

**Design and Applications of Advanced Optical  
Modulation Formats for Optical Metro/Access  
Transmission Systems**

**LIU, Zhixin**

A Thesis Submitted in Partial Fulfillment

of the Requirements for the Degree of

Doctor of Philosophy

in

Information Engineering

The Chinese University of Hong Kong

June 2012

# Acknowledgement

Pour ma famille, mes amis, et vous.

When I applied CUHK three years ago, I actually didn't have a good reason. The only thing I wanted was to quit the job and gave myself one more chance to pursuit my dream. If it was not Professor Chan, I wouldn't be here, learning, working, and fighting for the future. There was a dark time of life, in such time, a drop of water is worth more than a fountain in the bright time. Luckily, I got the precious drop. Therefore I would like to express my deepest gratitude to Professor Calvin, Chun-Kit Chan, who gave that drop of water. Thanks for your tolerance, guide, support, and precious help.

Success is difficult in real life, especially for people who started with nothing. We read many fantastic stories about success and happy life. But it rarely happens in the real life, or it may never happen if one doesn't receive support from family, friends, and sometimes strangers. In these respects, I am a lucky person, and I am grateful to the support from my family, who give me home; my girlfriend, who is always my "funny nut". And my friends, together we discuss work, life, philosophy, we deal with tough problems and innovate inspiring technologies. Your help, teach, and cooperation are my most valuable experience and memories. And for some strangers, though we may never know each others' name, I thank your suggestion and care.

There are numerous books, thesis, and articles. How many of them will be remembered in 10 years? 20 years? People don't get remembered by words, words are remembered because of the people. All the creations - poem, lyric, comment, scientific papers, will be buried in the dust if we are nobody. So my very dear audience, with all the help we get, let's keep trying, seeking, and fighting. Hope one day, we will be remembered.

~~我總在最深的絕望裏，遇見最美麗的驚喜~~

# 滿江紅

劉智鑫

二十年來，離桑梓，為求名節。曾記否，  
牛馬風塵，飄零如葉。獅子山下仰聖賢，吐  
露港前聽曉月。最難忘，滴水重金銀，恩情  
切。

貞元書，逸翁節。橫渠志，憑誰列？看  
兒孫，奮力星火相接。為立生民天地心，往  
聖開泰繼絕學。朝聖祖，不負男兒身，壯士  
血！

# Abstract

The increasing demands for bandwidth have aroused a myriad of industry and academic activities in developing high-speed and cost-effective optical networks, among which optical broadband access networks was the main driving force for such growth in recent years. The most promising solution to optical broadband access network is the passive optical network (PON), which is a point-to-multipoint tree-topology network that connects optical line terminal (OLT) with many optical network units (ONUs) via a long fiber feeder and many short distribution fibers. Promising the concept it is, it raises many detailed technical challenges, such as colorless ONUs, burst mode transmission, bi-directional transmission with mitigated backscattering noise, long-reach PON, and integrating network functionalities. All of the technical requirements are motivated by the “original requirements” of telecommunication – faster, cheaper, and more robust.

To fulfill the technical requirements, different researchers take different angles to design system and to study the enabling technologies. For example, devices, system architectures, network protocols, etc. In this thesis research, we have tried to deal with one or multiple problems by employing advanced modulation formats for the optical signals. In particular, we have studied IRZ-duobinary, Manchester-duobinary, and Manchester formats, including the modulation/demodulation techniques, transmission properties, and system applications. The research topics are classified according to the type of modulation formats.

In the first topic, IRZ-duobinary format is proposed for optical signal transmission. It has desirable properties of large dispersion tolerance (as compared to conventional RZ/IRZ) and finite optical power in each bit. In this study, we firstly show the advantages of IRZ-duobinary and the corresponding modulation techniques. Then, we demonstrate a 10-Gb/s per channel optical multicast overlay scheme and an

80-km-reach system with re-modulated ONU, both in wavelength division multiplexing (WDM) PON.

In the second topic, Manchester-duobinary format, which has the advantages including easy clock/level recovery, compressed bandwidth, and zero DC component, is studied. We propose an efficient and cost-effective Manchester-duobinary transmitter by properly modulating a chirp managed laser (CML) with electrical Manchester signal. Then, a cost-effective CLS 70-km-Reach full-duplex WDM-PON with downstream 10-Gb/s Manchester-duobinary signal and upstream 1.25-Gb/s re-modulated NRZ-OOK signal is proposed and experimentally demonstrated. This design simultaneously solves the problems of colorless ONU, bi-directional transmission, and long-reach, using cost-effective system design and devices.

Finally, we investigate the performance of electronic dispersion compensation (EDC) technique on 10-Gb/s Manchester coded optical signal, so as to further improve its dispersion tolerance and may enables its applications in long-reach PON. In this study, feed forward equalizer (FFE), decision feedback equalizer (DFE), and maximum-likelihood sequence estimation (MLSE) are employed as the equalizers Utilizing off-line signal processing, the performance of different equalizers with different parameters (number of taps, sampling rates, number of states, etc.) under both cases of single-ended and balanced detection are studied and compared. Experimental results show that the transmission distance of Manchester coded signal can be increased by a factor of three with four-sample-per-symbol FFE-DFE.

# 摘要

光纖通信技術與光網絡在過去三十年間極大地改變了人們的生活。雖然整個光通信行業因為 2000 年互聯網泡沫的破滅受到了影響，但近年來由於高清電視，移動多媒體和社交網絡的興盛，互聯網對通信網絡傳輸帶寬的需求達到了前所未有的高度，進而推動了光通信行業的再一次興盛。站在行業的高度來看，寬帶接入網無疑是推動行業發展的最主要領域。而實現寬帶接入網的最主要技術則是無源光網絡技術。無源光網絡的本質是一個樹型拓撲的光網絡，其主要的傳輸光纖可被多用戶共享，且在中央基站和用戶之間無任何有源器件，從而大大降低了網絡的成本。然而，在具體實踐中，仍然有許多的技術難題需要解決，例如：無色光網絡單元、突發性傳輸、全雙工傳輸、長距離無源光網絡和網絡功能集成等。這些技術需求亦反應了市場對通信技術發展的要求，及“更快，更便宜，更靈活。”

為滿足無源光網絡的技術要求，研究者們從不同的角度提出了各種解決方案，研究領域囊括光傳輸技術、新型器件、系統結構、網絡協議等等。本論文研究從傳輸碼型的角度來解決上述一項或幾項問題。研究碼型包括雙二進制反歸零碼，雙二進制曼切斯特碼，還有常規曼切斯特碼。研究內容則包括上述碼型的產生、接收、傳輸特性和系統應用等等。論文首貳章為概要和背景技術介紹，其餘幾章則按照不同的碼型分類討論。

本論文第一項研究課題為雙二進制反歸零碼。相比傳統的歸零碼和反歸零碼，雙二進制反歸零碼具有更大的色散容限，且每個傳輸符號均有能量。我們先研究了它的優勢，調製/解調方法，而後研究了該碼型在無源光網絡中的具體應用，包括 10-Gb/s 全光組播系統和基於重調製的 80 公里長距離波分複用無源光網絡系統。

第二項研究課題為雙二進制曼切斯特碼型，該碼型的優勢包括較大的時鐘分量，窄帶寬，無直流分量等。我們提出了一種基於直接調製的雙二進制曼切斯特碼產生方法。該方法具有高效，低價，高輸出功率等特點。基於該雙二進制曼切斯特碼發射機，我們實現了 70 公里雙向傳輸的波分複用無源光網絡。該系統下

行傳輸採用雙二進制曼切斯特碼型，上行傳輸採用直接調製的反射式半導體激光器，所以系統成本大大降低。

最後，我們研究了電色散補償技術對於傳統曼切斯特碼型的傳輸性能的改善。所使用的電均衡技術包括前向均衡器、判決反饋均衡器和極大似然估計均衡器。通過離線處理的方法，我們對曼切斯特碼型在三種均衡器下的傳輸性能進行了實驗驗證。研究內容包括前向均衡器和判決反饋均衡器抽頭數的優化、不同採樣率下系統性能、極大似然估計中狀態機個數的影響和不同的曼切斯特接收機的影響等等。

# Table of contents

Acknowledgement .....	1
Abstract .....	3
摘要 .....	5
Table of contents .....	7
List of figures and tables .....	13
Chapter 1. Introduction	
1.1 Optical Broadband Access .....	18
1.1.1 Bandwidth requirement .....	19
1.1.2 Passive optical networks .....	22
1.2 Research Challenge of Next-Generation Optical Access Network .....	25
1.2.1 Colorless ONU .....	25
1.2.2 Burst Mode Transmission .....	27
1.2.3 Backscattering Noise in PON .....	28
1.2.4 Long-Reach Access Network .....	30



1.2.5 Enriching Network Functionalities .....	31
1.3 Major contribution of this thesis .....	32
1.3.1 IRZ-duobinary transmitter and application.....	32
1.3.2 Manchester-duobinary transmitter and application .....	33
1.3.3 Receiver with electronic equalizer for Manchester signal..	34
1.4 Outline of this Thesis.....	35
 Chapter 2. Optical Modulation Technique and Transmission Impairments	
2.1 Optical Modulation techniques .....	38
2.1.1 Chirp managed laser.....	38
2.1.2 Mach-Zehnder modulator.....	41
2.2 Transmission Impairments .....	47
2.2.1 Noise.....	47
2.2.2 Chromatic dispersion .....	49
2.2.3 Fiber nonlinearity .....	50
2.3 Impairment Mitigation Techniques .....	51
2.3.1 In-line compensation techniques.....	51

2.3.2 Post-compensation techniques .....	52
Chapter 3.    Optical Multicast and Re-modulation Based on Inverse-RZ-duobinary Transmitter	
3.1 Introduction .....	53
3.2 IRZ-duobinary transmitter.....	55
3.2.1 Generation of IRZ-duobinary format.....	55
3.2.2 Comparison of different configurations of IRZ-duobinary generation .....	56
3.3 IRZ-duobinary format for optical multicast in WDM-PON .....	60
3.3.1 Optical multicast in WDM-PON.....	60
3.3.2 Proposed system architecture.....	61
3.3.3 Experimental demonstration of the proposed optical multicast system .....	65
3.4 IRZ-duobinary for long-reach PON .....	68
3.4.1 Long-reach PON using DI based IRZ-duobinary transmitter .....	69

3.4.2 Long-reach PON using CML based IRZ-duobinary transmitter.....	75
3.5 Summary.....	81
Chapter 4. Manchester-duobinary Transmitter for Bi-directional WDM-PON	
4.1 Introduction .....	83
4.2 Manchester-duobinary transmitter .....	85
4.2.1 Mach-Zehnder modulator based Manchester-duobinary transmitter.....	85
4.2.2 Chirp managed laser based Manchester-duobinary transmitter.....	87
4.3 Rayleigh noise mitigated bi-directional WDM-PON based on Manchester-duobinary transmitter .....	94
4.3.1 CLS Bi-directional long-reach WDM-PON. ....	94
4.3.2 Proposed system architecture.....	97
4.3.3 Experimental demonstration .....	99
4.4 Summary.....	102

## Chapter 5. Electronic Equalizer for Manchester Coded Signal

5.1 Introduction .....	103
5.2 Electronic equalizer for CD compensation .....	104
5.2.1 Channel model .....	104
5.2.2 FFE-DFE .....	106
5.2.3 MLSE .....	107
5.3 FFE-DFE for Manchester signal .....	109
5.3.1 Experimental setup for CD compensation of Manchester signal using FFE-DFE .....	110
5.3.2 Results and discussion.....	112
5.4 MLSE equalizer for Manchester signal.....	121
5.4.1 Experimental setup for CD compensation of Manchester format using MLSE.....	121
5.4.1 Results and discussion.....	122
5.5 Summary.....	124

## Chapter 6. Conclusion

6.1 Summary of this thesis .....	125
----------------------------------	-----

6.2 Future work.....	127
References .....	128
Appendix:.....	1499
A. List of abbreviations .....	149
B. List of publications .....	154

# List of figures and tables

Fig. 1.1 Hierarchical architecture of global communication infrastructure .....	19
Fig. 1.2 Worldwide FTTH Deployment Forecast (Households, 2005-2012) [5].	21
Fig. 1.3 FTTH Households & Penetration by Top Ten Countries (2011) [6] .....	21
Fig. 1.4 Architecture of passive optical network.....	22
Fig.1.5 Architecture of TDM-PON .....	23
Fig.1.6 Architecture of WDM-PON.....	24
Fig. 2.1 Principle of operation of chirped manager lasers [15] .....	40
Fig. 2.2 Performance comparison between CMLs and external modulators.....	41
Fig. 2.3 Schematic of the Mach-Zehnder Modulator .....	42
Fig. 2.4 (a) Operation of the MZM for NRZ-OOK modulation, (b) eye diagram, (c) optical spectrum.....	44
Fig. 2.5 Configuration of MZM for optical duobinary modulation.....	45
Fig. 2.6 (a) Operation of the MZM for AM-PSK duobinary modulation, (b) eye diagram (c) comparison of optical spectra for NRZ-OOK, RZ-OOK, NRZ-DB, RZ-DB .....	45
Fig. 3.1 An IRZ-duobinary transmitter.....	55
Fig. 3.2 Illustration of the principle of optical IRZ-duobinary modulation. ....	56
Fig. 3.3 Required OSNR for BER = $10^{-3}$ versus residual dispersion at 10.709 Gb/s for different modulation formats of pure IRZ (solid line, simulation), RZ (dot line, simulation), and IRZ-duobinary (dash line, type 1 configuration, simulation).....	58
Fig. 3.4 Required OSNR for BER = $10^{-3}$ versus residual dispersion at 10.709 Gb/s for different types of IRZ-duobinary transmitters in table 3.1. ....	59
Fig. 3.5 Schematic diagram of the proposed WDM-PON with proposed optical multicast overlay.....	62

Fig. 3.6 Signal at the output of MZM1 when multicast is enabled/disabled. (a) & (b): Principles of (a) enabling, and (b) disabling the multicast data transmission .....	63
Fig. 3.7 Simulated signal spectra and experimental eye diagrams at the output of MZM1 and MZM 2 under (a) multicast-enabled case, and (b) multicast-disabled case. ....	64
Fig. 3.8 BER measurements of upstream, downstream PtP and multicast signals when multicast is enabled or disabled. ....	66
Fig. 3.9 Receiver sensitivities (at BER= $10^{-9}$ ) of the downstream signals versus the transmission distance. ....	67
Fig. 3.10 Receiver sensitivities (at BER= $10^{-9}$ ) of the downstream signals, after 30-km transmission, under different timing misalignment values. ....	67
Fig. 3.11 Architecture of the proposed system. ....	69
Fig. 3.12 Principle of generating IRZ-duobinary signal with PM and MZDI. ....	70
Fig. 3.13 Optical spectra of conventional IRZ and IRZ-duobinary signals. ....	71
Fig. 3.14 Eye diagrams of (a) optical BtB IRZ-duobinary, (b) optical IRZ-duobinary after 80-km transmission, (c) electrical BtB IRZ-duobinary, (d) electrical IRZ-duobinary after 80-km transmission, (e) electrical BtB remodulated signal, (f) electrical remodulated signal at OLT. ....	72
Fig. 3.15 BER measurements of the 10-Gb/s downstream and the 2.5-Gb/s upstream signals. ....	73
Fig. 3.16 Measured dispersion tolerance for Inverse-RZ-Duobinary and conventional Inverse-RZ signal. ....	73
Fig. 3.17 Measured nonlinear tolerance for Inverse-RZ-Duobinary and conventional Inverse-RZ signal. ....	74
Fig. 3.18 Architecture of the proposed system. ....	76
Fig. 3.19 (a) Schematic of CML. (b) Illustration of principle of operation of IRZ-duobinary modulator using CML. ....	77
Fig. 3.20 Experimental setup. ....	78

Fig. 3.21 (a) The spectra of IRZ-duobinary signal generated by CML. (b) The spectra of the experiment wavelengths.....	79
Fig. 3.22 Eye diagrams. (a) Optical eye diagram of back-to-back IRZ-duobinary signal. (b) Optical eye diagram of IRZ-duobinary signal at ONU. (c) Optical diagram eye of back-to-back upstream signal. (d) Optical eye diagram of back-to-back upstream signal at OLT. (e) Electrical eye diagram of back-to-back upstream signal. (f) Electrical eye diagram of back-to-back upstream signal at OLT. ....	80
Fig. 3.23 BER measurements of the 10-Gb/s downstream and the 2.5-Gb/s upstream signals .....	81
Fig. 4.1 Experimental setup of MZM based Manchester-duobinary transmitter and corresponding receiver system. CLK: clock signal. FD: frequency doubler. T-FF: toggle flip-flop. PD: photodetector. Pre-AMP: preamplifier. LA: limiting amplifier. [18] .....	85
Fig. 4.2 Principle illustration of generation of Manchester-duobinary signal based on MZM. [18] .....	85
Fig. 4.3 Eye diagrams of (a) electrical Manchester-duobinary signals applied to modulator, (b) optical Manchester-duobinary signals before demodulation, and (c) electrical Manchester-duobinary signals after balanced detection. [18] .....	87
Fig. 4.4 (a) Schematic of CML-based Manchester-duobinary transmitter. (b) Illustration of the generation of the Manchester-duobinary signal.....	88
Fig. 4.5 Experimental setup for studying the CML based Manchester-duobinary transmitter.....	89
Fig. 4.6 Optical spectra of 10-Gb/s conventional Manchester (dashed line) and Manchester-duobinary (solid line) signals. ....	90
Fig. 4.7 BER performance for 10-Gb/s Manchester-duobinary signal and conventional Manchester signal. ....	91
Fig. 4.8 Chromatic dispersion tolerance for 10-Gb/s Manchester-duobinary signal and conventional Manchester signal.....	92



Fig. 4.9 Optical spectra of the output Manchester-duobinary signal under different OSR operating points.....	93
Fig. 4.10 Receiver sensitivities as a function of transmission distance for different OSR operating points.....	94
Fig. 4.11 Architecture of the proposed WDM-PON .....	97
Fig. 4.12 Generation of the Manchester-duobinary signal using CML.....	98
Fig. 4.13 Experimental setup.....	99
Fig. 4.14 BER measurements of (a) the 1.25-Gb/s upstream signal and (b) the 10-Gb/s downstream signal. ....	100
Fig. 4.15 Comparison of upstream sensitivity for re-modulating CW seeding and Manchester-duobinary downstream signal. ....	100
Fig. 4.16 Measured RF spectra for (a) upstream and (b) downstream paths with and without LPF and HPF. (Res: 10 MHz).....	101
Fig. 5.1 Direct detected optical fiber communication OOK system with electronic equalizer.....	104
Fig. 5.2 Structure of FFE-DFE .....	106
Fig. 5.3 Architecture of MLSE receiver.....	108
Fig. 5.4 Experimental setup for CD compensation of Manchester signal using FFE-DFE. PPG: pattern generator, XOR: exclusive-OR, OSA: optical spectrum analyzer, OBPF: optical bandpass filter.....	110
Fig. 5.5 Receivers for Manchester signal and the structure of FFE-DFE .....	110
Fig. 5.6 Optical eye diagrams of Manchester signal and corresponding sampling schemes for equalization. (a) 4 spb sampling. (b) 2 spb sampling. ....	112
Fig. 5.7 Required OSNR vs. Residual CD for 10.709-Gb/s Manchester signal with different number of FFE/DFE taps using single-ended detection. (a) FFE with different number of taps followed by DFE(2). (b): FFE(17) followed by DFE with different number of taps. ....	113
Fig. 5.8 Required OSNR vs. Residual dispersion for 10.709-Gb/s Manchester signal with different number of FFE/DFE taps using balanced detection. (a)	

FFE with different number of taps followed by DFE (2). (b): FFE (17) followed by DFE with different number of taps.....	114
Fig. 5.9. Required OSNR vs. Residual dispersion for 10.709-Gb/s Manchester signal using different detector and 2 samples per symbol scheme with different number of FFE/DFE taps. (a): Single-end detector (b): Balanced detector .....	116
Fig. 5.10 Required OSNR vs. sampling phase error for 2-spb scheme at back-to-back. ....	117
Fig. 5.11 Comparison of 2-spb scheme and 4-spb scheme for equalizer with different number of FFE taps.....	118
Fig. 5.12 Simulated eye diagrams for Manchester signal and corresponding FFE tap coefficients for FFE(9)-DFE(2) at different CD values. (a),(e): 380 ps/nm; (b),(f):480 ps/nm; (c),(g): 580 ps/nm; (d),(h): 680 ps/nm. ....	120
Fig. 5.13 Comparison of Manchester and NRZ for equalizer with different number of FFE taps.....	120
Fig. 5.14 Experimental setup for CD compensation of Manchester format using MLSE.....	121
Fig. 5.15 Required OSNR vs. Residual dispersion for 10.709-Gb/s Manchester signal with/without equalization using (a) single-end detection and (b) balanced detection. ....	122

# Chapter 1. Introduction

## 1.1 Optical Broadband Access

The use of fiber-optic technology in telecommunications systems occurred first in late 1970s. Since then the fiber-optic telecommunications systems have been deployed worldwide and have revolutionized the telecommunication technology. Entering the 21st century, we witnessed the explosive growth of the Internet and the rapid development of global communication infrastructure, which are driven by increasing user bandwidth demands and emerging multimedia applications, such as video-on-demand, high-definition television (HDTV), digital cinema. These tremendous changes in technologies and demands, together with government deregulation and competition among data, telecom, and community antenna television (CATV) operators, have overturned the conventional communication services and created new challenges and opportunities to society and economy. To cope with those challenges, service providers are striving to develop new telecommunication networks. The biggest opportunity of current Internet development is the access network.

Today's global communication network is built and operated within a hierarchical structure, consisting of access networks, metropolitan networks, and core networks [1] (as shown in Fig. 1.1). As a part of the global communication infrastructure, broadband access networks connect millions of users to the Internet, providing various kind of services, including voice, data, and video.

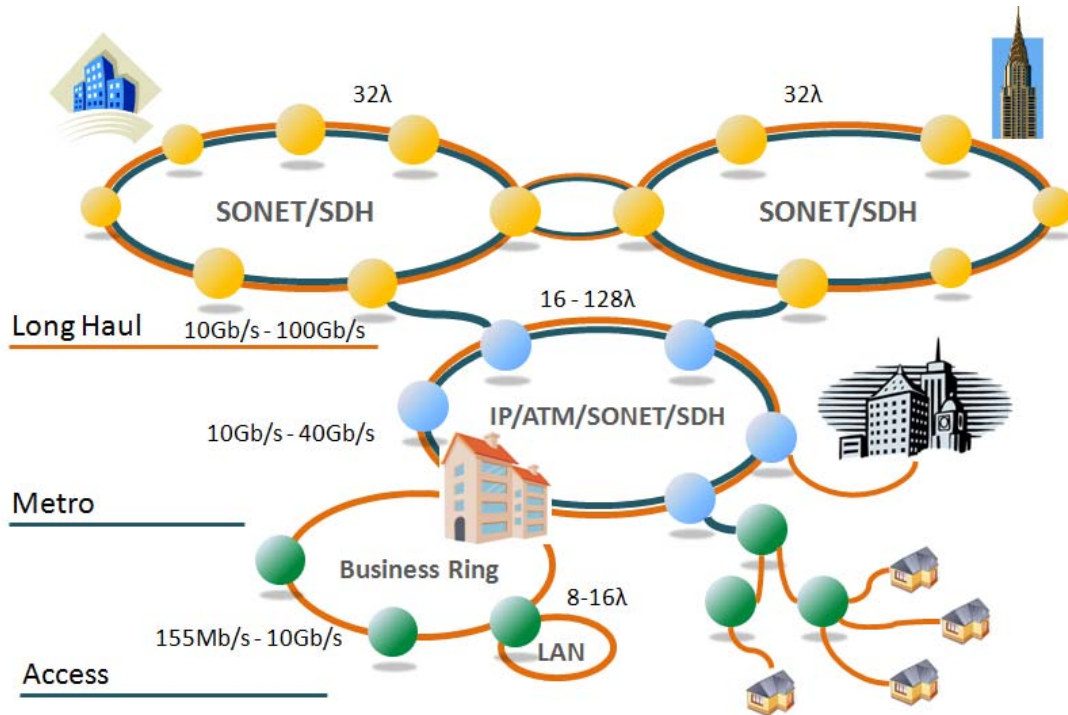


Fig. 1.1 Hierarchical architecture of global communication infrastructure

As bandwidth demands for multimedia applications continuously increase, customers require high bandwidth and flexible access at lower cost. A variety of broadband access technologies are emerging to meet those challenging demands. Though the wired access network is still dominated by digital subscriber line (DSL) and cable modem, the limited bandwidth-distance product of the copper wires will soon be the bottleneck for broadband access. Meanwhile, fiber to-the-x (FTTx) has become a promising access technology and is believed to be the ultimate solution for broadband access service in the future [2]. As new technology continues to be developed, the future access technology will be more flexible, higher speed, and lower cost. In this section we discuss current status of access network and review current and emerging optical access technologies.

### 1.1.1 Bandwidth requirement

The field of telecommunications suffered a significant setback in the beginning of this century because of the bursting telecom “bubble” [3]. After some years of stagnancy,

demands for bandwidths are now growing again, and have become the driving force for the recent enthusiasm in FTTx and passive optical networks (PON) developments.

The demand for bandwidth is driven by the contents available on the network. The drastic improvement in the performance of personal computers and consumer electronic devices has impact the way people live and made possible expanding demands of multimedia services, such as video on demand, video conferencing, e-learning, interactive games, VoIP, and others. Table 1.1 summarizes the bandwidth requirements for different applications in a typical household. As a result of the constantly increasing bandwidth demand, users may require more than 50 Mb/s in the near future.

Table 1.1 Bandwidth requirements for different IP services [4]

Application	Bandwidth	QoS
Video (SDTV)	3.5 Mb/s	Low loss, low jitter, constant bit rate
Video (HDTV)	15 Mb/s	Same as above
Voice over IP (VoIP)	64 kb/s	Low loss, low jitter, constant bit rate
Video conference	2 Mb/s	Protection
Video gaming	10 Mb/s	Low loss, low jitter, bursty
Telecommuting	10 Mb/s	best effort, bursty
Peer-to-peer downloading	100 kb/s - 100 Mb/s	best effort

According to the ‘FTTH Worldwide Market & Technology Forecast’ published by Heavy Reading [5], USA, the total number of homes connected to fiber will grow from about 11 million at the end of 2006 to about 89 million at the end of 2012, representing about 5% of all households worldwide. This growth is dominated by

Asia, where the number of connected households will grow to 65 million by the end of 2012. Over the next five years, it is expected that most other developed countries will join that list, and fiber will also have a significant impact in relatively less developed telecom markets, including, Russia, India, and the Middle East.

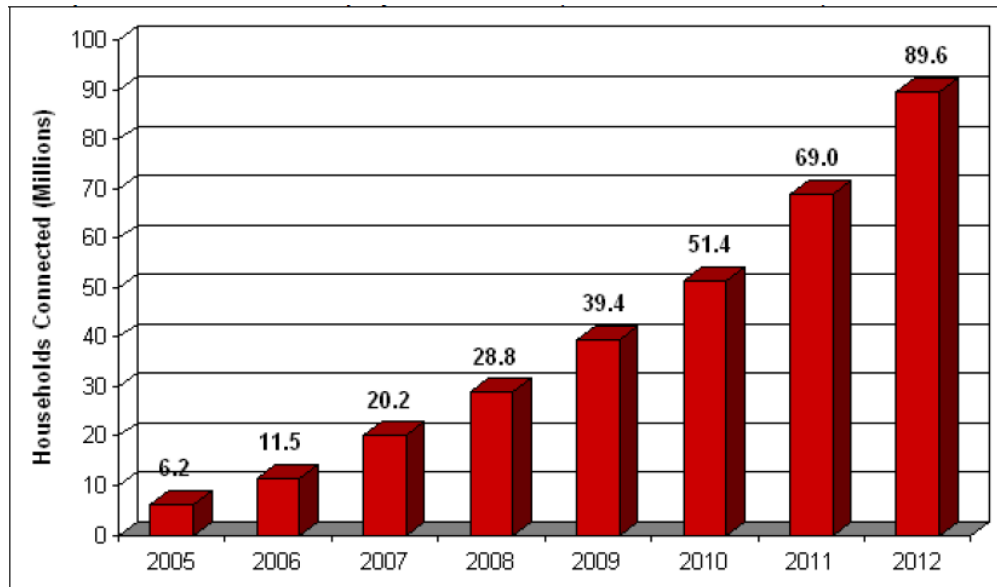


Fig. 1.2 Worldwide FTTH Deployment Forecast (Households, 2005-2012) [5]

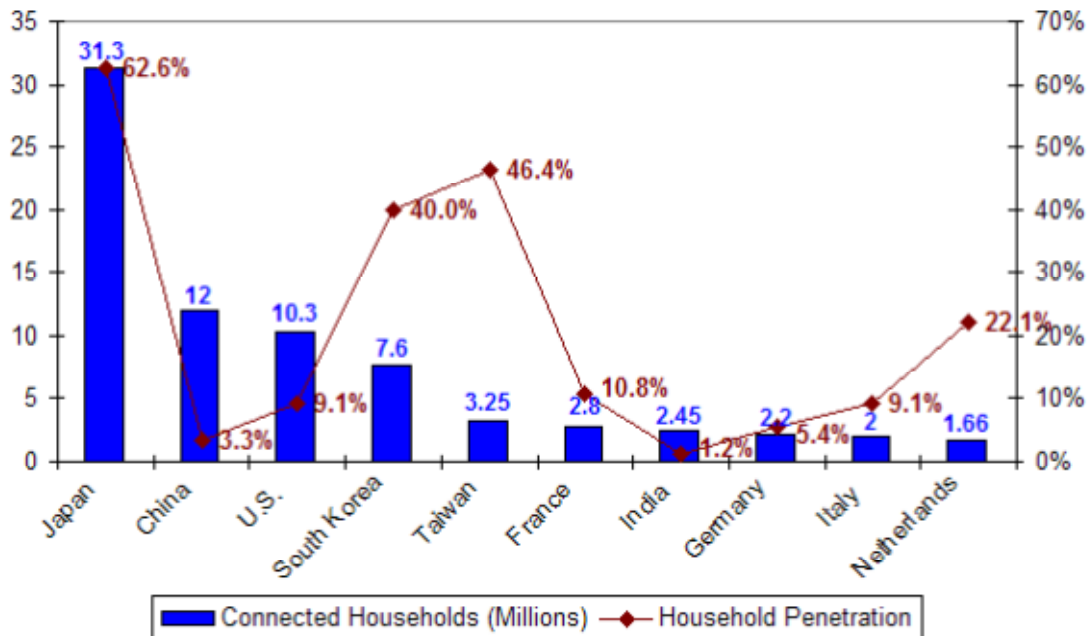


Fig. 1.3 FTTH Households & Penetration by Top Ten Countries (2011) [6]

## 1.1.2 Passive optical networks

The passive optical network (PON) is an optical fiber based network architecture, which is a promising solution to enable high-speed broadband access. As shown in Fig. 1.4, a PON is a point-to-multipoint optical network on which the optical line terminal (OLT) or the central office (CO) delivers services, via a long fiber feeder, to the remote node (RN), where light is split and deliver to many optical network units (ONUs) through one or multiple 1:N optical splitters or wavelength demultiplex. Then the downstream data are transmitted to the ONUs located at end user premises, via several shorter distribution fibers. At the ONU, the downstream data is received by users, while the upstream data, such as users' request information or upload files will be forwarded to the OLT after being combined or multiplexed at the RN. As the RN and feeder fiber are shared by all ONUs in the network, thus the total fiber length is much less than the case of direct connection between the OLT and all ONUs. Thus the total cost is significantly reduced. Besides, the infrastructure between the OLT and the ONU is passive, i.e., it does not require any power supply. Therefore it can greatly ease the network management of the outside plant facilities [4].

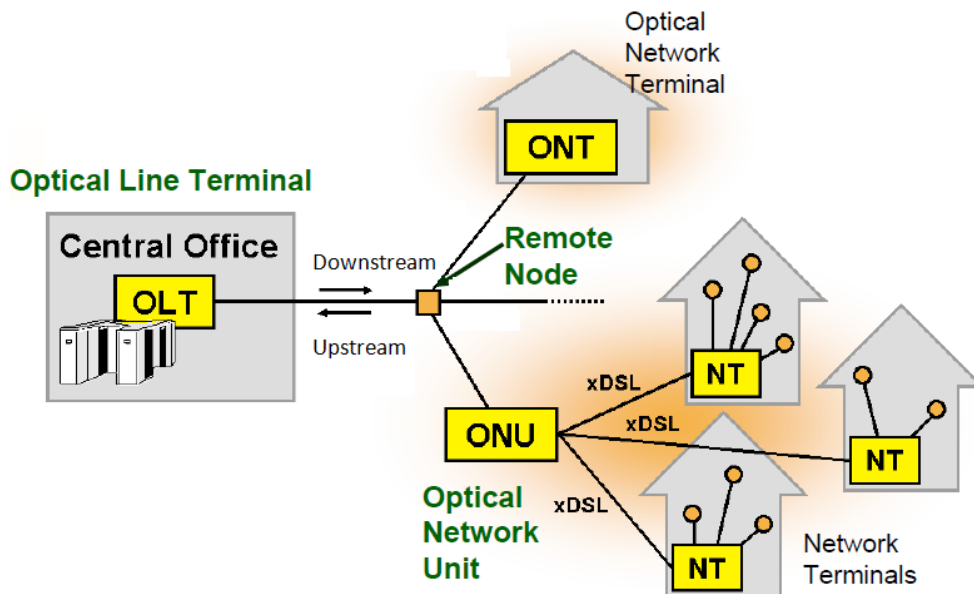


Fig. 1.4 Architecture of passive optical network [2]

Under this network architecture, PON can be further divided into several types according to the mechanisms to control the shared media access, including time-division-multiplexed PON (TDM-PON), wavelength division multiplexed (WDM-PON), and optical code-division multiple-access PON (CDMA-PON), etc. [7]. Nowadays, TDM-PON and WDM-PON are two most popular structures of the PON technologies. Thus, our discussion here will mainly focus on these two technologies.

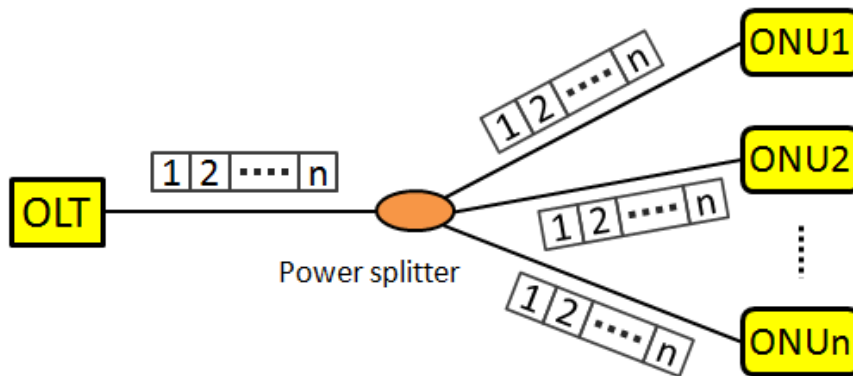


Fig.1.5 Architecture of TDM-PON

- *TDM-PON*

Fig. 1.5 shows the architecture of a TDM-PON. A TDM-PON uses a passive power splitter as the remote terminal. A single wavelength is employed at the OLT to carry the downstream traffic, which is broadcast to all ONUs via the power splitter. The upstream signal has a relatively lower bit rate and is usually carried on another wavelength. Both the upstream and the downstream employ TDM techniques. Most of the commercial PONs systems are based on TDM techniques, including BPON [8], EPON [9], and GPON [10], which have been standardized and deployed by network operators for access network applications.

In a BPON, downstream traffic at 622-Mb/s is carried by a 1.49- $\mu$ m optical carrier, while the upstream traffic at 155-Mb/s is carried by a 1.3- $\mu$ m optical carrier. GPON can provide a symmetric downstream/upstream data rate up to 2488 Mbps, while EPON which are originally standardized for a symmetric transmission speed of 1 Gb/s



for both downstream and upstream. In recent years, the advent of the 10-Gb/s Ethernet technology is also increasing the transmission speed of EPON, which is now working toward 10-Gb/s.

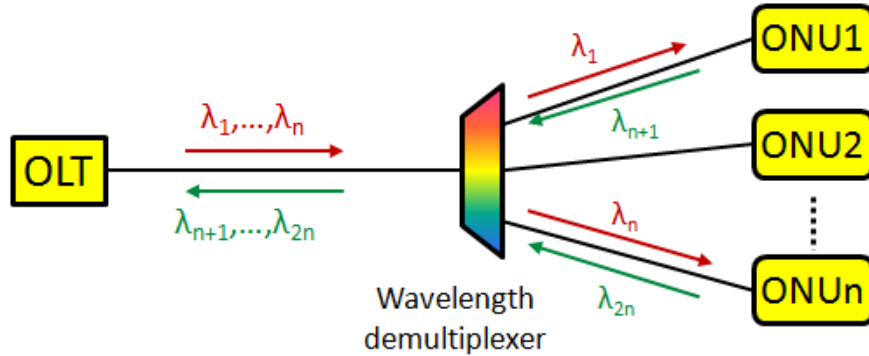


Fig.1.6 Architecture of WDM-PON

- *WDM-PON*

Fig. 1.6 shows the typical architecture of a WDM-PON in a tree-topology. In a WDM-PON, each ONU will be served by a dedicated wavelength to communicate with the OLT, with similar architecture as TDM-PON except a wavelength demultiplexer is employed at the RN to replace the power splitter. Signals for different ONUs are carried on different wavelengths and routed by the wavelength demultiplexer to the dedicated ONU. Each ONU detects the destined downstream wavelength and retrieves the received data or further distribute the data to more subscribers through DSLs or mobile connections. Upstream transmission is realized on another designated upstream wavelength. Although at this moment the WDM devices are still expensive, WDM-PON offers “unlimited” bandwidth and better privacy and scalability. Many leading network operators have shown growing interest in research and development in WDM-PONs, such as NTT in Japan [11], Verizon [12], etc.

## **1.2 Research Challenge of Next-Generation Optical Access Network**

Next-Generation (NG) optical access networks promise fast and flexible connectivity to fulfill the bandwidth requirement of end users and at the same time raise many technical challenges in order to ensure a flexible and reliable transmission, and mostly importantly, to bring down the cost. These technical problems bring research opportunities and require innovations in devices, network architecture, and transmission techniques. In this section, the major research challenges in current optical access networks will be briefly discussed, with the focus on physical-layer research problems, which contribute most to capital expense on NG optical access networks. Some existing technologies for each research problem will also be reviewed in the sub-sections.

### **1.2.1 Colorless ONU**

Colorless ONU is a critical requirement of WDM-PON [13]. In a WDM-PON, each ONU sends data back to the OLT via the upstream wavelengths. Therefore, the most straight forward way to realize the wavelength-specific upstream transmission is to employ light source of specific wavelength at the ONUs. In such a system, the upstream wavelengths have to match the respective passband of the wavelength multiplexer at the RN. Besides, the wavelength alignment is needed as any wavelength drift may lead to excessive power loss and distortion. These greatly increase the system complexity and the cost of deployment, administration and maintenance. Therefore, the concept of *colorless ONUs* has also been proposed such that the ONUs are not installed with any wavelength-specific devices. This greatly eases the inventory, maintenance and management of the wavelengths at the subscriber side and thus the cost of the ONUs can be kept low with mass production of identical ONU modules.

Much research efforts have been made for the implementation of colorless ONUs. For example, spectrum-slicing is proposed to realize colorless ONUs, in which a centralized broadband light source resides at the OLT, emitting broadband light is spectrally-sliced at the RN before being fed to the ONUs as the light source for upstream modulation. Instead of installing light sources at the ONUs, such scheme only requires cost-effective broadband light source at the OLT. System performance using different broadband light sources are characterized in early publications, including light emitting diode (LED) [14], Fabry-Perot (FP) laser [15], amplified spontaneous emission (ASE) light sources [16], and supercontinuum-based broadband light source [17]. Cost-effective as it is, the modulation speeds in schemes based on broadband light sources are low due to some inherent noise sources [17-18]. With the purpose of increasing transmission speed, injection-locking and wavelength seeding schemes have been proposed, where Fabry-Perot (FP) laser diodes [19], reflective semiconductor optical amplifiers (RSOA) [20-21] or vertical-cavity surface-emitting laser (VCSEL) [22] are adopted at the ONU sides and injected with the seeding wavelengths. By employing these schemes, the data rates can be increased to 1.25 Gb/s. To further improve the upstream data rate and to save wavelength resources, re-modulation schemes are proposed in [23-26], in which the downstream wavelengths are used as upstream light source to facilitate upstream modulation. Since the downstream carriers are reused for upstream transmission, the downstream data should either be erased or coded to avoid absence of optical power when performing upstream re-modulation. Studies in this field mainly focus on modulation techniques. Different modulation formats are employed to achieve upstream re-modulation, such as DPSK with different extinction ratio [23], OOK and DPSK [24], OOK and IRZ [25], DPSK and SCM [26], Manchester-duobinary and OOK [27], etc.

With the above mentioned schemes, the wavelengths of light sources are not determined by the gain media. As a result, it is easier to manage the wavelengths

without worrying about temperature changes or aging effects. Nowadays a lot of research has gone into making RSOAs, one of the most popular choices to realize colorless ONUs. However, the technology trend is still unclear as noise level of RSOA is still high and the speed that can be modulated is still low. Moreover, systems based on RSOA have to deal with Rayleigh backscattering (RBS) noise [28]. Researchers are also investigating the possibility of using cost-effective tunable laser [29] or reflective electro-absorption modulators (REAMs) [30].

### **1.2.2 Burst Mode Transmission**

Up to now, TDM-PON is the dominantly deployed PON system worldwide. In such system, the downstream traffic is continuously broadcast to all ONUs and conventional continuous-mode receiver are used at ONUs. However, for the upstream link, ONU transmitters are only active at their scheduled time slots to avoid collision. Thus, burst-mode transmitters are requested at OLT side. To correctly receive the discrete and asynchronous bursts with varying optical power levels, burst-mode receivers are required. In addition to TDM-PON, burst-mode transceivers are also required for some hybrid TDM/WDM-PON architectures [31-32].

A burst-mode transmitter requires fast burst on/off speed, sufficient power suppression during idle period, and stable power emission when turns on. These functionalities are usually performed by specially designed laser drivers, which play the most critical role in burst-mode transmitters [33].

A burst-mode receiver needs to handle burst-by-burst power fluctuation and the path-length differences induced burst-arrival timing jitter, which is probably the most challenging problem in burst mode transmission. To achieve such wide dynamic range, fast clock recovery and level recovery, many innovations at both device and system technologies are proposed. For instance, at device level, dc-coupled burst-mode receivers with auto-threshold level tracking circuit have been deployed [34-39]. For level recovery, feedback and feedforward structured circuits have been

reported. In the feedback design, the loop consists of a differential input/output trans-impedance amplifier and a peak detection circuit [34]. In the feedforward design, the signal from preamplifier is fed forward into a peak detection circuitry to determine the threshold [35]. By optimizing burst-mode automatic gain control (AGC) and automatic threshold control (ATC), a 10.3-Gb/s burst mode receiver, with dynamic range of 20.5 dB is achieved [36]. For fast clock recovery, feedforward architectures such as gated voltage-controlled oscillator [37] and oversampling [38] have been proposed. A burst mode receiver with 37-ns clock and data recovery (CDR) lock time based on 82.5-GS/s sampling IC has been reported [39].

Other than circuit techniques, several system-level innovations are also employed in designing burst mode transmission systems. Manchester code, with its inherent properties of abundant clock component and zero-dc, is adopted for easier clock and level recovery [40]. SOA based fast automatic level controlled amplifier with input dynamic range of more than 28 dB is also reported [41].

### **1.2.3 Backscattering Noise in PON**

In optical access systems, especially bi-directional transmission systems, the main contribution of backscattering noise is linear scattering noises, including Rayleigh scattering and Fresnel scattering. In practice, Fresnel scattering, which arises from interface discontinuity and is proportional to the power, is usually negligible, because it can be much alleviated by using specially designed connectors and fiber connections are usually achieved by splicing. Therefore, Rayleigh scattering is the dominant backscattering noise, when the system is working in linear regime.

The Rayleigh scattering results from the elastic scattering of light by particles much smaller than the wavelength of the light. It is a fundamental loss mechanism arising from density fluctuation during fiber fabrication [42]. As light travels through the fiber core, some scattered light is reflected back toward the light source and thus it

is called Rayleigh backscattering (RBS). For a input power of  $P_{in}$ , the average backscattered power  $P_{RB}$  is modeled as,

$$P_{RB} = P_{in} \alpha_s S (1 - e^{-2\alpha_p L}) / 2\alpha_p$$

where  $\alpha_s$ ,  $\alpha_p$ ,  $S$ ,  $L$  being the attenuation coefficient due to Rayleigh scattering, fiber attenuation coefficient, recapture factor, and fiber length, respectively [43], [44]. Rayleigh backscattering is a linear scattering and will not create new frequency component. However, the power and polarization of the backscattered light at different positions are random [45]. Hence, the reflected back signal is usually considered as a noise and the name Rayleigh backscattering noise (RBS) is used to describe this phenomenon.

The RBS problem in PON is also motivated by the cost-effective implementation of future broadband access network, especially in WDM based systems. Technically, it arises from the purpose to save wavelength resources while keeping the colorless property of ONUs. To realize such system, bi-directional transmission over the same fiber is necessary. In aforementioned carrier distributed schemes and re-modulation schemes, when the optical carrier or signal for upstream modulation is distributed from the OLT to the ONU, the back-reflected light generated by RB and Fresnel back-reflections will also be received by the upstream receiver. Though the scattered signal arrived at OLT has a relatively small power due to the loss of the round-trip propagation, the beating between the upstream signal and the back-reflected light will create much noise in the electrical domain. This RBS induced signal quality degradation must be resolved in order to achieve satisfactory system performance.

Much research have been done to solve the RBS problem. A straightforward way to avoid RBS is to implement dual-fiber architecture to support both downstream and upstream transmissions. However, it will drastically increase the network cost and is

currently not welcome by system operators. To realize bi-directional transmissions in single wavelength band in a single fiber, much effort have been paid on how to reduce the spectral overlap between the upstream signal and the backscattering noise. Without loss of generality, techniques can be categorized in reducing the spectral overlap in optical domain and electrical domain. Detailed technological review will be performed in Chapter 4.

### **1.2.4 Long-Reach Access Network**

Like Olympic game, the research in optical communication has a slogan of faster, longer, and stronger. It is not only true in research in long-haul transmission, but also true in access networks. However, the motivation for “longer” is a little bit different. The reason of doing long-reach access network is similar to other research problems – to save money. By extending the physical reach of the network from 20 km to around 100 km, end users can be directly connect to the core network, and thereby removes the need for additional equipment to connect outer core/metro backhaul network. Besides, the cost of the shared equipment can also be reduced by increasing the split size. Thus, long-reach optical access networks have potential to further reduce the installation and operation cost for operators.

To make optical access networks more economically attractive, we want to extend the reach and increase the split size, both of which introduce new technical challenges. In a standard PON, optical powers and losses define the available optical power budget. However, with the increased transmission distance and split size, both the upstream and the downstream transmissions face a large amount of attenuation, due to split loss and link loss. Research work in combating the large insertion loss is mainly focused on optical amplification and high sensitivity receiver. Long-reach PON based on EDFA pre-amplification and Raman amplification have been demonstrated [46-47]. To consolidate with deployed GPON system, SOA is also used for bi-directional amplification for both downstream and upstream signals, which

operate at different wavelength ranges [48]. Research in optical receiver includes RSOA-based upstream transmitter and high sensitivity receiver [49-50], etc. Many good reviews have summarized the progresses and achievements of long-reach access networks [48, 51].

In addition to power budget, we should also be noted that with the increased data rate and transmission distance, chromatic dispersion will also introduce impairment on optical signal. For standard single mode fiber (SSMF), the bandwidth-distance product at 1550 nm is around 500 GHz-km, which means apparent power penalty would occur when transmission distance increases to about 50 km. Therefore, the design of long-reach PON should consider power budget, dispersion, and aforementioned issues.

### **1.2.5 Enriching Network Functionalities**

PON offers broadband access, but it is still a point-to-point transmission system which links OLT and the individual subscribers. With the growth of video stream business such as HDTV, broadcast service delivery is needed in the optical access network. In TDM-PON, broadcast can be easily realized because the power splitter at RN inherently broadcast the downstream signal to all ONUs. In WDM-PON, however, is more challenging due to the dedicated wavelength assignment. Compared with broadcast service, the concept of multicast can significantly enhances the network resource utilization for multiple destination traffic and further improves the networking flexibility. Therefore, lots of research work has been done to realize broadcast or multicast in WDM-PON.

Conventional system realize optical multicast in higher layers. Contrary to conventional schemes, optical multicast can also be realized in optical domain. The advantage of doing so is to reduce the loading of the electronic network processors or routers on the network layer and to achieve much higher processing speed. Several interesting schemes have been proposed to overlay optical multicast onto a



WDM-PON, either by using additional light sources [52], subcarrier multiplexing technique [53], or the characteristics of modulation formats [54-55].

## **1.3 Major contribution of this thesis**

Research carried out in this thesis aims at system level innovation for the next generation optical access network, with main focus on modulation format and its corresponding transmitter and receiver realization to fulfill the system requirement. As discussed in section 1.2, next generation optical access network requires joint consideration of all the above mentioned problems. Our research work aims at solving one or multiple research problems with innovation in signal modulation format, transmitter, and receiver techniques.

### **1.3.1 IRZ-duobinary transmitter and application**

In this work, we investigate a new optical modulation format, namely inverse-return-to-zero duobinary (IRZ-duobinary), for optical transmission, especially in optical access networks. The work can be classified into three stages. In the first stage, we systematically study various methods of signal generation. Then we study its performance, i.e. complexity, dispersion tolerance, etc. and compared with commonly used optical modulation formats. Finally, we study its application in optical access network, including optical multicast and other possible applications in long reach system.

IRZ-duobinary format is a combination of IRZ and duobinary. It preserves several unique properties (i.e. finite optical power in every bit) while incorporating some desired property of optical duobinary (i.e. compressed bandwidth). Four different configurations for IRZ-duobinary generations are proposed and compared. Compared with conventional IRZ format, IRZ-duobinary show improved dispersion tolerance and may be more practical in many interesting applications in and optical access network, such as optical multicast and long-reach re-modulation system.

In the application of optical multicast in WDM-PON, we propose and demonstrate an optical multicast scheme employing the bandwidth efficient IRZ-duobinary signal. Multicast control is easily realized by tuning the bias of the downstream modulator at the OLT. At the ONU, one photo-detector with two decision modules is used to receive point-to-point (PtP) and multicast data, which makes the system low-cost and the ONUs are colorless. 10-Gb/s operation of the proposed selective broadcast overlay and 2.5-Gb/s upstream transmission with carrier distributed technology are experimentally demonstrated.

In another study, we demonstrate an 80-km-reach WDM-PON with 10-Gb/s downstream and 2.5-Gb/s upstream re-modulated signals. IRZ-duobinary signal is employed as the downstream signal format while upstream NRZ-OOK re-modulation is performed via a reflective semiconductor optical amplifier and electroabsorption modulator at the optical network unit. Two methods of generating IRZ-duobinary signal utilizing chirp managed laser (CML) are studied in similar system configurations.

### **1.3.2 Manchester-duobinary transmitter and application**

In this work, another novel modulation format – Manchester-duobinary is studied. Manchester-duobinary is a modulation format incorporating Manchester and duobinary. It is first proposed by Y. Dong et. al. in [56]. However, the MZM based Manchester-duobinary transmitter is complex. In our work, we propose a novel and simple scheme of generating optical Manchester-duobinary signal format using directly-modulated CML and experimentally demonstrated at 10 Gb/s. The generated optical Manchester-duobinary signal has narrow spectrum and has shown to achieve three times more chromatic dispersion tolerance in optical fiber transmission than that of conventional Manchester signal. The impact of the optical spectrum reshaper on the dispersion tolerance of the directly modulated optical Manchester-duobinary transmitter is also experimentally characterized.

By employing Manchester-duobinary format and our proposed cost-effective Manchester-duobinary transmitter, we propose and demonstrate a cost-effective centralized light source (CLS) 70-km-reach full-duplex WDM-PON with downstream 10-Gb/s Manchester-duobinary signal and upstream 1.25-Gb/s re-modulated NRZ-OOK signal. The downstream pre-chirped Manchester-duobinary signal is generated by directly modulating a CML with an electrical Manchester coded signal, at the OLT. Upstream re-modulation is realized via an RSOA, resided at the ONU. The CML-based downstream transmitter offers many advantages to cost-sensitive metro/access applications, including compactness, high output power, and no costly and bulky external modulators required. The reflected optical RBS noise in both downstream and upstream paths are mitigated by the electrical low-pass filter (LPF) and high-pass filter (HPF) at the OLT and the ONU, respectively. The experimental results show that the dispersion-tolerant Manchester-duobinary signal can well support data re-modulation and RBS noise suppression in bi-directional transmission.

### **1.3.3 Receiver with electronic equalizer for Manchester signal**

Manchester code is attractive in optical fiber communications due to its several unique properties, such as rich clock component, shaped spectrum. Its applications in access network include burst mode transmission, re-modulation, beat noise alleviation, and recently RBS noise mitigation. Nevertheless, Manchester code offers these advantages at the expense of broader signal bandwidth, which is twice as that of the conventional NRZ signal. Therefore, the chromatic dispersion (CD) tolerance of the Manchester signals is only one fourth of their NRZ counterparts, which limits their practical applications. To mitigate the CD induced signal impairment, we investigate the performance of electronic chromatic dispersion compensation of 10-Gb/s Manchester coded optical signal. Two types of electrical equalizers, feed forward equalizer (FFE) - decision feedback equalizer (DFE) and maximum-likelihood

sequence estimation (MLSE) are utilized to study their capabilities of CD mitigation. Utilizing off-line signal processing, the performance of FFE-DFE with different number of taps and input sampling rates under both cases of single-ended and balanced detection are compared. Experimental results show that the transmission distance of Manchester coded signal can be increased by a factor of three with four-sample-per-symbol FFE-DFE. Similarly, the performance of MLSE with different number of states for both single-end and balanced detection is compared. Experimental results show that the transmission distance of Manchester coded signal can be significantly enhanced by MLSE.

## **1.4 Outline of this Thesis**

The remaining chapters of this thesis are organized as follows:

Chapter 2 reviews the basic of optical transmitter, receiver, and common transmission impairments as well as compensation techniques in optical access networks. In addition to conventional direct modulated optical transmitter and MZM, CML will be reviewed in details. The background knowledge in this chapter will help the understanding of technology proposed in this thesis.

Chapter 3 explains the principle and applications of our proposed IRZ-duobinary format. Four different configurations to generate the IRZ-duobinary signal are studied and compared. Applications in WDM-PON multicast and long-reach PON are experimentally demonstrated.

Chapter 4 proposes a novel and simple Manchester-duobinary transmitter. The performance of the proposed transmitter and its application in suppression RBS noise in a bi-directional long-reach WDM-PON are experimentally studied.

Chapter 5 studies the performance of EDC for optical Manchester signal, including FFE-DFE and MLSE, with the purpose of finding proper EDC aided receiver for Manchester coded signal.

Chapter 6 gives the summary of this thesis and suggests the possible future work.

# Chapter 2. Optical Modulation Technique and Transmission Impairments

In the physical layer of optical communication, OOK in either NRZ or RZ have been the choice of optical modulation format since 1980s [57]. Though NRZ-OOK has still been employed in most transmission systems, even in long-haul system, it is not suitable for future high-speed optical networks, due to its low spectral efficiency and tolerance to transmission impairments [58]. In the past decades, advanced optical modulation formats have become a key ingredient to the design of modern optical communication networks, with different focus on core networks, metro networks, and access networks. Albeit the modulation formats that being studied in core, metro, and access networks are different, the research in modulation format is mainly motivated by two reasons: to fulfill the capacity demand and to lower down the cost. Because of these reasons, advanced modulation formats have received much interest with purposes to enhance signal tolerance to transmission impairments and to take advantage of some particular properties to increase the robustness of networks [59].

For access networks, various kinds of modulation formats have been studied to meet the growing demand for higher bit rates and bring down the system cost. The properties and requirements for desired optical access networks have been discussed in section 1.2 in the first chapter of this thesis, in which modulation formats play important role in some enabling technologies for the desired system. Applications, modulation, and demodulation technologies of different modulation formats are being actively studied.

In this chapter, we review the modulation techniques of generating different modulation format, with focus on the most significant binary modulation formats that are deployed in optical access networks. In addition to commonly used Mach-Zehnder

modulator (MZM), we highlight the principle and application of chirp managed laser (CML), which is an important device for this thesis research. Three basic transmission impairments in optical access networks – noise, chromatic dispersion, and fiber nonlinearity, are reviewed in order to help readers understand the content in the rest chapters. Common used technologies for impairment compensation have also been discussed.

## **2.1 Optical Modulation techniques**

### **2.1.1 Chirp managed laser**

The CML is an alternative transmitter technology that allows a directly modulated laser (DML) to be used in high-performance applications with a smaller size, lower power consumption, less device complexity, and lower cost [60].

It takes advantage of the chirp when directly modulating a DML to introduce phase shift such that the phase-related format can be generated. The bias current for a CML is usually about five times larger than that of the threshold current so that adiabatic chirp is dominated when modulating. The continuous phase shift of the optical carrier associated with the adiabatic chirp of the laser upon modulation, together with the action of a passive optical filter for spectral reshaping generates certain phase rule when bias, modulation current, and temperature are properly controlled, i.e. 1 bits separated by odd number of 0 bits are  $\pi$  out of phase. This kind of phase shift leads to a modulation format named duobinary, which increases dispersion tolerance by the destructive interference of the light in the bits that are leaving their time slots to spill into adjacent time slots [61]. Besides its dispersion tolerance, the phase-coding property of CML has been used to demonstrate return-to-zero alternate mark inversion (RZ-AMI) [62] and RZ-DPSK [63], RZ-DQPSK [64], IRZ-duobinary [65], and Manchester-duobinary [66], etc., both in compact butterfly packages. In this sub-section, we will first review the chirp property

when doing direct modulation on a DML, and then explain the principle of operation of CML.

### A Chirp in direct modulation

The chirp of directly modulated DFB lasers can be characterized by the time dependence of wavelength variation  $\Delta\lambda(t)$ , which is given by the equation [67]

$$\Delta\lambda(t) = a_1 \frac{1}{S} \frac{dS}{dt} + a_2 S \quad (2.1)$$

where

$$a_1 = \frac{\lambda^2 \alpha}{4\pi c} \quad (2.2)$$

and

$$a_2 = \varepsilon G a_1 \quad (2.3)$$

$\lambda$  is the wavelength,  $\alpha$  is the linewidth enhancement factor expressed in negative value [68],  $S$  is the optical power density,  $c$  is the velocity of light,  $\varepsilon$  is the nonlinear gain coefficient, and  $G$  is the threshold mode gain.

The first term of (2.1) denotes the transient component of chirp which depends upon the time rate of change of the optical intensity. The second term denotes the adiabatic component of chirp which depends only on the instantaneous value of the optical intensity, because it is introduced by the effect of the injection current on the refractive index of the cavity. Since the coefficients of the transient and adiabatic parts depend on different laser parameters, they will have different relative magnitudes depending on the individual DFB laser [69]. Without losing generality, transient chirp is dominated when the current injecting is around the threshold, while adiabatic chirp is dominated at higher bias current. In addition to transient chirp and



adiabatic chirp, thermal chirp also exists in DML [70]. However, as the thermal chirp is slow, we ignore it when illustrating the principle of CML.

## B Principle of CML operation

A conventional DML is operated to generate large amplitude modulation in which the laser is biased near threshold and modulated to achieve 8 to 10 dB ER. This will in turn enhance the transient chirp, which causes fast pulse spreading in SSMF because of the sign of the chirp. Since SMF has anomalous dispersion, the blue shifted rising edge of the output of a DML travels faster than the red shifted falling edge causing the pulses to quickly spread. Hence, the chirp of the laser in standard DML degrades the transmission performance, and is therefore, unwanted. The DML in a CML operates in a completely different regime, where the chirp is actually used to get advantage.

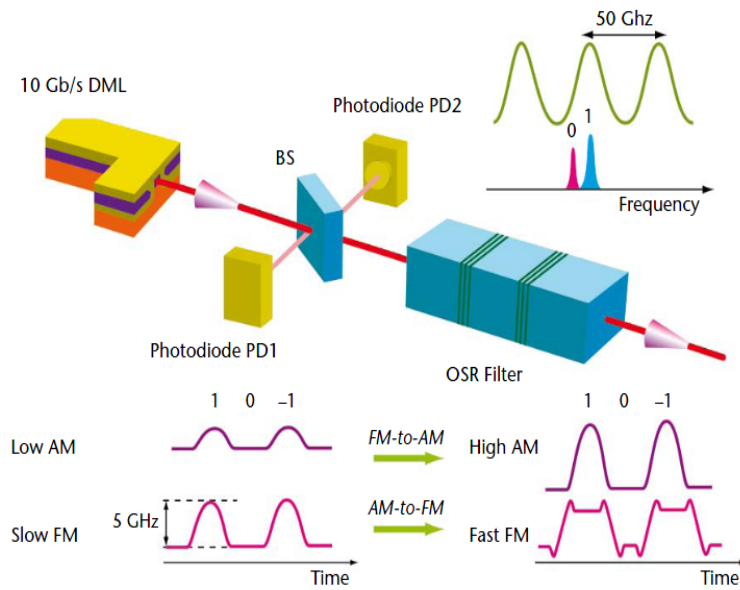


Fig. 2.1 Principle of operation of chirped manager lasers [71]

Fig. 2.1 shows the schematic of the CML and its principle of operation [72], [73]. The CML comprises a DML and an optical spectrum resaper (OSR) filter. A standard high-speed DFB laser is biased high above threshold, typically at  $\sim 5 \times$  threshold and directly modulated, this results in a low ER ( $\sim 1-3$  dB) intensity modulation. This mode of operation of the DML generates frequency-shift keying

(FSK) modulation. The other benefits of high bias of the DFB are high-output power, wide modulation bandwidth, stable single-mode operation, low timing jitter, and importantly suppression of transient chirp. The laser wavelength is tuned to the transmission edge of the OSR in order to attenuate the red-shifted 0 bits relative to the blue-shifted 1 bits. In this way, the OSR increases the ER to  $> 10$  dB and produces a clean eye and duobinary format is generated. The OSR also forms a wavelength locker together with two photodiodes and a beam splitter (as shown in Fig. 2.1).

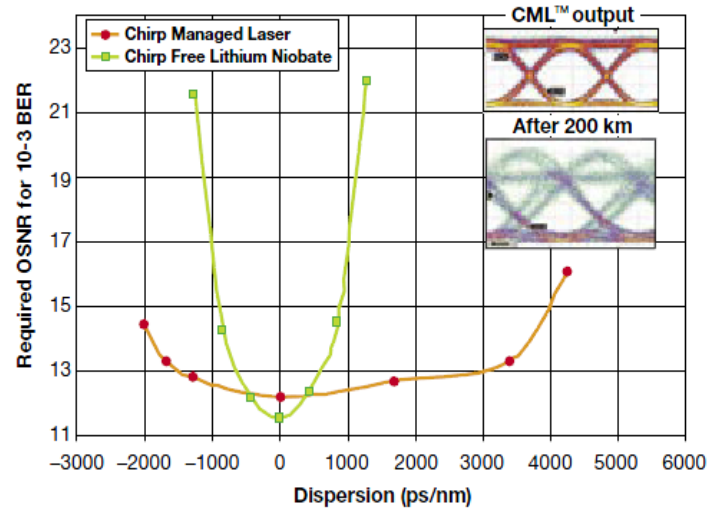


Fig. 2.2 Performance comparison between CMLs and external modulators [71].

In the duobinary application, the biggest advantage of CML based duobinary is the dispersion tolerance. Fig. 2.2 shows the required OSNR to reach the FEC threshold at 10.7 Gbits/sec for CML and LiNbO<sub>3</sub> MZM transmitters without dispersion compensation [71]. A CML can reach 250 km (4250 ps/nm) at an OSNR of 16.5 dB/0.1 nm. The performance of a CML is comparable to the best duobinary transmitters; it can also be used for reaches of 80-120 km and offers a higher optical power (4-7 dBm) and better dispersion tolerance than MZM based NRZ-OOK format.

### 2.1.2 Mach-Zehnder modulator

Mach-Zehnder modulator (MZM) is the most popular external electro-optic modulator for intensity or phase modulation. A typical structure of MZM is shown in

Fig. 2.3. Input light is split into two branches at position A in Fig. 2.3 and propagate through the LiNbO<sub>3</sub> waveguides and combined at position B in Fig. 2.3. The refractive index of the two LiNbO<sub>3</sub> waveguide branches will change with the applied voltages such that the phases of the light propagate through will be changed. At position B, the light in transmit through the two arms will interfere constructively. The intensity of the output signal is then controlled the by the applied electrical signal.

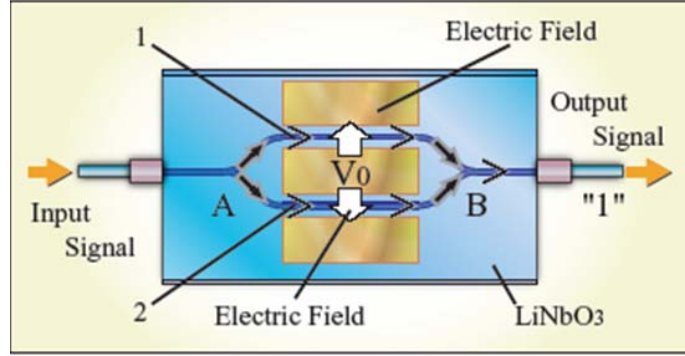


Fig. 2.3 Schematic of the Mach-Zehnder Modulator

### A. Principle of modulation

Assuming the voltages apply on two electrodes are  $V_1$  and  $V_2$ , the phase of the signal after propagate through the waveguides are

$$\phi_1 = \frac{\omega}{c} n_{eff} L + \frac{\omega}{2c} n_{eff}^3 \gamma_{33} \frac{V_1}{G} \Gamma L = \frac{2\pi n_{eff} L}{\lambda} + \pi \frac{V_1}{V_\pi} \quad (2.4)$$

$$\phi_2 = \frac{\omega}{c} n_{eff} L + \frac{\omega}{2c} n_{eff}^3 \gamma_{33} \frac{V_2}{G} \Gamma L = \frac{2\pi n_{eff} L}{\lambda} + \pi \frac{V_2}{V_\pi} \quad (2.5)$$

where  $G$  is the distance between electrodes,  $L$  is the length of electrodes,  $n_{eff}$  is the effective refractive index of the LiNbO<sub>3</sub> waveguide,  $\Gamma$  is the confinement factor which is defined as the ratio of the change in the effective index of refraction of the waveguide mode to the change in index of refraction of the electro-optic material,  $\omega$  is the radial frequency of light,  $c$  is the vacuum light speed,  $\gamma_{33}$  is the lightning

tensor,  $\lambda$  is the light wavelength,  $V_1$  and  $V_2$  are the voltages applied on two

electrodes, 
$$V_\pi = \frac{\lambda G}{n_{eff}^3 \gamma_{33} \Gamma L}$$

After combined at position B, the field of the output light is

$$\begin{aligned} E_{out} &= (0 \ 1) \begin{pmatrix} \sqrt{\rho_2} & j\sqrt{1-\rho_2} \\ j\sqrt{1-\rho_2} & \sqrt{\rho_2} \end{pmatrix} \begin{pmatrix} \exp(j\phi_1) & 0 \\ 0 & \exp(j\phi_2) \end{pmatrix} \begin{pmatrix} \sqrt{\rho_1} & j\sqrt{1-\rho_1} \\ j\sqrt{1-\rho_1} & \sqrt{\rho_1} \end{pmatrix} \begin{pmatrix} E_{in} \\ 0 \end{pmatrix} \\ &= jE_{in} (\sqrt{\rho_1(1-\rho_2)} \exp(j\phi_1) + \sqrt{\rho_2(1-\rho_1)} \exp(j\phi_2)) \end{aligned} \quad (2.6)$$

where  $\rho_2$  and  $\rho_1$  are the power splitting ratio of the two couplers at A and B,

respectively. Most MZM use 3-dB coupler, which means  $\rho_1 = \rho_2 = \frac{1}{2}$ . Therefore

$$\begin{aligned} E_{out} &= jE_{in} \exp(j\frac{\phi_1 + \phi_2}{2}) \cos(\frac{\phi_1 - \phi_2}{2}) \\ &= jE_{in} \exp(j\beta L) \exp(j\frac{\pi}{2} \frac{V_1 + V_2}{V_\pi}) \cos(\frac{\pi}{2} \frac{V_1 - V_2}{V_\pi}) \end{aligned} \quad (2.7)$$

where  $\beta$  is the propagation constant and  $\beta = \frac{2\pi n_{eff}}{\lambda}$ . To achieve chirp free

modulation, input voltages should fulfill the constrain  $V_1 = -V_2$ . The output power is

$$I_{out} = E_{out} E_{out}^* = I_{in} \cos^2(\frac{\phi_1 - \phi_2}{2}) = I_{in} \cos^2(\frac{\pi}{2} \frac{V_1 - V_2}{V_\pi}) \quad (2.8)$$

where  $I_{in} = |E_{in}|^2$ , the transmission curve of the MZM is squared cosine function and is shown in Fig. 2.4 (a).

## B. Generation of NRZ-OOK signal

As discussed in section 2.1, NRZ-OOK generated by directly modulating a DFB laser will suffer from large transient chirp and its CD tolerance is very small. Therefore,

external modulation with a MZM is normally preferred to reduce the residual chirp in the modulated signal.

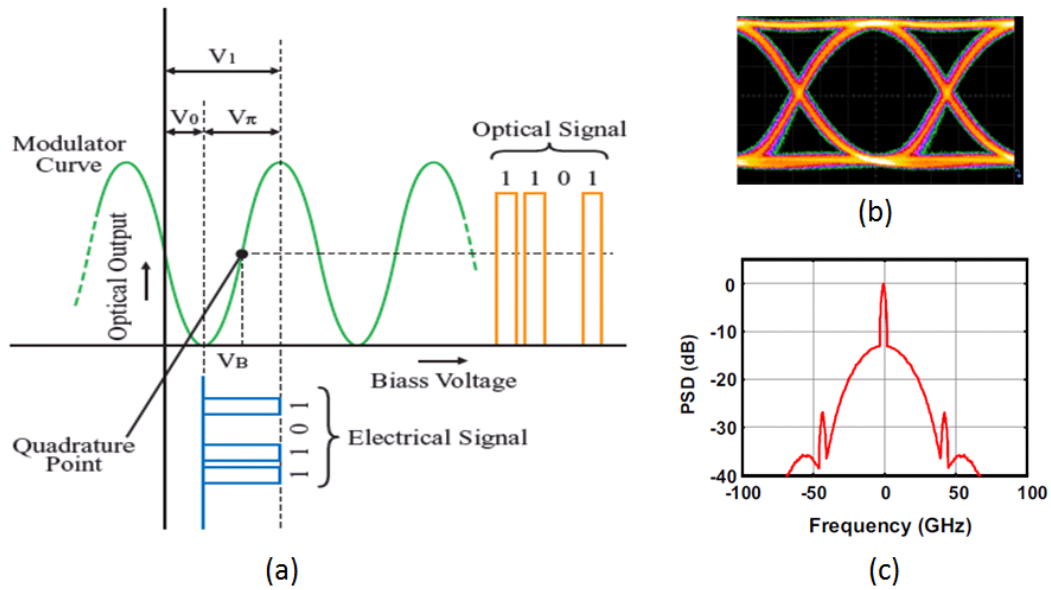


Fig. 2.4 (a) Operation of the MZM for NRZ-OOK modulation, (b) eye diagram, (c) optical spectrum

The operation of NRZ-OOK modulation with a MZM is depicted in Figure 2.4 (a). The MZM is biased in the quadrature point and is driven from minimum to maximum transmittance. The electrical drive signal requires a peak-to-peak amplitude of  $V_\pi$ . Note that due to the nonlinear transmission function of the MZM, overshoots and ripples on the electrical drive signal can be suppressed during modulation.

The eye diagram and optical spectrum of NRZ-OOK signal is shown in Figures 2.4 (b) and (c), respectively. It can be seen from the spectrum that NRZ-OOK has a strong component at the carrier frequency, which contains half of the optical power and is referred to as the carrier. The clock tones are spaced at multiples of the symbol rate, but are strongly reduced as compared with the carrier component. The bandwidth of the optical spectrum is approximately twice symbol rate.

### C. Generation of Duobinary signal

Duobinary have been introduced into Optical transmission experiments since mid-90's [72]. The main characteristic of duobinary modulation is a strong correlation between consecutive bits, which results in a more compact spectrum. It can either be generated as a 3-level amplitude signal ('0', '0.5', '1') or as a 3-level signal that combines phase and amplitude signaling ('-1', '0', '+1'), which is referred to as AM-PSK duobinary [73]. The use of AM-PSK duobinary generation is advantageous in optical communication as it has ideally the same or an even better OSNR requirement than OOK modulation [74]. At the same time the narrower optical spectrum and strong correlation between consecutive bits result in an increased dispersion tolerance [72].

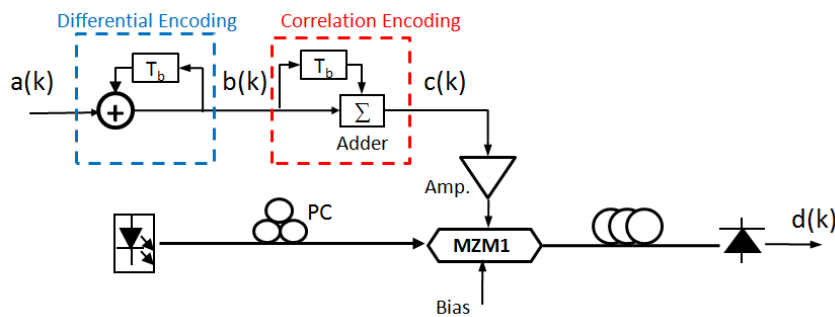


Fig. 2.5 Configuration of MZM for optical duobinary modulation

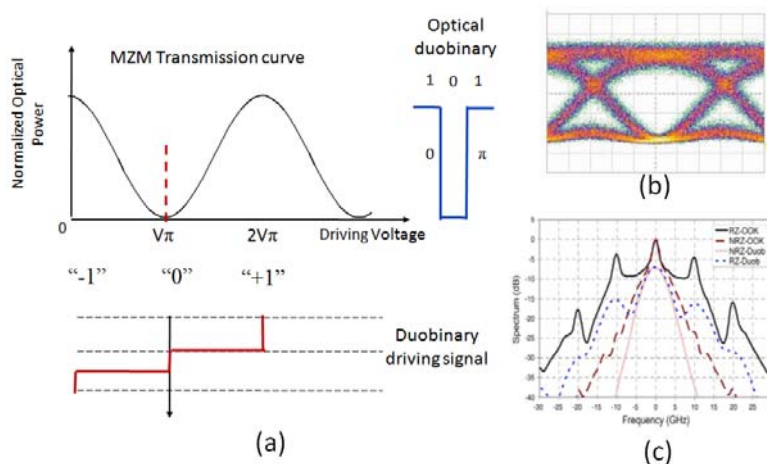


Fig. 2.6 (a) Operation of the MZM for AM-PSK duobinary modulation, (b) eye diagram (c) comparison of optical spectra for NRZ-OOK, RZ-OOK, NRZ-DB, RZ-DB

The configuration of MZM for optical duobinary modulation depicts in Figure 2.5. To generate proper driving signal for optical duobinary, precoder is needed. The duobinary precoder consists of a differential encoder and a correlation encoder (Fig. 2.5). They implement logic operation as follows:

$$\begin{aligned} b(k) &= a(k) \oplus b(k-1) \\ c(k) &= b(k) + b(k-1) \end{aligned} \quad (2.9)$$

The PD follows square-law detection achieves the mod2 detection

$$\begin{aligned} d(k) &= c(k) \bmod 2 = (b(k) + b(k-1)) \bmod 2 \\ &= (a(k) \oplus b(k-1) + b(k-1)) \bmod 2 \\ &= a(k) \oplus b(k-1) \oplus b(k-1) \\ &= a(k) \end{aligned} \quad (2.10)$$

Fig. 2.6 (a) illustrates the operation condition of the MZM for AM-PSK duobinary modulation. After precoding, the electrical duobinary driving signal has three levels “-1”, “0”, “+1”. The MZM is biased such that “0” is biased at transmission null while “-1” and “+1” are biased at transmission peak. The peak-to-peak voltage of the driving signal is  $2V_\pi$ , therefore the output optical signal for “-1” and “+1” have the same intensity but opposite sign ( $\pi$  phase difference). Fig. 2.6 (b) shows the eye diagram of the optical duobinary signal. Fig. 2.6 (c) shows the measured spectra at 10 Gb/s for RZ- and NRZ-duobinary and OOK for comparison [75]. As with the NRZ-duobinary, the RZ-duobinary shows a clear spectral compression compared to its OOK counterpart. This spectral compression results in better dispersion tolerance for duobinary compared to OOK [76].

## 2.2 Transmission Impairments

### 2.2.1 Noise

There are many sources of noise in optical communication systems. For example, light source have phase noise and intensity noise. Optical amplifier such as EDFA and SOA will add amplified spontaneous emission (ASE) noise to the signal. At the receiver side, shot noise and thermal noise are the two fundamental noises that limit the receiver sensitivity. In optical communication systems, different noises will be dominated in different communication systems. Without loss of generality, thermal noise will be the limitation in system without optical amplification (i.e. PON), and the optical noise results from ASE or SOA will be dominated in an optically amplified system. In the later scenario, optical signal to noise ratio (OSNR) is used to describe signal quality, or more specifically, how well a receiver can recover the information-carrying signal from its corrupted version. In this section, we describe the fundament of noises mentioned above.

#### A. Shot noise

Shot noise is a manifestation of the fact that photon arrivals are discrete and random in nature, which results in an electric current consists of a stream of electrons that are generated at random times. The probability of receiving photons in time interval obeys Poisson distribution. Assuming the average number of photons received in unit time interval  $\tau$  is  $\bar{n}$ , the mean number of photoelectron generated is  $\bar{m} = \eta\bar{n}$ , where  $\eta$  is the quantum efficiency. The mean and variance of photocurrent generated are  $i_p = \left(\frac{q}{\tau}\right)\bar{m}$  and  $\sigma_i^2 = \left(\frac{q}{\tau}\right)^2 \sigma_m^2$ . Since both n and m are Poisson distributed, the noise variance can then be obtained

$$\sigma_i^2 = 2q\bar{i}_p B \quad (2.11)$$



In the presence of dark current  $i_D$  of PN junction, the noise variance is modified

$$\sigma_i^2 = 2q(\bar{i}_p + i_D)B \quad (2.12)$$

### B. Thermal noise

At a certain temperature, electrons move randomly in any conductor. This random thermal motion of electrons in a resistor manifests as a fluctuating current even in the absence of an applied voltage. The load resistor in the front end of an optical receiver adds such fluctuations to the current generated by the photodiode. This additional noise component is referred to as thermal noise. Mathematically, thermal noise is modeled as a stationary Gaussian random process with a spectral density that is frequency independent up to 1 THz and is given by [57]:

$$\sigma_T^2 = \frac{4k_B T B}{R_{eq}} \quad (2.13)$$

where  $k_B$  is the Boltzmann constant ( $1.38 \times 10^{-23} \text{ J / K}$ ),  $T$  is the absolute temperature, and  $R_{eq}$  is the load resistor.

In the presence of FET preamplifier,

$$\sigma_T^2 = \frac{4k_B T F_t B}{R_{eq}} \quad (2.14)$$

where  $F_t$  is the amplifier noise figure.

### C. ASE noise

The spontaneous emission in EDFA is a random process and the emitted photons are in all directions. Some spontaneous emission is captured and amplified as it propagates along fiber. The ASE appears at the output of the EDFAs. Assume an optical amplifier with uniform gain  $G$  over an optical bandwidth  $B$ . The ASE spectral density in a single polarization is [57]

$$N_0 = n_{sp} h\nu(G-1) \quad (2.15)$$

where  $n_{sp}$  is the spontaneous emission noise factor and  $h\nu$  is the photon energy.

As the ASE noise can be modeled as additive white Gaussian noise and the ASE noise is typically unpolarized, the total ASE noise power in bandwidth B is given as:

$$P_{ASE} = 2n_{sp} h\nu(G-1)B \quad (2.16)$$

When ASE noise dominates in a transmission system, an important parameter used in evaluating signal quality is OSNR, which is define as:

$$OSNR = 10\lg \frac{P_i}{N_i} + 10\lg \frac{B_m}{B_r} \quad (2.17)$$

where  $P_i$  is the signal power in  $i_{th}$  channel,  $B_r$  is the resolution (0.1 nm in ITU standard),  $B_m$  is the equivalent noise bandwidth, and  $N_i$  is the noise power within the equivalent bandwidth.

### 2.2.2 Chromatic dispersion

When an electromagnetic wave interacts with the bound electrons of a dielectric, the medium response, in general, depends on the optical frequency  $\omega$ . As a result, different spectral components of the pulse travel at slightly different group velocities, which will limit the performance of the optical communication systems by broadening optical pulses. If we assume a Gaussian pulse with normalized amplitude  $U(z, \tau)$ , the effect of CD can actually be viewed as a linear filter in the frequency domain [77]:

$$U(z, \omega) = U(0, \omega) \exp\left(\frac{i}{2} \beta_2 \omega^2 z\right) \quad (2.18)$$

where  $\beta_2$  is the group velocity dispersion (GVD) parameter.

CD is usually characterized by the CD parameter  $D = -2\pi c\beta_2 / \lambda^2$ . The pulse broadening (assuming Gaussian pulse) from CD for a fiber length L is given by

$$\Delta T = DL\Delta\lambda \quad (2.19)$$

where  $\Delta\lambda$  represents the wavelength width. One of them is the use of lasers with a wavelength in the region around 1310 nm, where chromatic dispersion reaches a minimum. However, in long-haul and metro links, wavelength in the 1550 nm region, where the fiber attenuation is minimum and significantly lower than at 1310nm, are generally preferred. CD can also be compensated by the use of dispersion compensation fiber [78]. These are fibers where the slope of the delay versus wavelength curves has an opposite sign compared with normal fibers. Reels of appropriate lengths of dispersion compensating fiber (DCF) are placed at certain points in the link to compensate dispersion. Unfortunately, DCFs also cause significant attenuation, and their length has to be manually adjusted to achieve proper compensation, so link provisioning become expensive and time consuming. Although other optical techniques to compensate dispersion exist, in general, they suffer from the problems of being costly and requiring manual adjustment.

### **2.2.3 Fiber nonlinearity**

Fiber transmission channel will become nonlinear when the input signal's power exceeds a certain level, i.e. too high or too many carriers are injected into the same device at the same time. Non-linear effect in the fiber induces various types of crosstalk. There are two categories of fiber nonlinearities. The first one is due to the scattering between the input signal and the phonons in the silica medium. Stimulated Brillouin scattering (SBS) and stimulated Raman scattering (SRS) belong to this category [77]. These two effects would cause transfer of power from the original wavelength to another wavelength and would consequently cause power reduction and channel crosstalk. The second category is due to the fact that the refractive index of a fiber depends on the optical power. Four-wave mixing (FWM), self-phase

modulation (SPM) and cross-phase modulation (XPM) fall to this category. FWM would generate new frequency components, inducing crosstalk, while SPM and XPM would cause spectral broadening and therefore increase the chromatic dispersion penalties.

## **2.3 Impairment Mitigation Techniques**

### **2.3.1 In-line compensation techniques**

The most common in-line compensation technique is regeneration. It is well known that system transmission limits stem from a combined effect of amplifier noise accumulation, fiber dispersion, fiber nonlinearity, and inter/intrachannel interactions. There are two solutions for signal regeneration. The first is to segment the systems into independent trunks, with electronic transceivers in between, which is regarded as O-E-O regeneration. The second solution, all-optical regeneration, performs the same signal-restoring functions as the electronic approach, except doing the signal processing in optical domain, such that complexity of the regenerator can be reduced and processing capacity can be improved [79]. In regeneration, the three basic signal-processing functions are reamplifying, reshaping, and retiming.

A special kind of fiber, dispersion compensating fiber (DCF), has been developed for dispersion compensation along the transmission line in a periodic fashion. The use of DCF provides an all-optical technique that is capable of compensating the fiber GVD completely if the average optical power is kept low enough that the nonlinear effects are negligible. However, DCFs offers the advantages at expense of large attenuation, and their length has to be manually adjusted to achieve proper compensation, which makes the link compensation expensive and time consuming.

### 2.3.2 Post-compensation techniques

Electronic equalization was proposed to mitigate transmission distortion including CD and PMD for optical communication systems since early 1990s [80-81]. However, it only becomes reality with the recent development of high speed microelectronics, i.e. digital signal processors, analog-to-digital and digital to analog converters. 80 GSamples/s, 6-bit D/A has been innovated. In this section we briefly introduce the receiver-side electronic equalization techniques, which can be classified into following categories:

- *Feed-forward equalizer (FFE)*. In such filter, the signal is delayed by a tapped delay line. The delayed signal is then weighted by the tap coefficients and summed together [82]. The FFE is realized by tuning the tap coefficients. However, because a linear FFE enhances the noise, a pure FFE is less preferable.
- *Decision feedback equalizer (DFE)*. DFE is a nonlinear filter which eliminates post-cursors of distorted signals. It consists of a decision circuit and a feedback path. The feedback signal from the decision circuit is delayed by one bit period, weighted and subtracted from the original input signal. This technique does not introduce noise enhancement but has little capability to reduce the influence of precursors. A preferred method is to employ DFE to take into account the postcursors while using a FFE before the DFE to compensate the interference from the precursors.
- *Maximum likelihood sequence estimation (MLSE)*. MLSE is regarded as the most efficient electronic equalizer and has better performance than DFE and FFE [82]. In an MLSE receiver, the detected signal is firstly A/D converted. Then MLSE algorithms with pure digital signal processing are performed in digital signal processing (DSP). Details about FFE, DFE, and MSLE will be discussed in chapter 5.

# Chapter 3. Optical Multicast and Re-modulation Based on Inverse-RZ-duobinary Transmitter

## 3.1 Introduction

Inverse-return-to-zero (IRZ) format, which is formed by inverting the intensity level of a conventional return-to-zero (RZ) signal, has found many interesting applications in optical transmission systems and optical access networks, such as multi-bit per symbol transmission, optical multicast overlay, optical labeling switching, and wavelength reused PON, etc [83-93]. Its feature of carrying optical power in both “one” and “zero” bits allows superposition of different data streams, and thus enabling all the interesting applications.

The purpose of doing multi-bit per symbol transmission is to boost transmission data rate and increase the spectrum efficiency. Because the intensity of IRZ signal only changes in first (or second) half of every symbol and left the other half with constant power, phase information can be superimposed on the second half so that multi-bit can be transmitted in one symbol. By combining IRZ with DPSK or DQPSK are superimposed on the “light” half of IRZ signal to achieve 2-bit per symbol and 3-bit per symbol transmissions [83-85]. A later work further push the spectrum efficiency to 4-bit per symbol by employing a 4-level IRZ (say IRZ-QASK) and superimpose QPSK on the second half of every symbol [86], which can actually be viewed as a TDM transmission technique using QASK and QPSK. In addition to superimposing phase information, polarization property is also exploited to realize a self-homodyne transmission, which has been demonstrated in [87]. Other than increasing spectrum efficiency, the idea of superimposing other format on IRZ has also been found applications in optical label switching and optical multicast in WDM-PON. Different from multi-bit per symbol transmission, the data source of the

IRZ signal and the one for superimposing are different, with a purpose to achieve optical labeling [88-90] or multicast service delivery [55],[91]. The property of finite power in every bit offers a good solution to the light source for upstream re-modulation in a wavelength reused WDM-PON. IRZ signal can transmit information while facilitate upstream re-modulation. This can eliminate the process of erasing the downstream data from the received optical carrier and can maintain high extinction ratio of the downstream data. Meanwhile, the downstream IRZ signal does not require extra demodulation circuit, except a simple inverting post-amplifier after the photodiode, which makes it a cost-effective solution [92-93].

As we can see from the above discussion, IRZ format is useful in addressing the research problems in optical access network. However, IRZ signal offers the advantages at the expense of requiring broader transmitter and receiver bandwidth, which is double that of the NRZ-OOK signal. Optical bandwidth of the IRZ signals is also two times that of the NRZ signals. As a result, optical spectral efficiency and dispersion tolerance of the IRZ signals are degraded. These drawbacks limit its practical application desired access networks, especially under the trend to increase the reach of PON. On the other hand, it is well known that optical duobinary modulation format is effective in narrowing signal optical spectrum [76]. Hence, we propose bandwidth efficient IRZ-duobinary format to improve the optical spectral efficiency and dispersion tolerance of IRZ signals [94].

In this chapter, we first study our proposed IRZ-duobinary format in details, including several feasible approaches and the respective transmitter design to generating IRZ-duobinary signals. Then, their dispersion tolerances in optical transmission are also numerically characterized and compared. The application of IRZ-duobinary in optical multicast overlay and wavelength reused WDM-PON are discussed in section 3.3 and 3.4.

## 3.2 IRZ-duobinary transmitter

### 3.2.1 Generation of IRZ-duobinary format

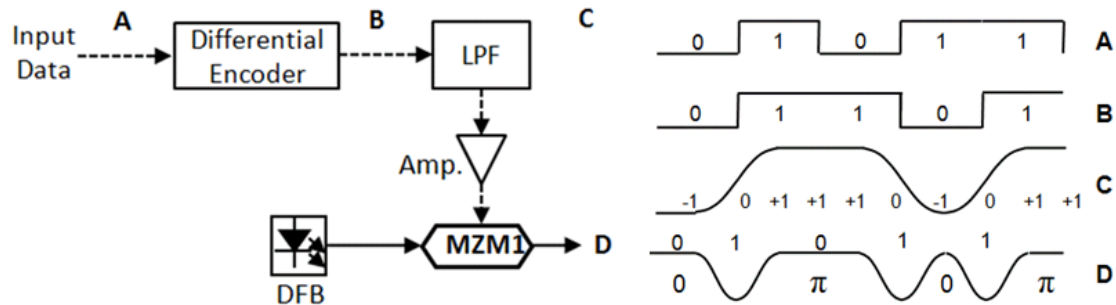


Fig. 3.1 An IRZ-duobinary transmitter

Fig.3.1 depicts the design of one of the feasible IRZ-duobinary transmitters. It consists of a differential encoder, a low pass filter (LPF), an electrical amplifier and a push-pull Mach-Zehnder modulator (MZM) [95]. The input NRZ signal is first differentially encoded before being passed through a LPF with 3-dB bandwidth of about half of the bit rate for correlation encoding. After the LPF, the input two-level electrical signal is transformed into a three-level driving signal, “+1”, “0,” and “-1”. The original data, the differentially encoded data and the correlation encoded waveform are illustrated as inset A, B and C in Fig.3.1, respectively. Then the three-level electric signal is amplified to a peak-to-peak voltage ( $V_{pp}$ ) of  $2V_{\pi}$ , so as to drive the MZM for optical signal generation. To generate optical IRZ-duobinary signal, the MZM should be controlled, such that level “0” is biased at the null transmission point while levels “+1” and “-1” are biased at the maximum transmission points. Under this driving condition, the “+1” and “-1” levels in the driving signal produce the same intensities but opposite phases in the generated optical signal. Hence, an optical IRZ-duobinary signal with duty cycle of  $\sim 50\%$  is obtained, as shown in Fig. 3.2. The inset spectrum diagram in Fig. 3.2 compares the optical spectra of the IRZ-duobinary signal and the conventional IRZ signal. It is shown that the IRZ-duobinary signal exhibits a more compact optical spectrum than the conventional IRZ case. At 10-Gbit/s, it is found that the 20-dB down bandwidth of



the IRZ-duobinary signal is about 16 GHz while that of the conventional IRZ signal is up to 23 GHz.

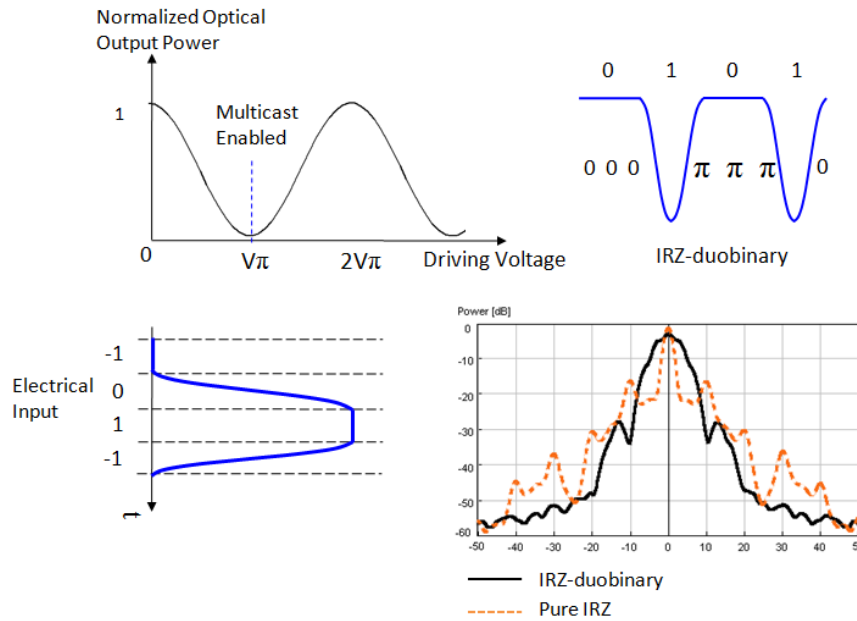
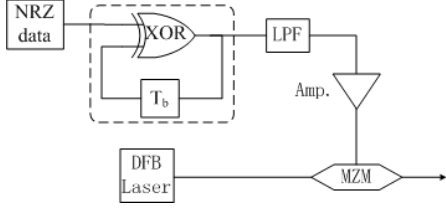
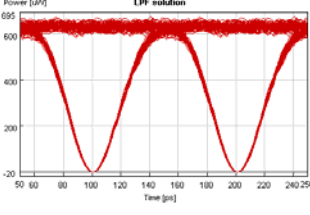
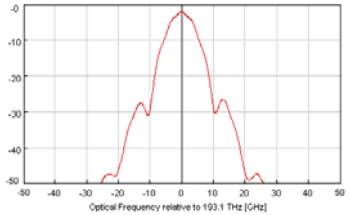
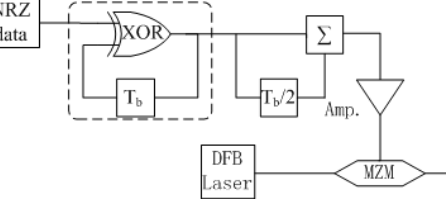
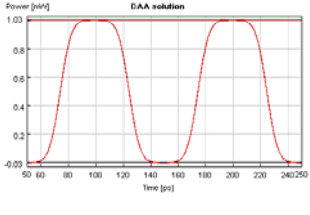
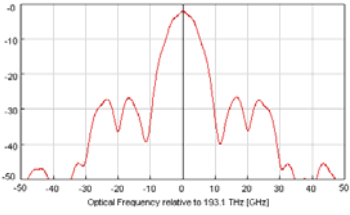
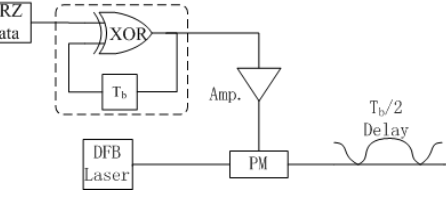
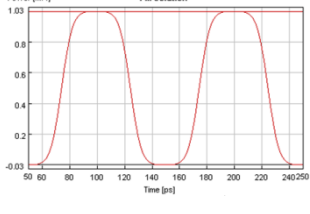
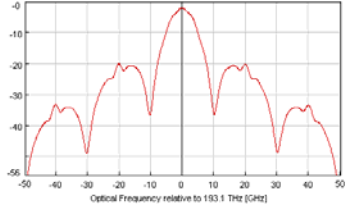
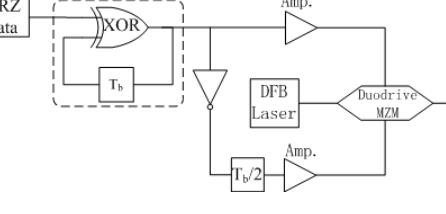
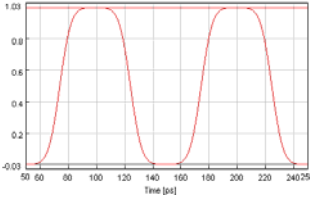
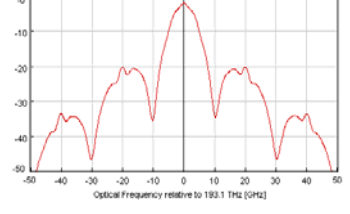


Fig. 3.2 Illustration of the principle of optical IRZ-duobinary modulation.

### 3.2.2 Comparison of different configurations of IRZ-duobinary generation

Optical IRZ-duobinary signals can be generated by several different transmitter configurations. In this section, we compare four different configurations for IRZ-duobinary modulation.

Table 3.1 Comparison of different configurations of IRZ-duobinary generation

Type	Configuration for IRZ-duobinary generation	Eye diagram	Optical spectrum
1			
2			
3			
4			

The first configuration (Type 1) is identical to the one discussed in section 3.2.1, as depicted in Fig. 3.1. Type 2 is similar to Type 1, except the correlation encoding is realized by adding half-bit period delayed data (ADD) to the present data in order to transform differential encoded signals into three-level signals. Type 3 employs an optical phase modulator (PM) followed by a half-bit delay interferometer. The PM is driven by a differentially pre-encoded electrical NRZ signal. Type 4 employs

dual-drive MZM, where one arm is driven by the input NRZ signal while the other is driven by the inverted signal with half-bit delay. A differential encoder is needed in each of all four configurations.

The eye diagrams in Table 1, obtained by numerical simulations at 10 Gb/s, show the back-to-back (BtB) eye diagrams (duty cycle 50%) of the four proposed transmitter configurations. The rise and the fall times of the NRZ signals are set to one quarter of the symbol duration. The rise and the fall times of the generated optical IRZ-duobinary signal in Type 1 is slower than that of the other three, as its driving signal has been shaped by the LPF. In practical applications, the shape of the LPF should be optimized to ensure optimum performance of the generated optical IRZ-duobinary signal. Since push-pull MZM is used in both Type 1 and Type 2, the generated optical IRZ-duobinary signal is not chirped, and its phase changes abruptly at “space” level. The main spectral lobe of the optical IRZ-duobinary signal generated by Type 1 is slightly wider than that by Type 2, but its spectral side lobes are more suppressed. The output signal of Type 3 and Type 4 are intrinsically the same. Their large side lobes are due to the chirp induced during the rise and the fall times.

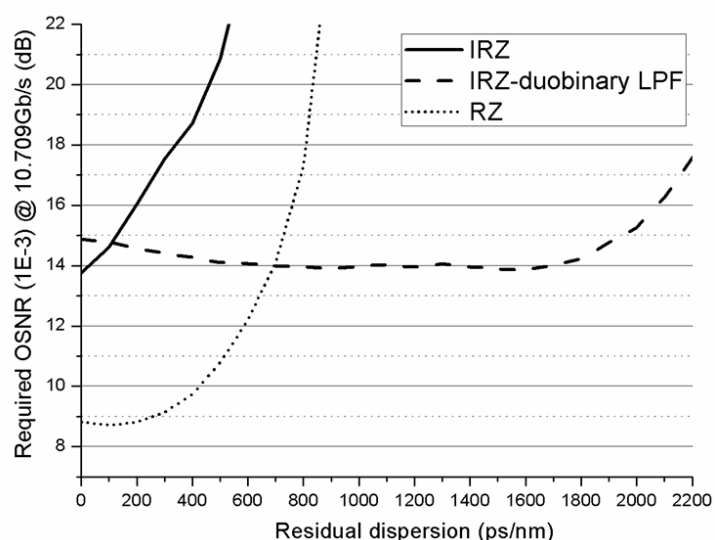


Fig. 3.3 Required OSNR for BER =  $10^{-3}$  versus residual dispersion at 10.709 Gb/s for different modulation formats of pure IRZ (solid line, simulation), RZ (dot line, simulation), and IRZ-duobinary (dash line, type 1 configuration, simulation).

We have also investigated and compared the dispersion tolerance in optical transmission among the IRZ-duobinary format (generated by Type 1 transmitter), conventional RZ format, and conventional IRZ format through Monte Carlo simulation. Fig. 3.3 depicts their respective required optical signal-to-noise ratio (OSNR) at  $\text{BER}=10^{-3}$ , for different residual dispersions. It is found that the conventional IRZ signal with direct detection quickly degrades in performance due to chromatic dispersion (CD) in fiber. RZ format follows a similar trend, albeit  $\sim 5$  dB better initial sensitivity, and slightly better tolerance to CD. IRZ-duobinary format, as expected, shows  $\sim 10 \times$  and  $\sim 4 \times$  tolerance to dispersion, as compared with conventional IRZ and RZ formats at 2-dB OSNR penalty, respectively.

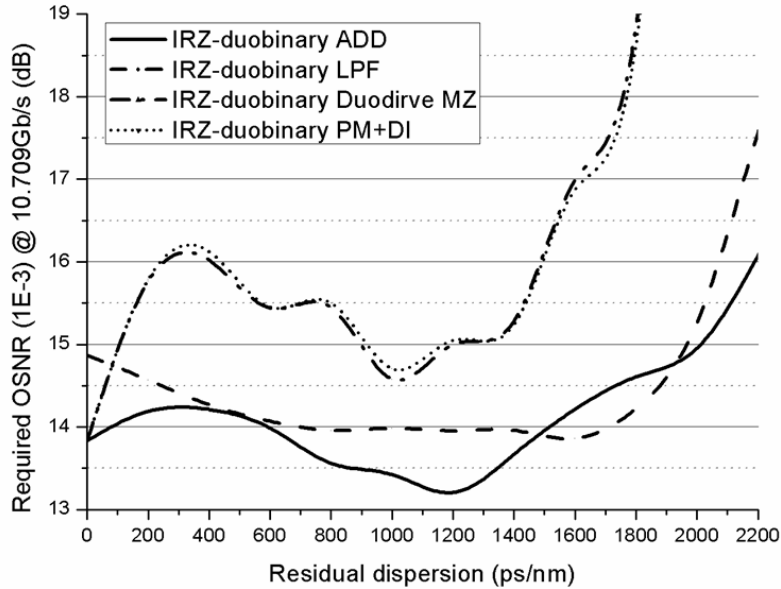


Fig. 3.4 Required OSNR for  $\text{BER} = 10^{-3}$  versus residual dispersion at 10.709 Gb/s for different types of IRZ-duobinary transmitters in table 3.1.

In Fig. 3.4, we have compared the CD tolerance for IRZ-duobinary signal generated by different transmitter configurations, as discussed in Table 1. Similar to the transmission performance of conventional duobinary signals [76], the optical IRZ-duobinary signals generated by Type 1 and Type 2 transmitters actually show small improvement in performance with some dispersion. At a dispersion value of 1200 ps/nm, Type 2 transmitter comes to -1.3-dB improvement for the required

OSNR, while Type 1 transmitter reaches -1.2-dB improvement at dispersion of 1600 ps/nm. Ideally, the optical signals generated by Type 3 and Type 4 transmitters are essentially identical. Thus, their performances show the same trend versus CD.

### **3.3 IRZ-duobinary format for optical multicast in WDM-PON**

#### **3.3.1 Optical multicast in WDM-PON**

One important application of IRZ-duobinary format is to realize flexible and cost-effective optical multicast. As discussed in the introduction of this chapter, optical multicast is needed in WDM-PONs in providing diverse multimedia and data services available for broadband access. And the most cost-effective way to upgrade the access network is to overlay such new kinds of services on the existing access network infrastructure. Therefore, various novel schemes have been proposed to support broadcast or multicast overlay on the WDM-PON architectures.

The reason of doing multicast in optical layer other than high layer is to ease the loading the electronic network processors or routers on the networking layer. Because the mass multicast data, which is usually video, would be limited by the processing bandwidth of electronic components as well as processing speed. Therefore, optical multicast realized by establishing one-to-many light paths on the optical layer is very attractive. An optical multicast design should be able to deal with two problems: 1. how to overlay the multicast traffic to the existing network infrastructure, which is carrying the two-way point-to-point traffic. 2. How to do the overlay control. In order to do so, several schemes have been proposed.

In [96], multicast was realized by means of subcarrier multiplexing. However, such a technique required high-speed electronic components at both transmitter and receiver sides. The allowable bit-rate for the PtP signal was also limited. In [54], [91], optical orthogonal modulation schemes offer large bandwidth for both PtP and

multicast data. However, at the ONU, a Mach-Zehnder delay interferometer (MZDI) was needed to demodulate the DPSK multicast signal. The use of MZDI significantly increased the complexity of the ONU and required stringent requirement for wavelength stability. The schemes in [55],[91] employed intensity modulation format to transmit the multicast and PtP data on one symbol, but the receiver sensitivity was intrinsically low, due to the small eye-opening and three-level detection. In general, a robust optical multicast scheme without MZDI and having relatively higher sensitivity at the ONU is highly desirable.

### **3.3.2 Proposed system architecture**

In this section, we demonstrated an optical multicast overlay on a WDM-PON employing 10-Gb/s IRZ-duobinary signal as the downstream format for both PtP and multicast data [97]. Multicast control is realized by adjusting the voltage bias of the PtP modulator at the OLT. The correlation encoding for generating the three-level electrical IRZ-duobinary driving signal can be generated by delay-and-add (ADD) circuit or be approximated by a LPF with a 3-dB bandwidth of about  $0.5R_b$  Hz, where  $R_b$  is the data bit rate. By adopting IRZ-duobinary, the system can simultaneously transmit 10-Gbit/s PtP signal and 10-Gbit/s multicast signal with 3-dB aggregate bandwidth of about 14 GHz. The dispersion tolerance is enhanced due to the improved spectral efficiency. At the ONU, a cost-effective photo-detector with two decision modules is proposed to receive the PtP and the multicast data.

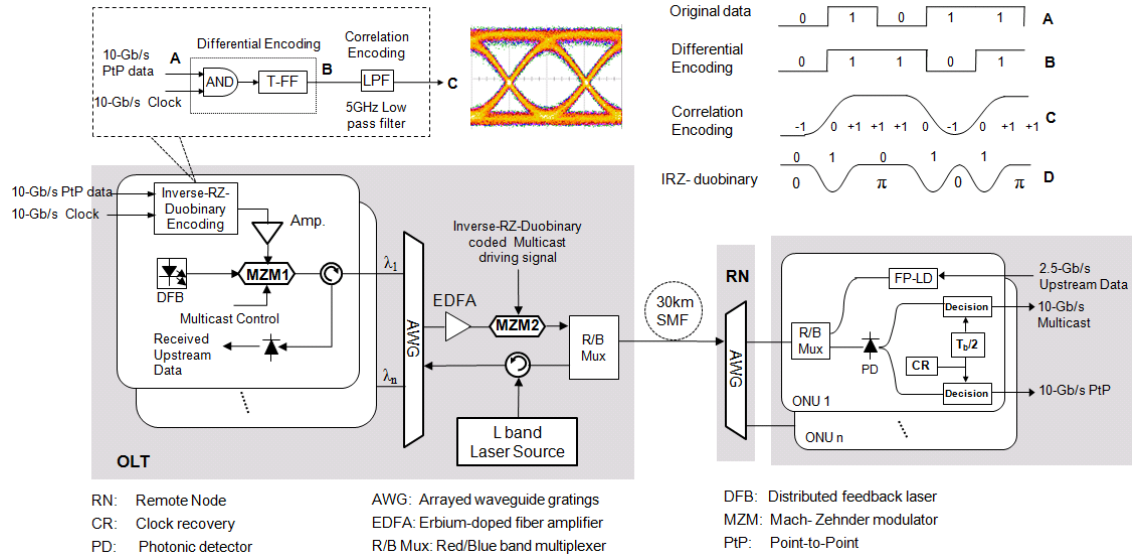


Fig. 3.5 Schematic diagram of the proposed WDM-PON with proposed optical multicast overlay.

Fig. 3.5 depicts the architecture of the WDM-PON. At the OLT side, C-band wavelengths from different downstream transmitters are first modulated with their respective IRZ-duobinary coded downstream PtP data. The top inset in Fig. 1 depicts the method of generating the IRZ-duobinary signal. The input NRZ data signal is first differentially encoded by an electrical logic AND-gate, followed by a toggle flip-flop circuit (T-FF). Then, correlation encoding is realized by a 5th-order LPF with 3-dB bandwidth of  $\sim 5$  GHz, in order to transform the differentially encoded signal into a three-level signal, with voltage levels “+1”, “0,” and “-1”. The input data, differentially encoded data, and correlation encoded waveforms are illustrated as insets A, B and C in Fig. 1, respectively. The generated three-level IRZ-duobinary driving signal is then amplified to  $V_{pp}=2V_{\pi}$  ( $\sim 10$  volts) and modulated onto the downstream carrier through an optical Mach-Zehnder modulator (MZM1) biased at  $V_{\pi}$ . All the downstream optical signals are multiplexed, via a cyclic arrayed waveguide grating (AWG), and are optically amplified before being fed into the common multicast transmitter (MZM2), where the multicast data, also encoded in IRZ-duobinary format, is optically superimposed onto all downstream carriers. Proper symbol synchronization is required, and could be achieved by employing fixed delay

line at the OLT. The composite signal is then multiplexed with the L-band CW carriers, dedicated for upstream transmissions at the ONUs, via a C-band/L-band multiplexer, before being delivered over a piece of 30-km SSMF feeder to the RN. At each ONU, the received downstream carrier is detected before being split and fed into two different paths for the recovery of the PtP and the multicast data, respectively. Each ONU requires only one photo-detector and all the modules can be potentially integrated, which saves the cost of the ONU. On the other hand, the received L-band carrier is used to injection-lock the Fabry-Pérot (FP) laser diode, which is directly modulated with 2.5-Gb/s upstream data, simultaneously. Thus L-band carrier-distributed upstream transmission is realized and the upstream signal is sent back to the OLT, via the RN and the fiber feeder.

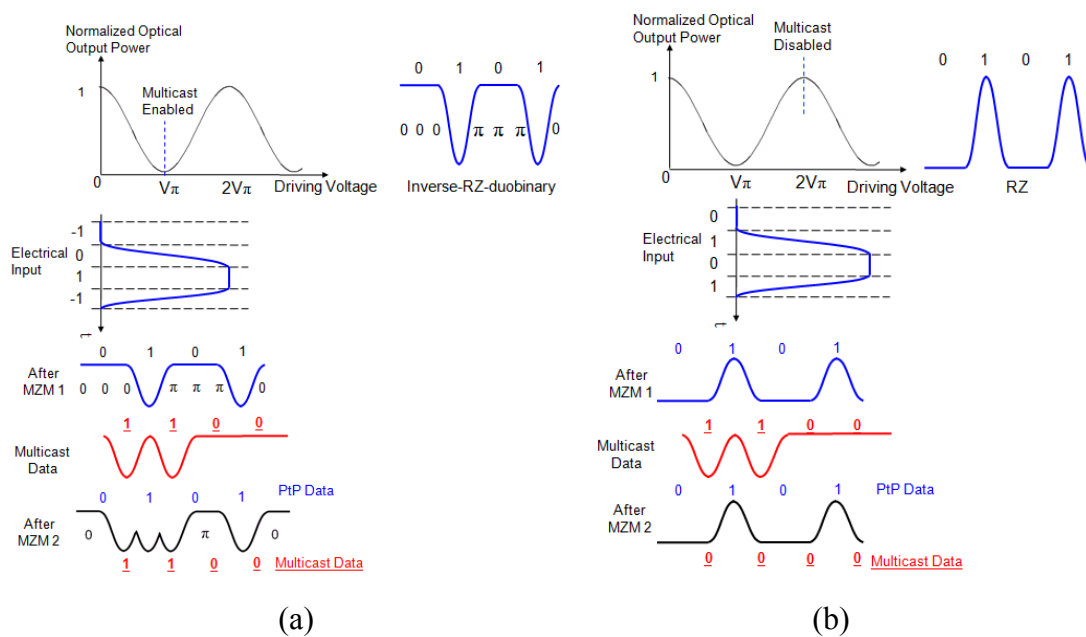


Fig. 3.6 Signal at the output of MZM1 when multicast is enabled/disabled. (a) & (b): Principles of (a) enabling, and (b) disabling the multicast data transmission

The control of the multicast transmission is performed at the OLT. When multicast is enabled on a particular downstream transmitter, the respective MZM1 is biased to a guarantee level “0” at the null transmission point and levels “+1” and “-1” at the maximum transmission points. Under this driving condition, the “+1” and “-1” levels will be transformed into the same optical intensities but opposite phases in the



output optical signal. As a result, an optical IRZ-duobinary signal with duty cycle of  $\sim 50\%$  is obtained (as shown in Fig. 3.6 (a)). Since the PtP information is only carried on the first half of each bit and there is always optical power at the second half of each bit, the multicast data can be successfully superimposed onto the second half of the PtP bits, via MZM2, as illustrated in Fig. 3.6(a). As the multicast data also introduces  $\pi$ -phase shift at bit “1”, the signal remains duobinary after the optical multicast overlay. To disable the multicast signal for a certain subscriber, the voltage bias (level “0” of the multicast data) of the respective MZM1 has to be shifted to the transmission maximum point. Thus, the levels “+1” and “-1” of the multicast data are at the null transmission points of MZM1. The output of PtP modulator becomes an RZ-like signal. In this case, the second half of each bit is always null. Therefore multicast signal cannot be superimposed onto the PtP signal, as depicted in Fig. 3.6(b). The stabilization of the voltage bias of the optical modulators can be realized, via optical power feedback control. The data logic of the two signal streams can be easily rectified by simple digital processing. The simulated signal spectra after MZM 1 & 2, under multicast-enabled and disabled modes are also illustrated in Fig. 3.7 (a) and (b), respectively, assuming 10-Gb/s PtP and multicast data. The respective measured eye diagrams are also shown in their insets.

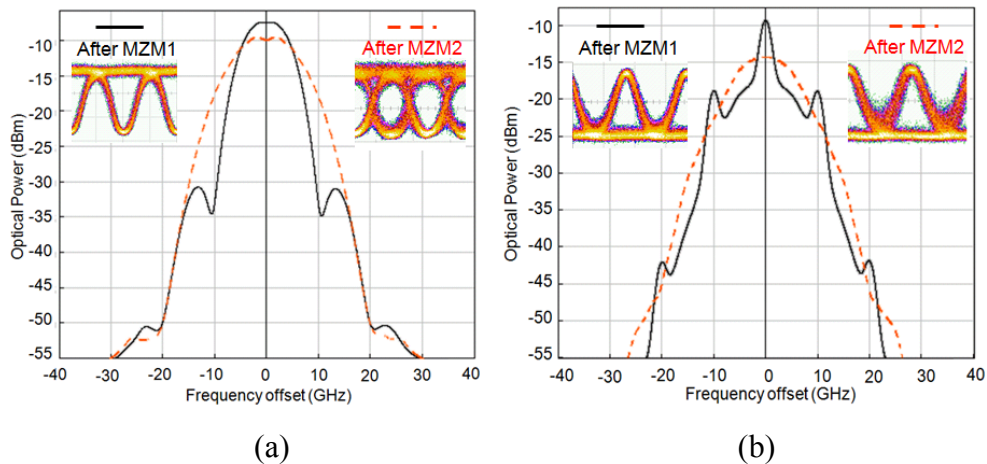


Fig. 3.7 Simulated signal spectra and experimental eye diagrams at the output of MZM1 and MZM 2 under (a) multicast-enabled case, and (b) multicast-disabled case.

At the receiver, the PtP data can be recovered by sampling the first half-bit of detected signal, while the multicast data can be restored by sampling the second half. After the clock recover, rising edge triggering and falling edge triggering can be used to recover PtP and multicast data, respectively. The link loss between the OLT and the corresponding receiver in an ONU is 12 dB, which consists of 3.6 dB for AWG at remote node (RN), 6 dB for the 30-km SMF, and 2.6 dB for the insertion losses of connectors and C/L multiplexer

### **3.3.3 Experimental demonstration of the proposed optical multicast system**

The feasibility of the proposed system has been experimentally verified on one particular channel for proof-of-concept demonstration. At the OLT, a continuous wave (CW) light from a DFB laser at 1550.13 nm was modulated by the 10-Gb/s IRZ-duobinary driving signal, which was generated from a 10-Gb/s NRZ pseudorandom binary sequence (PRBS) with a word length of  $2^{20}-1$ , via a MZM with a  $V_\pi$  of 5.3 volts. After superimposing the multicast signal, it was amplified by an EDFA with 15-dB gain before being multiplexed by an L-band seed wavelength for upstream modulation. The launched optical power into the fiber feeder was -0.7 dBm. At the ONU, a C/L band demultiplexer first separated the downstream wavelength and the upstream seed wavelength. The received 20-Gb/s downstream signal was detected by a 40-GHz photo-diode (PD) followed by a LPF with a 3-dB bandwidth of 16.7 GHz. The 10-GHz clock extracted by clock recovery module was used to recover the transmitted signal. The received upstream seed wavelength was also modulated by the upstream data before being delivered back to the OLT.

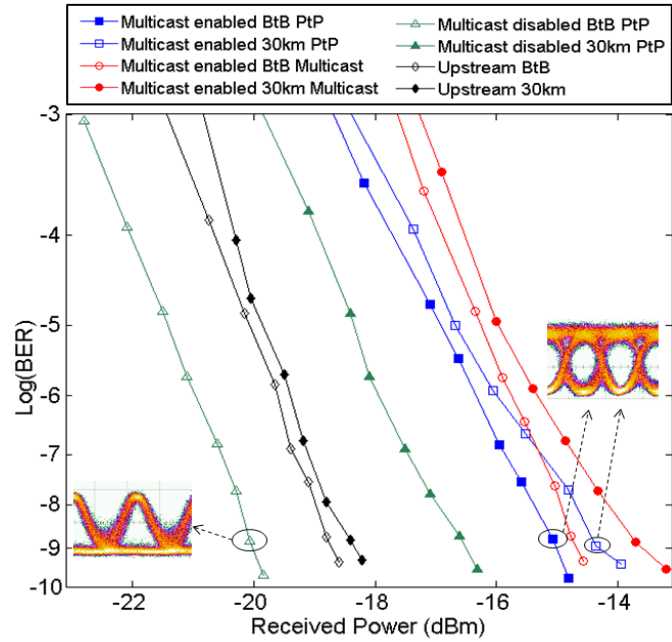


Fig. 3.8 BER measurements of upstream, downstream PtP and multicast signals when multicast is enabled or disabled.

The measured bit-error-rate (BER) results of PtP, multicast and upstream signals are shown in Fig. 3.8. When multicast was enabled, the receiver sensitivities (at BER of  $10^{-9}$ ) for PtP data and multicast data were -14.38 dBm and -13.66 dBm, having 0.76-dB and 1.05-dB power penalties after 30-km transmission, respectively. When multicast was disabled, the back-to-back (BtB) sensitivity at BER of  $10^{-9}$  for PtP data was -20.07 dBm with about 3.41-dB power penalty, after transmission. Besides, low-penalty upstream transmission was also achieved. The BtB of the upstream signal was -18.70 dBm, having 0.28-dB penalty, after transmission.

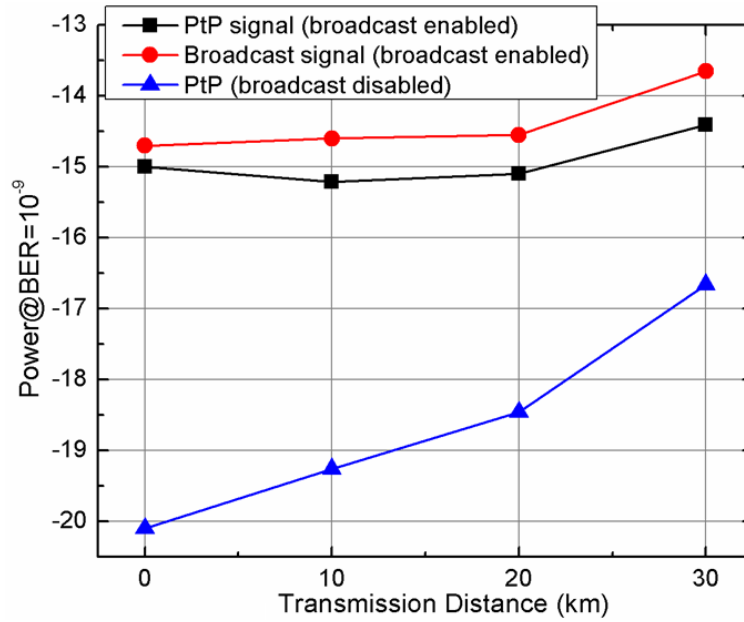


Fig. 3.9 Receiver sensitivities (at BER=10<sup>-9</sup>) of the downstream signals versus the transmission distance.

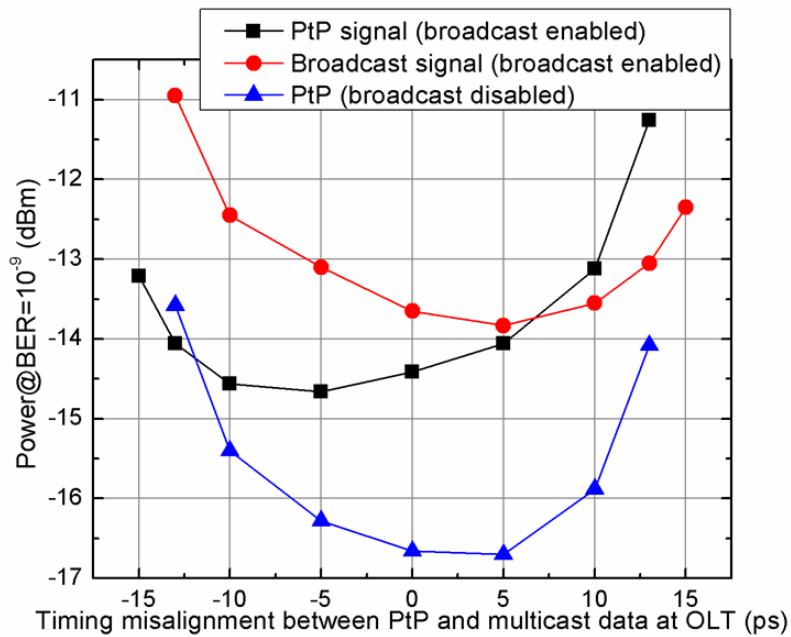


Fig. 3.10 Receiver sensitivities (at BER=10<sup>-9</sup>) of the downstream signals, after 30-km transmission, under different timing misalignment values.

Fig. 3.9 shows the measured receiver sensitivities (at BER of 10<sup>-9</sup>) and the respective transmission distance of the downstream signals. Although the BtB performance of the multicast-disabled PtP signal was much better than that of the

multicast-enabled PtP signal and the multicast signal, it degraded much faster as the transmission distance increased, as it became RZ-like format. In the proposed scheme, synchronization between the PtP and the multicast data are necessary. Fig. 3.10 shows their receiver sensitivities (at BER of  $10^{-9}$ ) after 30-km transmission, under various timing misalignment values. The 1-dB tolerance of timing misalignment for the multicast-disabled PtP signal was around 18 ps (-8 ps to +10 ps), while that for multicast-enabled cases was around 15 ps (-7.5 ps to + 7.5 ps).

In conclusion of this section, we have proposed and experimentally demonstrated an optical multicast overlay scheme for WDM-PONs, using bandwidth-efficient IRZ-duobinary signals. Optical multicast control can be easily achieved by tuning bias of the downstream PtP modulator. Satisfactory transmission performances of the PtP and multicast signals have been achieved, with sufficient system power budget. The system performances have been further characterized.

### **3.4 IRZ-duobinary for long-reach PON**

Colorless ONU and long-reach are two desired properties of optical access networks. To realize colorless ONU, one practical and cost-effective approach is to employ centralized light sources (CLS) at the OLT and directly re-use the downstream light as the upstream carrier at the ONUs. Since long-reach optical access networks can help save further cost, long-reach CLS WDM-PON has aroused much attention. In realization of CLS WDM-PON, IRZ, Manchester, and DPSK formats are among the feasible options for the downstream signal format, since they carry power in both “1” and “0” bits [92-93, 99-101]. However, they may not be suitable for 10-Gb/s long-reach PON because of their limited uncompensated transmission span.

In this section, we propose an 80-km-Reach WDM-PON utilizing IRZ-duobinary downstream signal and on-off-keying (OOK) upstream signal was demonstrated. Compared with IRZ and Manchester formats, IRZ-duobinary signal format has larger dispersion tolerance and it can be directly reused and re-modulated with the upstream

data at the ONU, without any synchronization. Compared with DPSK format, it does not require MZDI to do the demodulation and thereby saving the cost at ONU. In our studies, two kinds of IRZ-duobinary transmitters are employed as downstream transmitter. In the first study, type 3 IRZ-duobinary transmitter in section 3.2.2 is employed. An 80-km-reach WDM PON with 10-Gb/s downstream and 2.5-Gb/s upstream re-modulated signals is demonstrated [101]. In the second study, a CML based IRZ-duobinary transmitter is proposed as downstream transmitter, which does not require pre-coder as other transmitters. The system cost can be further brought down.

### 3.4.1 Long-reach PON using DI based IRZ-duobinary transmitter

In this work, we propose to generate the IRZ-duobinary downstream signal using an optical phase modulator (PM) followed by a half-bit DI at the OLT. This method does not require correlation encoder, as well as high power electrical amplifier to obtain  $2V_\pi$  driving voltage, as required in [101]. Therefore it is more cost-effective and practical.

#### A. System architecture

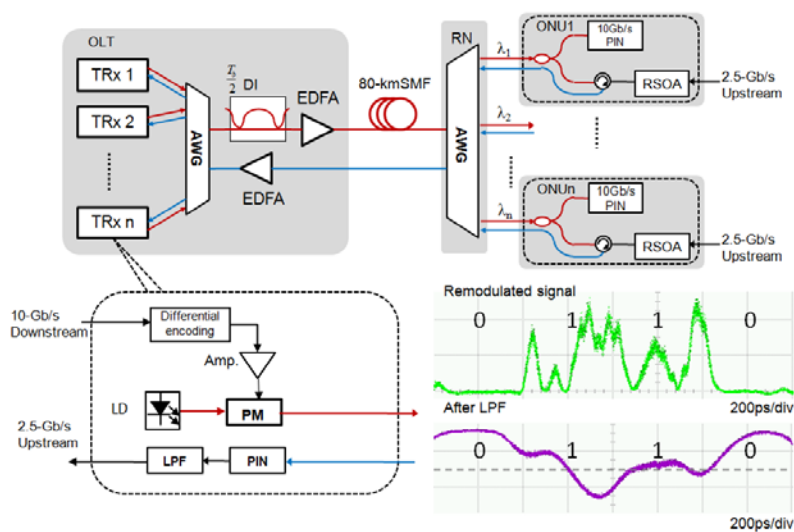


Fig. 3.11 Architecture of the proposed system.

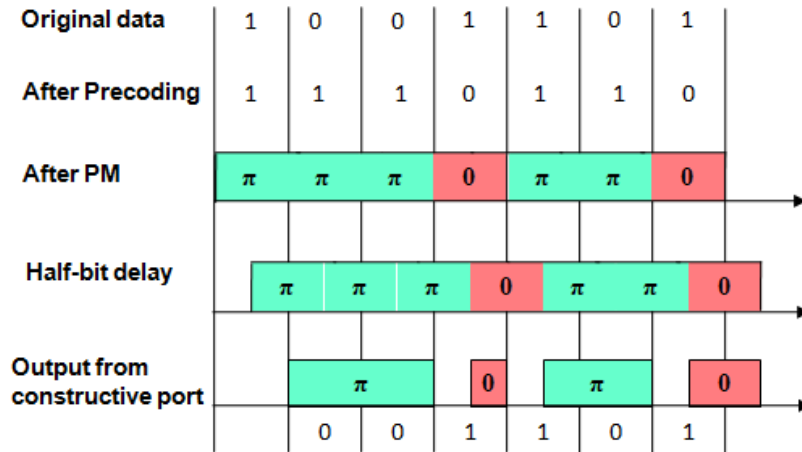


Fig. 3.12 Principle of generating IRZ-duobinary signal with PM and MZDI.

Fig. 3.11 illustrates the CLS WDM-PON architecture utilizing IRZ-duobinary as the downstream signal format. Each transceiver at the OLT generates its downstream IRZ-duobinary signal and receives its upstream re-modulated signals from its respective subscriber. At the OLT, differentially pre-coded downstream data is modulated onto a designated wavelength channel through an optical phase modulator. All downstream modulated wavelengths are multiplexed, via an AWG, before being fed into a common half-bit DI, where the DPSK signals on all wavelengths are converted into IRZ-duobinary signals at the DI's constructive port. Fig. 3.12 illustrates the operation principle of this format conversion from DPSK to IRZ-duobinary. In practical application, all laser frequencies should be precisely aligned to the spectral response of the DI to realize such format conversion. By proper setting of the time delay between the two arms in the DI, the duty cycle of the generated RZ signals is set to about 50%. All downstream wavelengths are then delivered to their destined ONUs, via a piece of 80-km feeder fiber and the individual distribution fibers.

At each ONU, a 3-dB optical coupler splits a portion of the received downstream signal power for detection, while the remaining power is fed into a RSOA for upstream data re-modulation. The finite optical power in each bit of the received downstream IRZ-duobinary signal provides the light source for the upstream

transmission. After re-modulation, the upstream NRZ-ASK signal was then transmitted back to the OLT, via another upstream fiber link. A pair of feeder fibers is used to avoid the possible Rayleigh backscattering induced performance degradation on both the downstream and the upstream signals. At the OLT, the upstream signal is recovered by an electrical LPF after detection. Fig. 3.11 insets show an example waveform of the received upstream signal and its corresponding electrical waveform after the LPF.

### ***B. Experimental demonstration***

The proposed system was experimentally demonstrated on one particular channel for proof-of-concept demonstration. A CW light from a DFB laser at 1550.13 nm was modulated by a 10-Gb/s PRBS downstream data with a length of  $2^{31}-1$ . The output IRZ-duobinary downstream signal was amplified by an EDFA to 6 dBm. After 80-km transmission, a portion of light is fed into the RSOA and re-modulated by 2.5-Gb/s  $2^{31}-1$  PRBS upstream data. The modulation condition of RSOA is set to maximize the ER of the modulated upstream signal. The upstream signal was then sent back to OLT, via another piece of 80-km fiber. At the OLT, an electrical LPF with 3-dB bandwidth of 1.87 GHz was used to recover the upstream data.

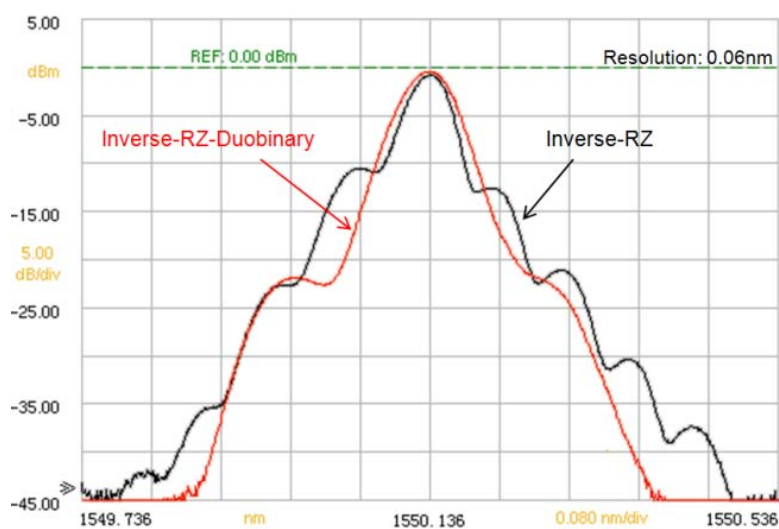


Fig. 3.13 Optical spectra of conventional IRZ and IRZ-duobinary signals.



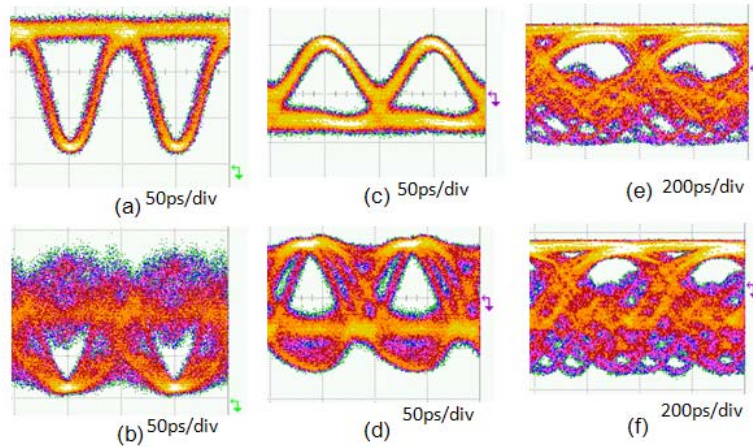


Fig. 3.14 Eye diagrams of (a) optical BtB IRZ-duobinary, (b) optical IRZ-duobinary after 80-km transmission, (c) electrical BtB IRZ-duobinary, (d) electrical IRZ-duobinary after 80-km transmission, (e) electrical BtB remodulated signal, (f) electrical remodulated signal at OLT.

Fig. 3.13 shows the optical spectrum of the IRZ-duobinary signal generated at the OLT. It has exhibited relatively more compact spectrum, as compared to that of a conventional IRZ signal. Thus it has better tolerance against fiber chromatic dispersion. Figs. 3.14 (a) and (b) show the eye diagrams of the generated IRZ-duobinary signal, obtained at the constructive output port of the DI, and that after 80-km transmission, respectively. Their corresponding electrical eye diagrams detected by 10-Gb/s receiver followed by an inverting pre-amplifier are shown in Figs. 3.14 (c) and (d), respectively. Figs. 3.14 (e) and (f) show the BtB eye diagram for the upstream signal before and after a 1.87-GHz electrical LPF, respectively. Fig. 3.15 shows the measured BER performance. Error-free transmissions were achieved for both the downstream and the upstream signals, after 80.4-km SSMF transmission. The BtB sensitivity (at BER of  $10^{-9}$ ) for the 10-Gb/s downstream IRZ-duobinary signal and the 2.5-Gb/s upstream re-modulated ASK signal were measured to be -16.27 dBm and -20.45 dBm, respectively. After 80.4-km transmission, their respective power penalties were measured to be 1.26 dB and 2.95 dB, respectively.

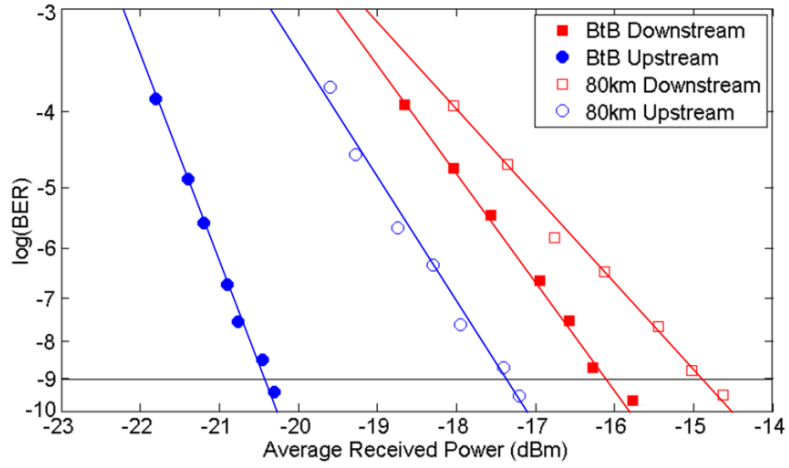


Fig. 3.15 BER measurements of the 10-Gb/s downstream and the 2.5-Gb/s upstream signals.

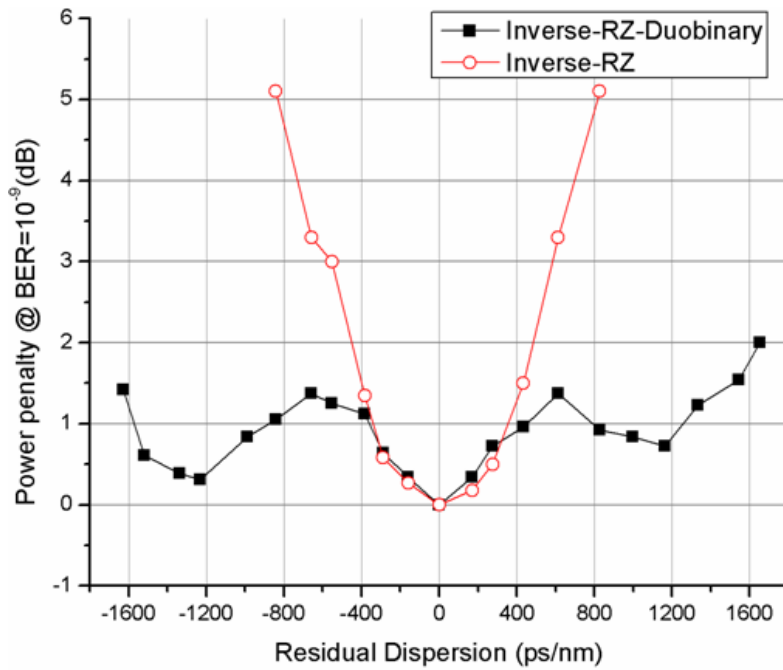


Fig. 3.16 Measured dispersion tolerance for Inverse-RZ-Duobinary and conventional Inverse-RZ signal.

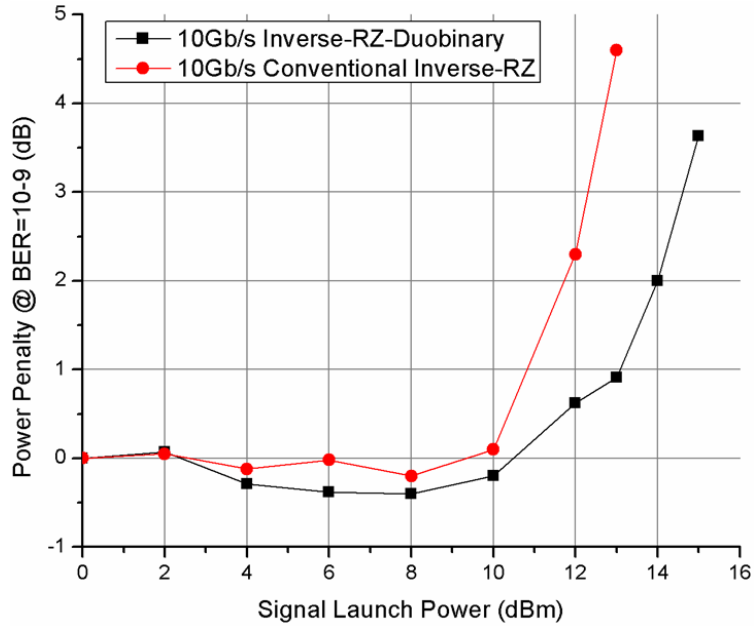


Fig. 3.17 Measured nonlinear tolerance for Inverse-RZ-Duobinary and conventional Inverse-RZ signal.

We have also investigated and compared the dispersion tolerance between the IRZ-duobinary format and the conventional IRZ format. Fig. 3.16 depicts their respective power penalties (at BER=10<sup>-9</sup>) measured at different residual dispersions. It was found that the 10-Gb/s IRZ-duobinary signal exhibited dispersion tolerance from -1634 ps/nm to +1626 ps/nm, at 2-dB power penalty. However, under the same condition, the conventional IRZ signal only exhibited dispersion tolerance from -460 ps/km to +500 ps/nm. The measurements showed that dispersion tolerance of the IRZ-duobinary format was more than three times superior to that of the conventional IRZ signal.

As the power budget is another important issue in long-reach WDM-PON, we have further investigated the nonlinear tolerance of the IRZ-duobinary signal. The IRZ-duobinary signal at different optical powers was launched into a piece of 80-km SSMF so as to evaluate the nonlinear tolerance. The chromatic dispersion of the SSMF was compensated with dispersion compensate module (DCM). The receiver sensitivities (at BER of 10<sup>-9</sup>) of both 10-Gb/s IRZ-duobinary signal and 10-Gb/s

conventional IRZ signal, at different launched power levels were measured and their induced power penalties were shown in Fig. 3.17. The results also proved that the IRZ-duobinary format has much better nonlinear tolerance and it exhibited 1-dB penalty at 13- dBm launched power.

### **3.4.2 Long-reach PON using CML based IRZ-duobinary transmitter**

In previous section, we demonstrate an 80-km-Reach WDM-PON utilizing IRZ-duobinary downstream signal and OOk re-modulation upstream. However, The DI based IRZ-duobinary transmitter requires the laser wavelengths to be precisely aligned to the DI, which would increase the cost by adding extra wavelength monitoring and feedback controlling modules.

In this session, we propose to generate IRZ-duobinary signal by directly modulating a CML with electrical IRZ signal. Similar as previous work, upstream re-modulation is realized by RSOA-EAM. The CML-based downstream transmitter offers many advantages to cost-sensitive metro access applications such as compact, high emit power, and do not require costly and bulky external modulators [102]. Moreover, unlike the previous schemes that require differential encoder to generate IRZ-duobinary signal, only IRZ encoder is needed in the CML-based IRZ-duobinary transmitter. Therefore the cost can be further decreased. The experimental results show that the IRZ-duobinary signal generated by CML has large dispersion tolerance and can well support the re-modulation at ONU.

### A. System architecture

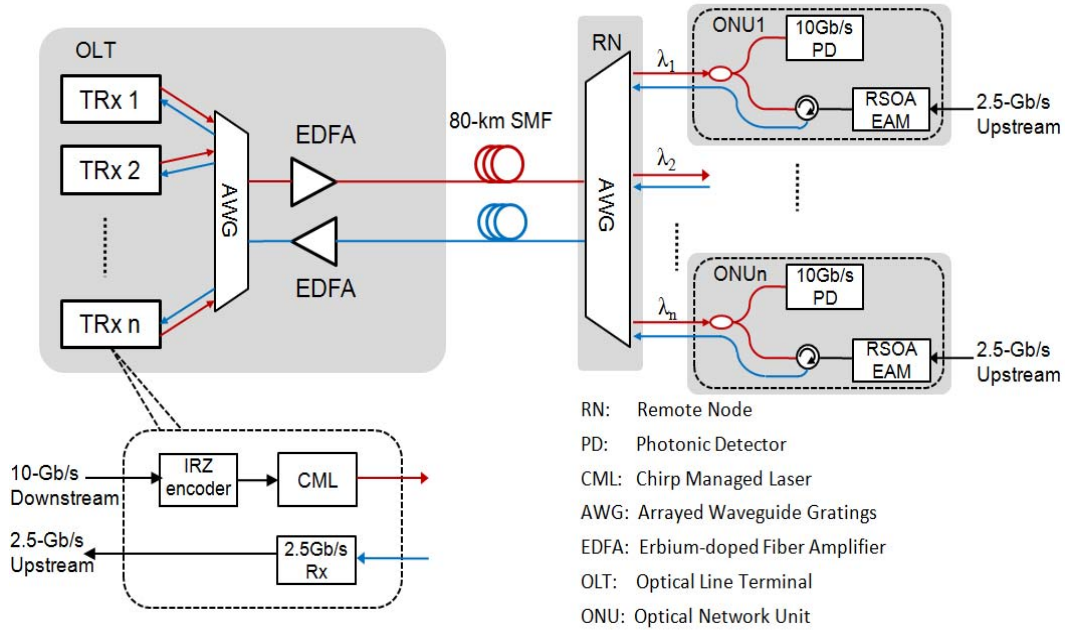


Fig. 3.18 Architecture of the proposed system

Fig. 3.18 illustrates the WDM-PON architecture utilizing IRZ-duobinary as the downstream signal format. Each transceiver at the OLT generates its downstream IRZ-duobinary signal and receives its upstream re-modulated signals from its respective subscriber. At the OLT, IRZ coded electrical downstream data is modulated onto a designated wavelength channel through a CML. By properly adjusting the central wavelength of the optical spectrum reshaper (OSR) integrated in the CML, IRZ-duobinary signal can be obtained. All downstream modulated wavelengths are multiplexed, via an AWG, before fed into an EDFA for boosting power. All downstream wavelengths are then delivered to their destined ONUs, via a piece of 80-km feeder fiber and the individual distribution fibers.

At each ONU, an optical coupler splits a portion of the received downstream signal power for detection, while the remaining power is fed into a RSOA-EAM for upstream data re-modulation. The finite optical power in each bit of the received downstream IRZ-duobinary signal provides the light source for the upstream

transmission. After re-modulation, the 2.5-Gb/s upstream NRZ-OOK signal is then transmitted back to the OLT, via another upstream fiber link. A pair of feeder fibers is used to avoid the possible rayleigh backscattering induced performance degradation on both the downstream and the upstream signals. At the OLT, the upstream signal is restored by an optical receiver with 2.5 GHz bandwidth.

### B. Generation of IRZ-duobinary signal using CML

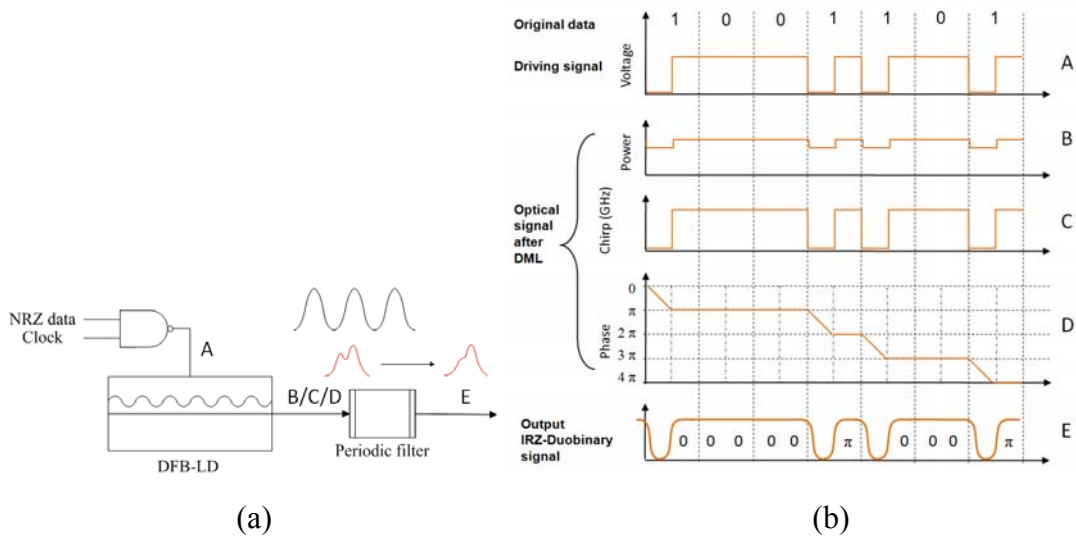


Fig. 3.19 (a) Schematic of CML. (b) Illustration of principle of operation of IRZ-duobinary modulator using CML.

Fig. 3.19 (a) shows the schematic of the CML-based IRZ-duobinary transmitter, which comprises an electrical NAND gate and a CML. The CML comprises a distributed feedback laser (DFB-LD) followed by an in-line OSR filter in a butterfly package. Fig. 3.19 (b) illustrates the principle of operation using time domain and frequency domain pictures, as well as a phasor representation. The NAND gate convert the input NRZ signal into IRZ signal that directly modulate the DFB-LD. As shown in Fig. 3.19 (b) A, the current swings down from high level to low level by  $\Delta I$  at the first half of bit “1” while remains high level at the second half of “1” and bit “0”. The drive amplitude is adjusted to generate blue adiabatic chirp of  $\Delta f = 1/T$ . The DFB-LD is biased around 5 times above its threshold to minimize transient chirp

while increase the adiabatic chirp. The adiabatic chirp makes the high intensity level blue shifted relative to the low intensity level by  $\Delta\phi = 2\pi \int_0^{T/2} \Delta f(t) dt$ . When the duty cycle of bit “1” is 50%, the frequency shift results in phase shift of  $\Delta\phi = 2\pi \times T/2 \times 1/T = \pi$  for the low level in bit “1”. However, the extinction ratio (ER) of the output signal is low due to the high bias. The intensity, chirp and phase of the optical signal generated by the DML are shown as **B**, **C**, and **D** in Fig. 3.19 (b). As shown in the inset of Fig. 3.19 (a), the laser wavelength is aligned on the transmission edge of the OSR filter, so as to pass the blue shifted high intensity level and attenuate the red low intensity level. The intensity modulated signal accompanied with frequency modulation is then converted to a two level IRZ signal by the OSR filter (As shown in Fig. 3.19(b) **E**), resulting in relatively high ER IRZ-duobinary signal. Besides, The OSR edge also converts the adiabatic chirp to flat-top chirp with abrupt phase transitions at the lower level.

### C. Experimental demonstration

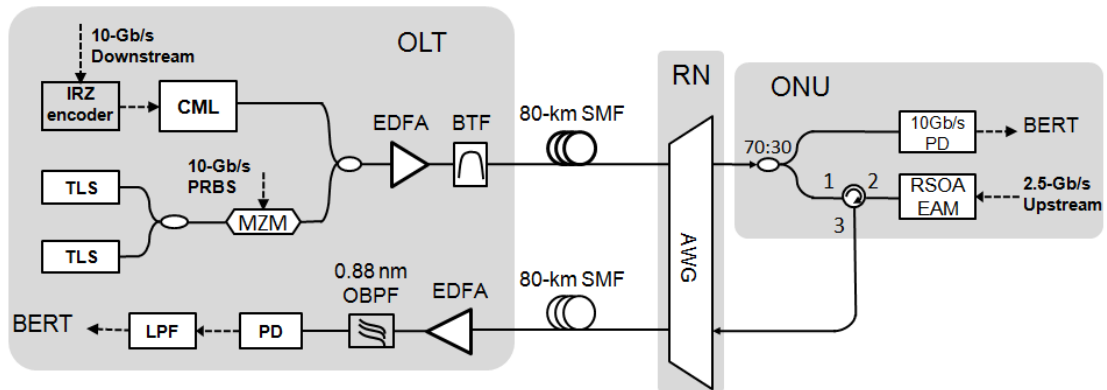


Fig. 3.20 Experimental setup.

The feasibility of the proposed system is experimentally assessed on one particular channel for proof-of-concept demonstration. We also study the BER performance of the nonlinear cross talk induced by two co-propagating 10Gb/s NRZ-OOK channels. As illustrated in Fig. 3.20, a standard CML module (Finisar DM80-01) is used for experimental setup. The DFB-LD at 1555.63nm is biased at 80

mA and modulated by electrical IRZ signal with PRBS with a word length of  $2^{31}-1$ . The  $V_{pp}$  of the driving signal is 2.23 Volt. The neighboring signals are generated using two tunable laser sources (TLSs) followed by a Mach-Zehnder Modulator, which is driven by 10Gb/s PRBS  $2^{31}-1$  data. The power per channel is adjust to be equal. Then the EDFA amplifies the power of each channel to 6 dBm and the out-of-band noise is suppressed by the following bandwidth tunable flat top filter (BTF). The spectrum of the signal launched into the fiber is shown in Fig. 3.21 (a). At the remote node, an AWG (45 GHz at 3-dB bandwidth) demultiplex the IRZ-duobinary signal into ONU. At the ONU, a 70:30 coupler is used to ensure enough power budget for downstream receiver. 70% power of the incoming signal is split to the downstream receiver while the rest is amplified and remodulated by a RSOA-EAM. The upstream signal is then sent back to OLT, via another piece of 80-km fiber, and recovered by an optical PD followed by an 5<sup>th</sup> order electrical LPF with 3-dB bandwidth of 1.87 GHz.

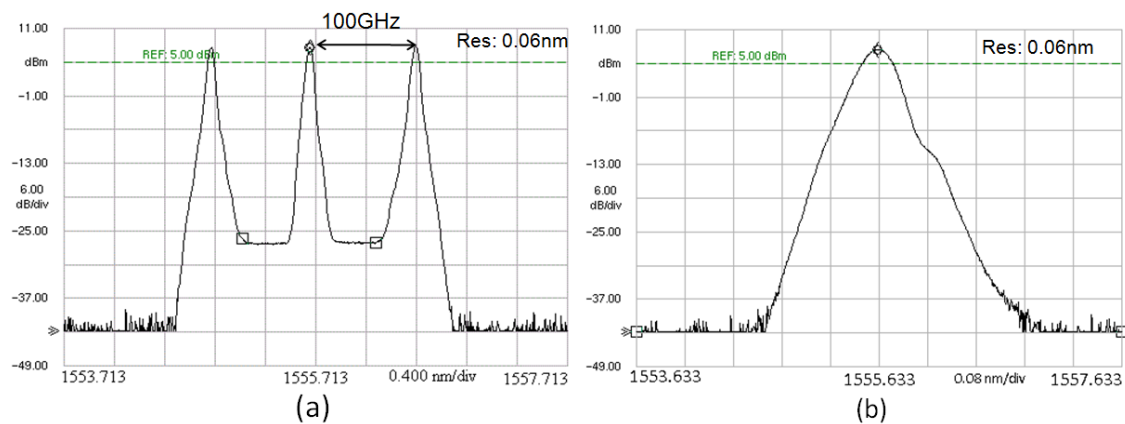


Fig. 3.21 (a) The spectra of IRZ-duobinary signal generated by CML. (b) The spectra of the experiment wavelengths.



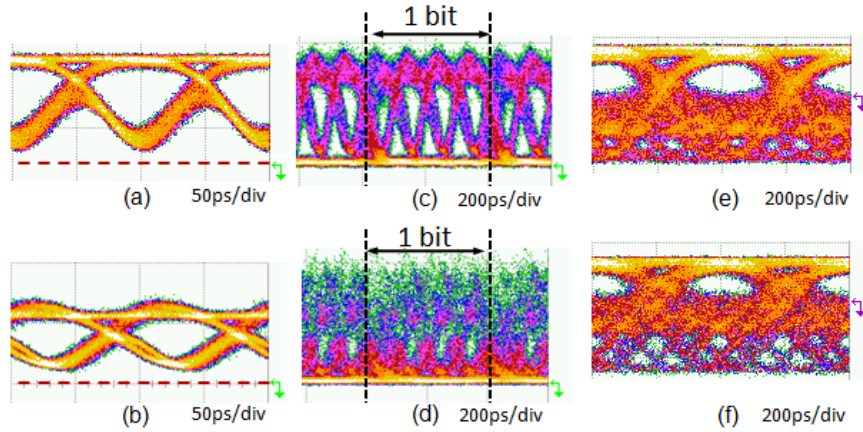


Fig. 3.22 Eye diagrams. (a) Optical eye diagram of back-to-back IRZ-duobinary signal. (b) Optical eye diagram of IRZ-duobinary signal at ONU. (c) Optical diagram eye of back-to-back upstream signal. (d) Optical eye diagram of back-to-back upstream signal at OLT. (e) Electrical eye diagram of back-to-back upstream signal. (f) Electrical eye diagram of back-to-back upstream signal at OLT.

Fig. 3.21 (b) shows the spectrum of the IRZ-duobinary signal generated by CML. The 20-dB bandwidth of the IRZ-duobinary signal is around 13 GHz. It has exhibited relatively more compact spectrum, as compared to that of a conventional IRZ signal. Thus it has better tolerance against fiber chromatic dispersion. Figs. 3.22 (a) and (b) show the optical eye diagrams of the generated IRZ-duobinary signal, obtained at the output of CML, and that after 80-km transmission, respectively. The duty cycle of the IRZ-duobinary signal is  $\sim 60\%$ , which is due to the limited modulation bandwidth of the CML. The ER of the signal at the transmitter is 6.7dB. The relative low ER is owned to the low slope of the OSR in the used CML ( $\sim 11\text{GHz}@3\text{dB}$ ). Low ER will decrease the BER sensitivity for downstream signal. However, downstream signal with low ER provides more power for upstream remodulation, which may improve the upstream sensitivity. Fig. 3.22 (c) and (d) are the optical eye diagrams of the remodulated signal at ONU and OLT, respectively. Each upstream bit contains four downstream bits. Figs. 3.22 (e) and (f) show the electrical eye diagrams for the upstream signal after a 1.87-GHz electrical LPF and an inverting amplifier at ONU and OLT, respectively. Clear eye opening is obtained.

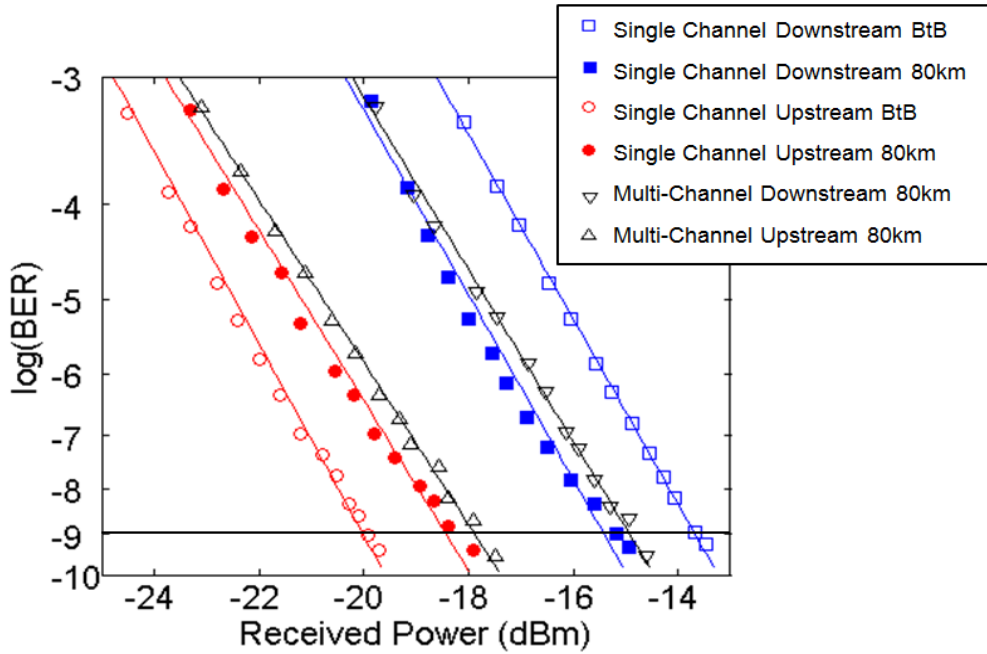


Fig. 3.23 BER measurements of the 10-Gb/s downstream and the 2.5-Gb/s upstream signals

Fig. 3.23 shows the measured bit-error-rate (BER) curves. Error-free transmissions were achieved for both the downstream and the upstream signals, after 80.4-km SSMF transmission. The BtB sensitivity (at BER of  $10^{-9}$ ) for the 10-Gb/s downstream IRZ-duobinary signal and the 2.5-Gb/s upstream re-modulated NRZ-OOK signal were measured to be -13.67 dBm and -20.07 dBm, respectively. After 80.4-km transmission, their respective sensitivities were measured to be -14.96 dBm and -17.88 dBm, having -1.29 dB and 2.19 dB penalty. Single channel results are also measured in order to determine the nonlinear penalty induced by multi-channel transmission. The single channel sensitivity at BER of  $10^{-9}$  for downstream at ONU and upstream at OLT were -15.12 dBm and -18.21. Small penalties are observed.

### 3.5 Summary

In this chapter, we have reviewed many applications of IRZ and then proposed an improved format named IRZ-duobinary. The relatively narrow IRZ-duobinary spectrum presents much better dispersion tolerance than conventional IRZ or RZ.

Methods of generating IRZ-duobinary signal and the performance of the signal generated by the proposed transmitters are compared.

After review IRZ-duobinary and its properties, we proposed and experimentally demonstrated a WDM-PON with optical multicast overlay by using the bandwidth efficient IRZ-duobinary signal. In the proposal, multicast control can be easily achieved by tuning bias of the downstream PtP modulator. Satisfactory transmission performances of the PtP and broadcast signals have been achieved, which provide sufficient power budget for the system.

Another typical application – wavelength reused WDM-PON, have also been characterized. In the study, we have experimentally demonstrated and characterized an 80-km-reach CLS WDM-PON. By employing IRZ-Duobinary as downstream format, 10-Gb/s downstream and 2.5-Gb/s upstream transmission over 80 km is realized. Error-free transmissions for both the downstream and the upstream signals have been achieved without dispersion compensation.

# Chapter 4. Manchester-duobinary Transmitter for Bi-directional WDM-PON

## 4.1 Introduction

Manchester code, which has one transition within every encoded bit period, is an attractive modulation format for various applications in optical fiber communication systems. Compared with the conventional NRZ, Manchester code has rich clock component and enables simple clock recovery and level recovery [103]. Besides, it has the feature of zero dc content, which makes it highly tolerant to signal intensity fluctuation when differential detection is used [104]. With these advantages, Manchester code was extensively studied in high-speed burst mode transmission systems [105]-[107]. Besides, it has also found application in WDM-PON. Having equal power in every bit, Manchester code has been employed as the downstream signal format in WDM-PONs so as to facilitate upstream data transmission, via re-modulating the downstream optical carrier at the ONUs [108]-[109]. In frequency domain, the main lobe of the Manchester coded signal is concentrated at the frequency which equals its data rate. Hence, such intrinsic property could effectively alleviate the optical beat noise between the optical line terminal (OLT) and the ONUs in bi-directional WDM-PONs [110]-[111]. In particular, one of its variants, the phase-shift-keying-Manchester signal [112], has been shown to have much stronger tolerance to the beat interference noise (BIN), compared with other modulation formats.

However, Manchester signals offer the above advantages at the expense of requiring broader transmitter and receiver bandwidth, which is double that of the nonreturn-to-zero (NRZ) signal. Optical spectrum of the Manchester signals is also two times that of the NRZ signals. As a result, optical spectral efficiency and

dispersion tolerance of the Manchester signals are degraded greatly [103]. These drawbacks affect its application to practical burst mode transmission link.

It has been known that the use of optical duobinary modulation format is an effective means in achieving narrow signal optical spectrum [113]. Many studies have shown the effectiveness of this modulation scheme for improving dispersion tolerance and spectral efficiency in high-speed optical transmission systems [114]–[119]. By combining the Manchester and duobinary coding together, a format with improved dispersion tolerance is proposed and demonstrated, namely Manchester-duobinary [120]. With the advantage of improved dispersion tolerance, Manchester-duobinary format has been found useful applications than conventional Manchester in optical access networks.

In this chapter, we discuss the principle of Manchester-duobinary, methods of generate Manchester-duobinary signal, as well as its application in bi-directional long-reach WDM-PON. Our contributions include a novel Manchester-dubinary transmitter using CML, and a Rayleigh noise mitigated 70-km-Reach bi-directional WDM-PON with our proposed Manchester-duobinary transmitter [121-122].

## 4.2 Manchester-duobinary transmitter

### 4.2.1 Mach-Zehnder modulator based

### Manchester-duobinary transmitter

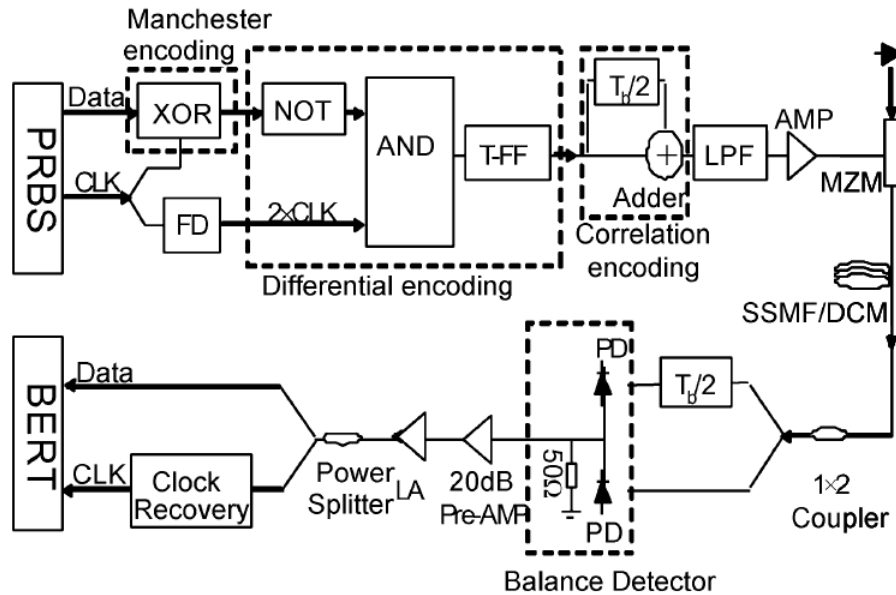


Fig. 4.1 Experimental setup of MZM based Manchester-duobinary transmitter and corresponding receiver system. CLK: clock signal. FD: frequency doubler. T-FF: toggle flip-flop. PD: photodetector. Pre-AMP: preamplifier. LA: limiting amplifier.

[120]

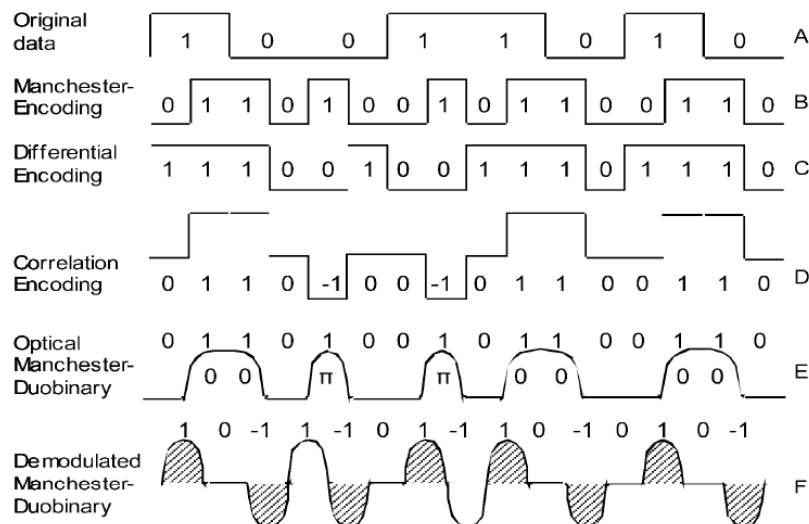


Fig. 4.2 Principle illustration of generation of Manchester-duobinary signal based on MZM. [120]

Fig. 4.1 shows the experimental setup in [120] for generating and receiving the Manchester-duobinary signal. The first module in the transmitter is a typical implementation of the Manchester encoder from NRZ data. In this module, the Manchester signal is realized by doing XOR operation between NRZ signal and its clock. The original NRZ data and its corresponding Manchester signal are shown as A and B in Fig. 4.2. Because of the level transitions of the Manchester signal, bandwidth of is doubled when it becomes Manchester signal. For example, if the original bandwidth of NRZ is 10 GHz, the bandwidth of the output Manchester signal is 20 GHz, albeit the data rate is still 10 Gb/s. The Manchester encoding module is followed by the duobinary encoding module, which consists of a differential encoder, a correlation encoder, and a LPF. The functionality of the differential encoder can be established by connecting an inverter and an AND-gate followed by a toggle flip-flop (TFF) circuit. The two times frequency clock signal for AND-gate is obtained by using a frequency doubler. Correlation encoding is realized by adding data delayed half bit period to the present data. In this way, differential encoded signals are converted to three-level signals, “+1”, “0,” and “-1”. Differential encoded signals and three-level signals are illustrated as C and D in Fig. 4.2.

Following the correlation encoding, one LPF with a bandwidth of half the bit rate of electrical Manchester is used to further compress the bandwidth of three-level signals by trimming its high-frequency components. As a result, the filtered three-level signals have narrower bandwidth than the Manchester signals. Then the three-level electric signals are amplified to a  $V_{pp}$  of about  $2V_{\pi}$  and modulated onto the optical carrier through a MZM. The MZM is biased in such a way, where level “0” is at the transmission null point and level “+1” and “-1” are at the transmission maximum points. Under this driving condition, the “+1” and “-1” levels in the duobinary signals have the same optical intensity but opposite phase after modulation. The optical duobinary signals are shown as E in Fig. 4.2.

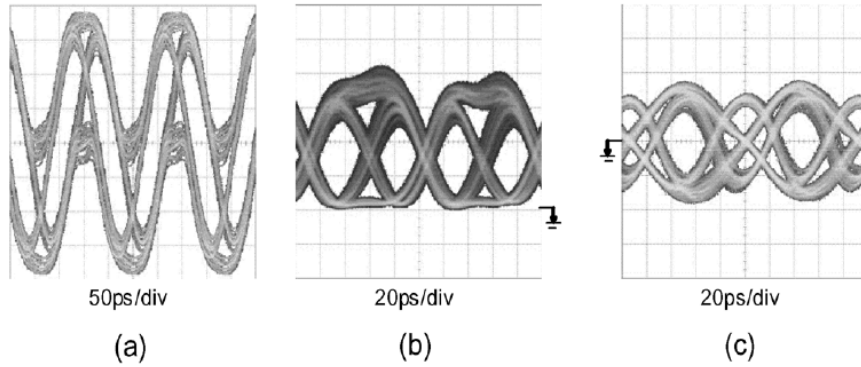


Fig. 4.3 Eye diagrams of (a) electrical Manchester-duobinary signals applied to modulator, (b) optical Manchester-duobinary signals before demodulation, and (c) electrical Manchester-duobinary signals after balanced detection. [120]

Fig. 4.3 (a) shows the eye diagram of the electrical Manchester-duobinary signal applied to the modulator, which corresponds to D in Fig. 4. 2. Fig. 3(b) shows the eye diagrams of the optical Manchester-duobinary signal before demodulation, which corresponds to E in Fig. 4.2. Fig. 4.3 (c) shows the electrical Manchester-duobinary signal after balanced detection, which corresponds to F in Fig. 2. It can be found that the DC component of the Manchester-duobinary signals is removed effectively by using balance detector. Experiment results in [120] show that the optical spectrum of Manchester-duobinary coding is more compact than that of the conventional Manchester signal and therefore has a larger CD tolerance.

#### **4.2.2 Chirp managed laser based Manchester-duobinary transmitter**

In the previous section we discuss the Manchester-duobinary format and a MZM based Manchester-duobinary transmitter that can help alleviate the problem of dispersion tolerance for conventional Manchester format. However, the transmitter proposed in [18] requires high-speed electronic encoders and is quite power inefficient. In this section, we propose and demonstrate a 10-Gb/s optical Manchester-duobinary transmitter using a directly modulated CML [123]. By properly modulating the CML with an electrical Manchester-coded driving signal,



optical Manchester-duobinary signal can be obtained [121]. This eliminates the need for complex electronic encoders and the costly and bulky external modulators. Thus, the complexity and the cost of the Manchester-duobinary transmitter are greatly reduced. The experimental result has showed that its chromatic dispersion tolerance is increased by nearly three times compared with that using conventional Manchester code. In this section, the conventional Manchester signal refers to Manchester signal without any phase transition. The proposed CML-based Manchester-duobinary transmitter has also been experimentally characterized.

#### A. Principle of the CML based Manchester -duobinary transmitter

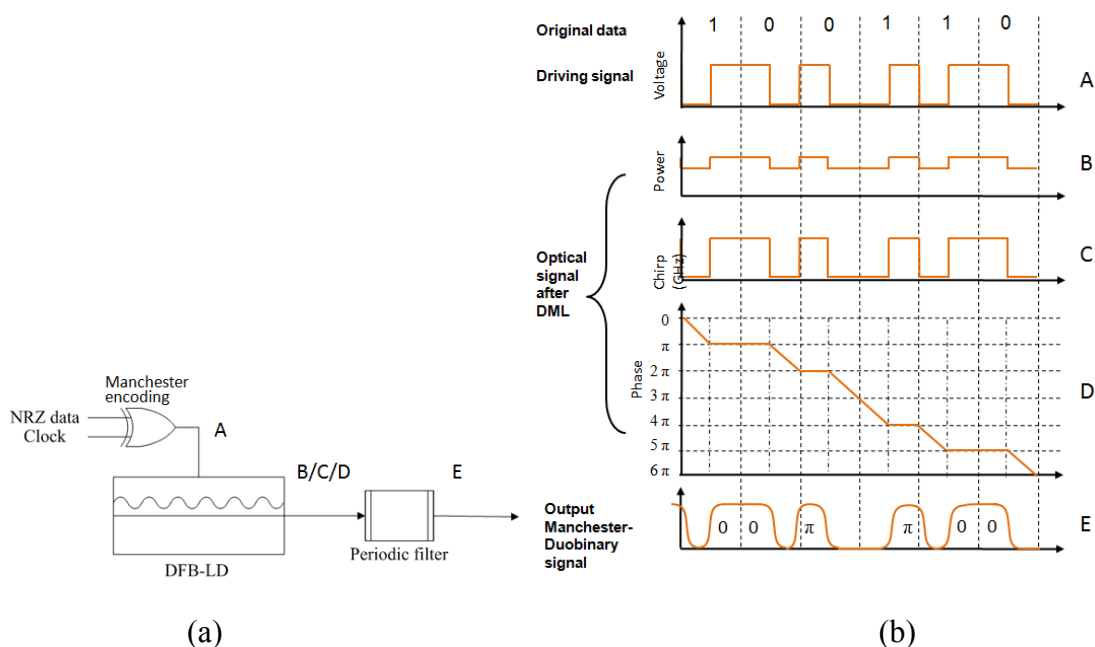


Fig. 4.4 (a) Schematic of CML-based Manchester-duobinary transmitter. (b) Illustration of the generation of the Manchester-duobinary signal.

Fig. 4.4 (a) shows the schematic of the proposed CML-based Manchester-duobinary transmitter, which comprises an electronic XOR gate and a CML. The CML comprises a distributed feedback laser (DFB-LD) followed by an in-line OSR filter in a butterfly package [123]. Fig. 4.4 (b) illustrates the principle of operation in time, frequency and phase domains. The XOR gate converts the input NRZ signal into

Manchester format before directly modulating the DFB-LD in the CML. The driving signal (trace **A**) is an electrical Manchester signal and its driving amplitude  $V_{pp}$  is adjusted to generate blue adiabatic chirp of  $\Delta f = 1/T$ , where  $T$  is the bit period at the high-intensity level in each bit. Such frequency shift results in a phase shift of  $\Delta\phi = 2\pi \int_0^{T/2} \Delta f(t) dt = \pi$ , to the low intensity level, in each bit. The DFB-LD is biased around five times above the laser threshold current so as to minimize the transient chirp but results in low ER in the DFB-LD output. The intensity, chirp and phase of the output optical signal from the DFB-LD are shown schematically as traces **B**, **C**, and **D** in Fig. 4.4(b), respectively. The laser wavelength is aligned on the transmission edge of the OSR filter, so as to pass the blue-shifted high intensity level and attenuate the red-shifted low intensity level. The intensity modulated signal accompanied with frequency modulation is then converted into a Manchester-duobinary signal with relatively high ER by the OSR filter (trace **E**). Besides, the OSR edge also converts the adiabatic chirp to flat-top chirp with abrupt phase transitions at the lower intensity level.

### B. Experimental demonstration and performance analysis

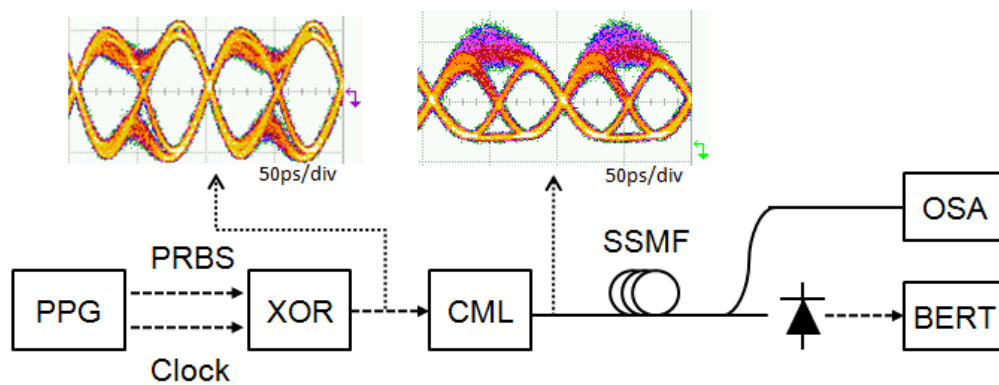


Fig. 4.5 Experimental setup for studying the CML based Manchester-duobinary transmitter

A standard CML module (Finisar DM80-01) was employed in our experimental setup, shown in Fig. 4.5. The DFB-LD at 1554.60 nm was biased at 75 mA and was

modulated by an 10-Gb/s electrical Manchester signal with pseudorandom binary sequence (PRBS) and a word length of  $2^{31}-1$ . The  $V_{pp}$  of the driving signal was 2.25 V. Different lengths of dispersion-compensation module or SSMF with  $\sim 17$  ps/(nm·km) chromatic dispersion were utilized to study the chromatic dispersion tolerance of the optical Manchester-duobinary signals. The optical power of the Manchester-duobinary signal was kept below 0 dBm, in order to avoid the impact from fiber nonlinearity. Single PD was used for signal detection.

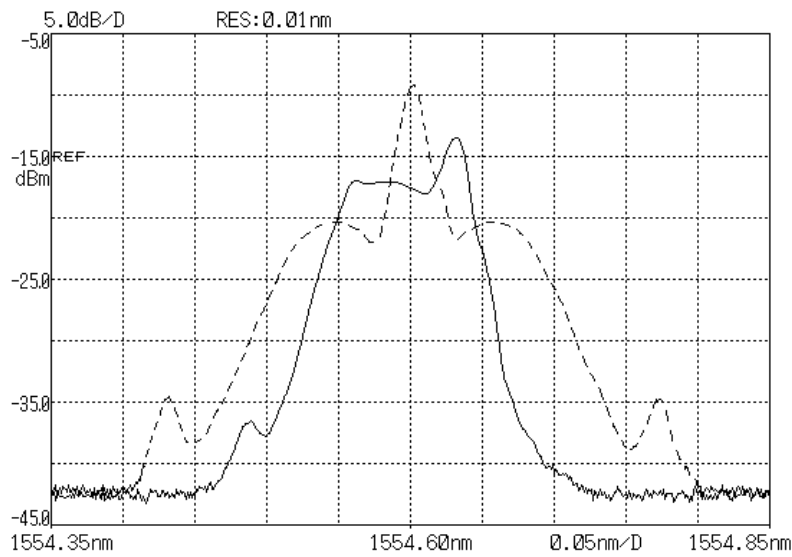


Fig. 4.6 Optical spectra of 10-Gb/s conventional Manchester (dashed line) and Manchester-duobinary (solid line) signals.

Fig. 4.6 shows the optical spectrum of the generated 10-Gb/s CML-based Manchester-duobinary signal (solid line) and it was compared with the 10-Gb/s conventional Manchester signal (dashed line). The tone of CML-based Manchester duobinary signal was shifted and the carrier was suppressed. The 20-dB bandwidths of the Manchester-duobinary signal and conventional Manchester signal were measured to be 18 GHz and 29 GHz, respectively. The Manchester-duobinary signal exhibited relatively more compact spectrum, as compared with that of a conventional Manchester signal. Thus it gave better tolerance against fiber chromatic dispersion in optical fiber transmission. The insets in Fig.4.5 show the eye diagrams of the electrical driving signal and the output optical signal. The ER of the output optical

signal was 8.7 dB. The relative low ER was attributed to the low slope of the OSR in the CML ( $\sim 11\text{GHz}@3\text{dB}$ ).

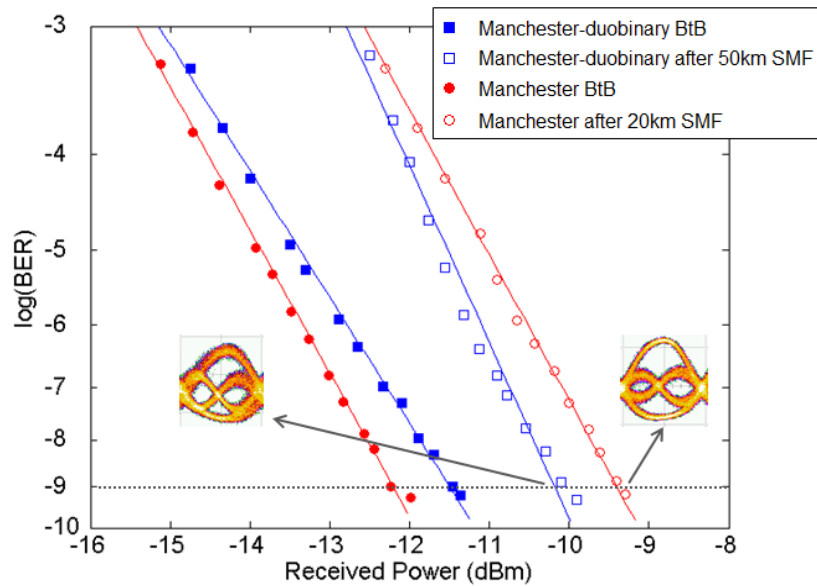


Fig. 4.7 BER performance for 10-Gb/s Manchester-duobinary signal and conventional Manchester signal.

As shown in Fig. 4.7, the back-to-back sensitivities (at the BER of  $10^{-9}$ ) for 10-Gb/s Manchester-duobinary signal and conventional Manchester signal were -11.45 dBm and -12.23 dBm, respectively. The 0.78-dB difference was mainly attributed to relatively low ER and overshoot of the Manchester-duobinary signal. The relatively low receiver sensitivities were mainly due to the insufficient electrical preamplifier gain in the photodetector. The power penalty of the Manchester-duobinary signal after 50-km SSMF transmission was 1.31 dB while that of the conventional Manchester signal after only 20-km SSMF transmission was 2.80 dB, showing the much longer optical reach for the Manchester-duobinary signal.

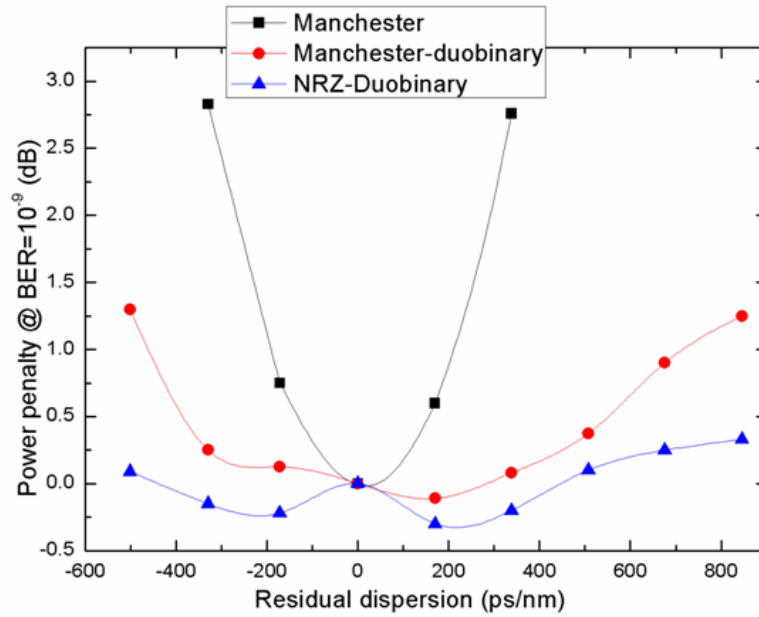


Fig. 4.8 Chromatic dispersion tolerance for 10-Gb/s Manchester-duobinary signal and conventional Manchester signal.

We have also investigated and compared the chromatic dispersion tolerance between the Manchester-duobinary format and the conventional Manchester format. Fig. 4.8 depicts their respective power penalties (at  $BER=10^{-9}$ ) measured at different residual chromatic dispersions. It was found that the 10-Gb/s Manchester-duobinary signal exhibited dispersion tolerance from -460 ps/nm to +720 ps/nm, at 1-dB power penalty. However, under the same condition, the 10-Gb/s conventional Manchester signal only exhibited dispersion tolerance from -190 ps/nm to +200 ps/nm, at 1-dB power penalty. The measurements showed that dispersion tolerance of the Manchester-duobinary format was around three times superior to that of the conventional Manchester signal.

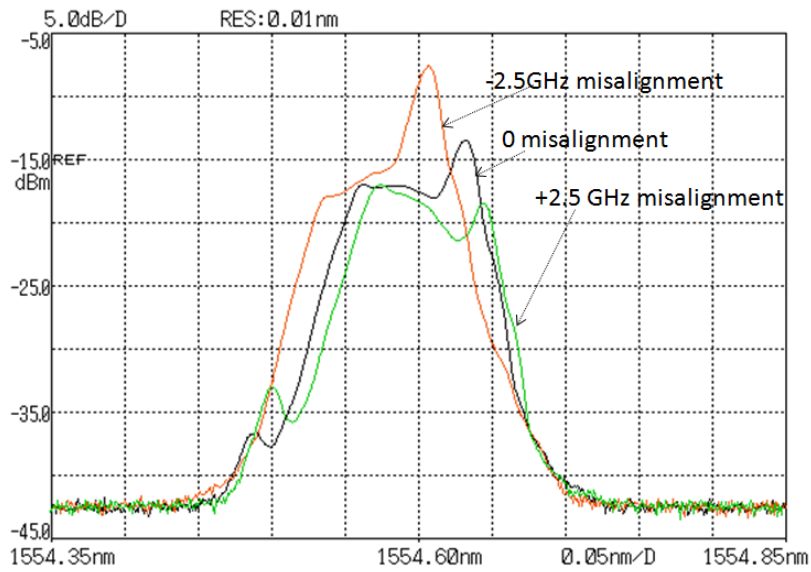


Fig. 4.9 Optical spectra of the output Manchester-duobinary signal under different OSR operating points.

The spectral property and transmission performance of CML-based Manchester-duobinary format varied with the OSR operating point in the CML. The optical spectra of the output Manchester-duobinary signal under different OSR operating points were shown in Fig. 4.9. The reference operating point (denoted as zero misalignment) was obtained by experimentally optimizing the OSR operating point such that the generated Manchester-duobinary signal gave the largest dispersion tolerance and exhibited a relatively flat top spectrum. Any small deviation from this reference operating point, say  $\pm 2.5$ -GHz misalignment, shown in Fig. 4.9, led to tilting of the top portion of the optical spectra.

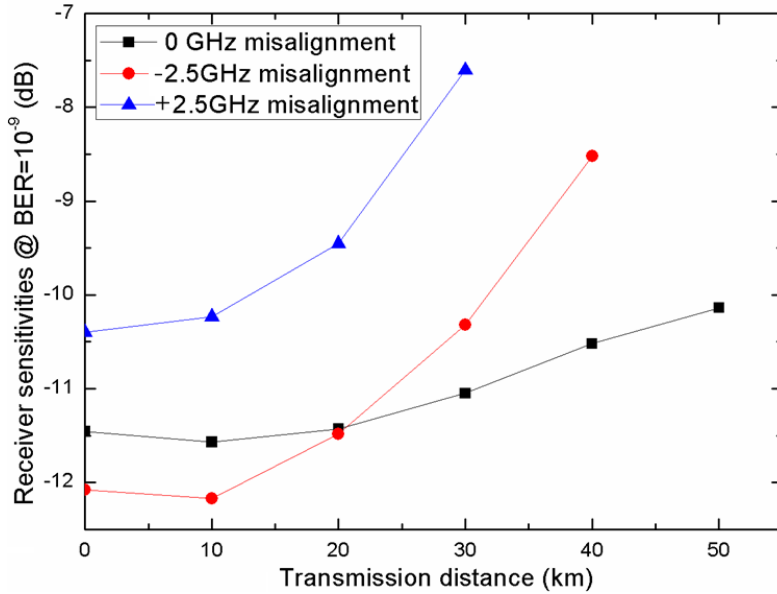


Fig. 4.10 Receiver sensitivities as a function of transmission distance for different OSR operating points.

Fig. 4.10 shows the chromatic dispersion tolerance curves measured under these three OSR operating points. It was shown that +2.5-GHz OSR misalignment would lead to quick degradation of the dispersion tolerance, which could be attributed to the large induced chirp when the mark bit was transmitted. For the case of -2.5GHz misalignment, it also exhibited similar trend in the dispersion tolerance degradation, albeit with  $\sim 0.6$  dB better back-to-back sensitivity, which could be attributed to the relatively higher ER resulted from the filtering at the OSR.

### **4.3 Rayleigh noise mitigated bi-directional WDM-PON based on Manchester-duobinary transmitter**

#### **4.3.1 CLS Bi-directional long-reach WDM-PON.**

We have discussed in chapter 1 that the WDM-PON has long been considered as a promising solution for the NG access network. Nevertheless, it still has not yet been massive deployed due to the high cost. Thus, one important mission of current

research in WDM-PON is to make it more cost-effective and thereby enhance its competitiveness for commercial success. This business requirement then raises the technology requirements that has been discussed in section 1.2, including colorless ONU, bi-directional transmission, long-reach, cost-effective devices, etc. Among all the colorless ONU solutions, centralized light source (CLS) with reflective ONU seems most promising. Therefore, the desired system is a CLS bi-directional long-reach WDM-PON [124-125].

In such single-fiber full-duplex wavelength-reused transmission system, signals propagating in the opposite directions using the same wavelength in the bidirectional transmission system suffer from impairment because of unavoidable Rayleigh backscattering (RB) and Fresnel back reflections [127-128]. Therefore a critical issue that needs to be addressed is how to mitigate the impairments arisen from optical beat noise (OBN) induced by possible back-reflections and Rayleigh backscattering (RBS) for both upstream and downstream signals.

To mitigate the impact of RBS in CLS PONs, different modulation formats have been considered, so as to reduce the spectral overlap between the signal and the interferer noise [128-129]. Several methods to mitigate the RB effects by introducing additional phase modulator at the ONU and optical notch filter at CO [130], wavelength offset detuning [131], frequency dithering [132], and cross-remodulation technique [133], etc. have also been proposed. However, these schemes either cannot completely eliminate the Rayleigh carrier backscattering (CB) and Rayleigh signal backscattering (SB) or require additional light sources for U.S. carriers or separate fiber links for DS and US signals. In [134], it has shown that downstream differential phase shift keyed (DPSK) signal, together with upstream subcarrier (SCM) signal could achieve 115-km bidirectional transmission. However, it required an expensive high-bandwidth modulator to facilitate upstream data re-modulation and an optical DI to demodulate the downstream signal, thus increased the cost of the ONU. A cost-effective solution was proposed to employ Manchester-coded downstream signal,



such that the OBN for upstream could be filtered out with a proper LPF [135]. However, as the Manchester-coded signal has twice the bandwidth than the non-return-to-zero (NRZ) signal, its dispersion tolerance is small. Thus, it cannot support 10-Gb/s downstream signals in CLS long-reach PONs.

In this work, we propose and demonstrate a cost-effective CLS 70-km-Reach full-duplex WDM-PON with downstream 10-Gb/s Manchester-duobinary signal and upstream 1.25-Gb/s re-modulated NRZ-OOK signal. The downstream pre-chirped Manchester-duobinary signal is generated by directly modulating a CML with an electrical Manchester coded signal, at the OLT [123]. Upstream remodulation is realized via a RSOA, resided at the ONU. The CML-based downstream transmitter offers many advantages to cost-sensitive metro/access applications, including compactness, high output power, and no costly and bulky external modulators required [124]. The reflected OBN in both downstream and upstream paths are mitigated by the electrical LPF and HPF at the OLT and the ONU, respectively. The experimental results show that the dispersion-tolerant Manchester-duobinary signal can well support data re-modulation and OBN suppression in bi-directional transmission.

### 4.3.2 Proposed system architecture

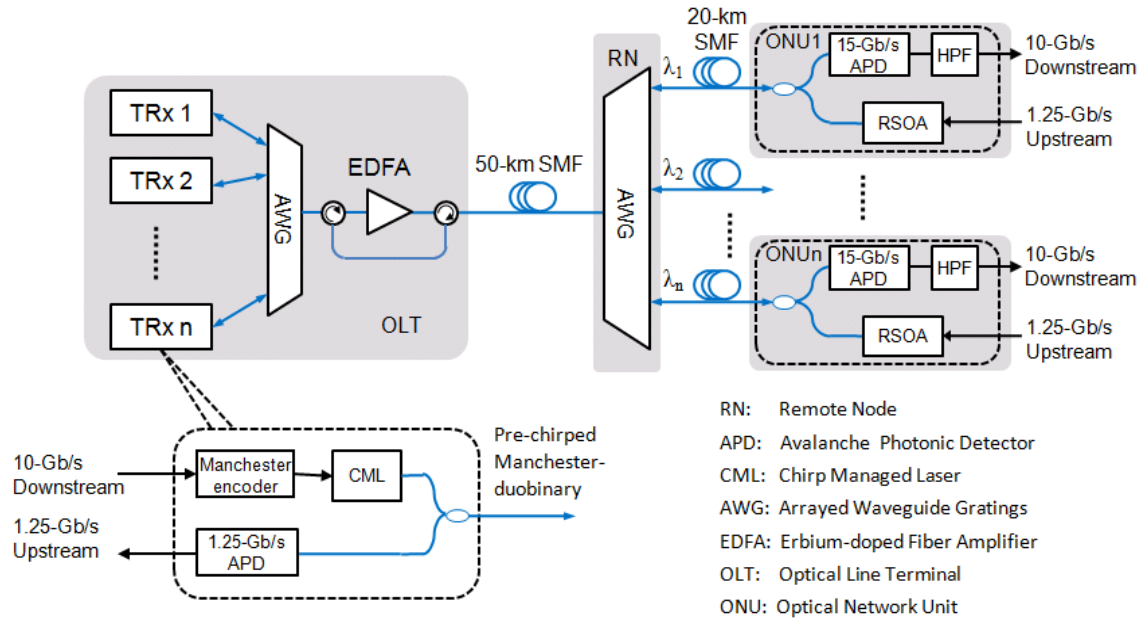


Fig. 4.11 Architecture of the proposed WDM-PON

Fig. 4.11 illustrates the proposed WDM-PON architecture utilizing Manchester-duobinary as the downstream signal format. Each transceiver at the OLT generates its downstream Manchester-duobinary signal and receives its upstream re-modulated signals from its respective subscriber. At the OLT, Manchester-coded electrical downstream data is directly modulated onto a designated wavelength channel through a CML. By properly adjusting the modulation current and the central wavelength of the OSR integrated in the CML, 10-Gb/s Manchester-duobinary signal is generated. To achieve optimum performance for the re-modulated upstream signal, pre-chirping is introduced to the downstream Manchester-duobinary signal by offsetting the OSR. All downstream modulated wavelengths are multiplexed, via an AWG, before being fed into an EDFA to boost up the transmitted power. Then the downstream wavelengths are delivered to their respective destined ONUs, via 50-km feeder fiber and 20-km distribution fiber.

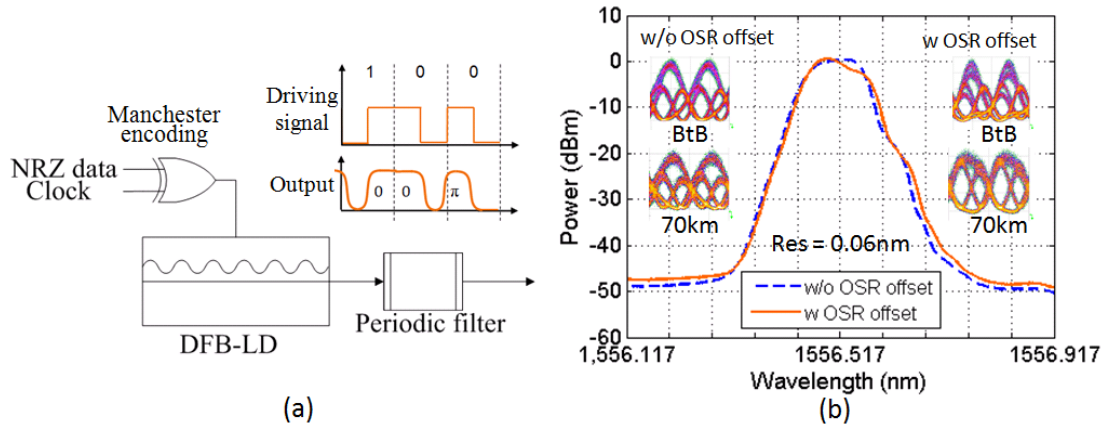


Fig. 4.12 Generation of the Manchester-duobinary signal using CML.

At each ONU, part of the received downstream signal power is tapped off for detection, while the remaining power is fed into a RSOA for upstream data re-modulation. The finite optical power in each bit of the received downstream signal provides the light source for the 1.25-Gb/s upstream NRZ-OOK data transmission, before being transmitted back to the OLT, via the same fiber link. A 15-Gb/s avalanche photo diode (APD) and a HPF are used to receive the signal and avoid the Rayleigh backscattering induced performance degradation on the downstream signal. At the OLT, the upstream signal is restored by a 1.25-Gb/s APD receiver and a LPF. As the downstream induced RBN spreads in higher frequency, LPF can filter out the OBN and recover the upstream signal.

The CML-based Manchester-duobinary transmitter, which comprises an electrical XOR gate and a CML, is schematically shown in Fig. 4.12(a). Standard Manchester-duobinary exhibited a relatively flat top spectrum. In our experiment, we have introduced pre-chirping to the CML-based Manchester-duobinary signal, via blue-shifting the OSR by about 2 GHz. With pre-chirping, the eye diagram obtained at ONU exhibited the minimal overshoot. This not only increased the downstream receiver sensitivity but also improved the signal quality for the re-modulated upstream signal. The optical spectra and the eye diagrams with and without OSR offset were compared in Fig. 4.12(b).

### 4.3.3 Experimental demonstration

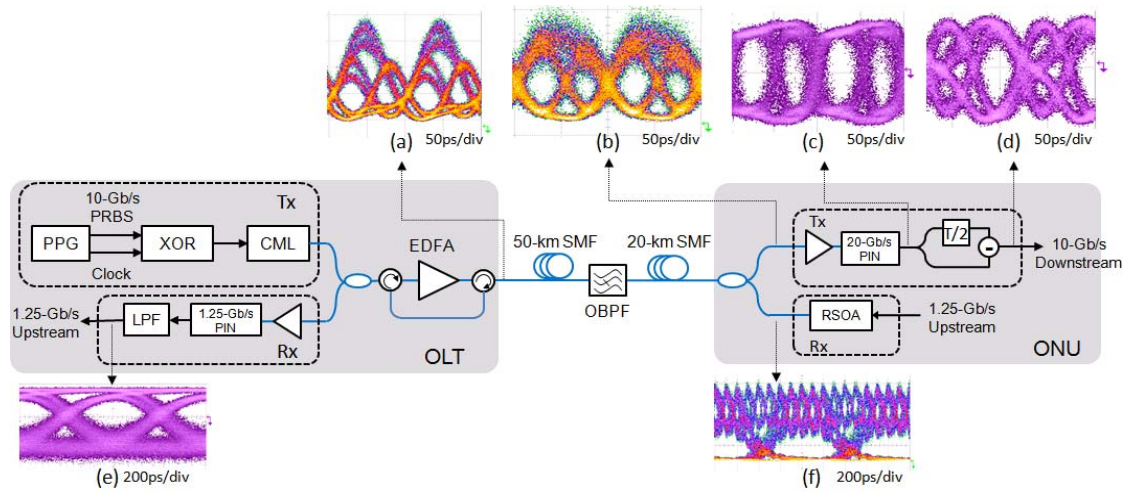


Fig. 4.13 Experimental setup

The feasibility of the proposed system has been experimentally assessed on one particular channel for proof-of-concept demonstration. As illustrated in Fig. 4.13, a standard CML module (Finisar DM200-01) was used in our experiment. The CML at 1556.51nm was biased at 75 mA and modulated by the electrical Manchester coded signal with pseudorandom binary sequence (PRBS) and a word length of  $2^{15}-1$ . The  $V_{pp}$  of the driving signal was 1.18 volts. The output signal was then fed into the EDFA and amplified to 2.3 dBm. The transmission link consisted of 50-km feeder fiber and 20-km distribution fiber. An optical bandpass filter (OBPF) with 3-dB bandwidth of 1.28 nm was used to emulate the RN. At the ONU, half of the received optical power was tapped off for downstream signal reception, while the other half was amplified and re-modulated by a RSOA. The RSOA was biased at 65 mA and modulated by an electrical NRZ signal with  $V_{pp}$  of 4 volts. The downstream optical power input into the RSOA was -18.6 dBm and the upstream power launched into the fiber link was 0.13 dBm. The re-modulated upstream signal was sent back to OLT, via the same transmission link, and was restored by a PD, followed by a 5<sup>th</sup>-order electrical LPF with 3-dB bandwidth of 798 MHz. The downstream signal was received by a 20-Gb/s photodiode, followed by a HPF constructed by a half-bit electrical delay line and a subtractor. The insets of Fig.4.123 show the eye diagrams at various strategic points.

The colored eye diagrams were the optical eye diagrams, while the grayed ones were the electrical ones. Clear eye opening for both downstream and upstream signals were obtained with the help of the HPF and the LPF.

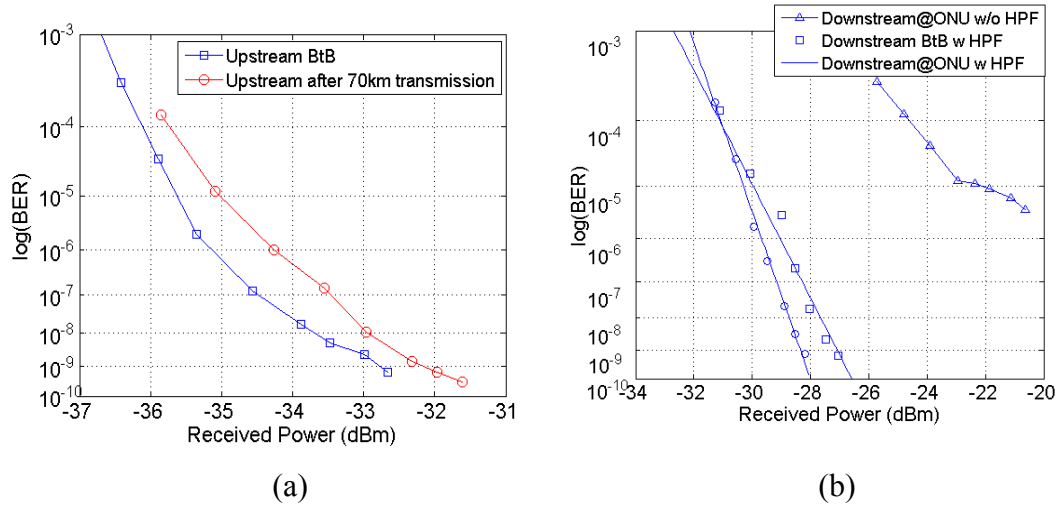


Fig. 4.14 BER measurements of (a) the 1.25-Gb/s upstream signal and (b) the 10-Gb/s downstream signal.

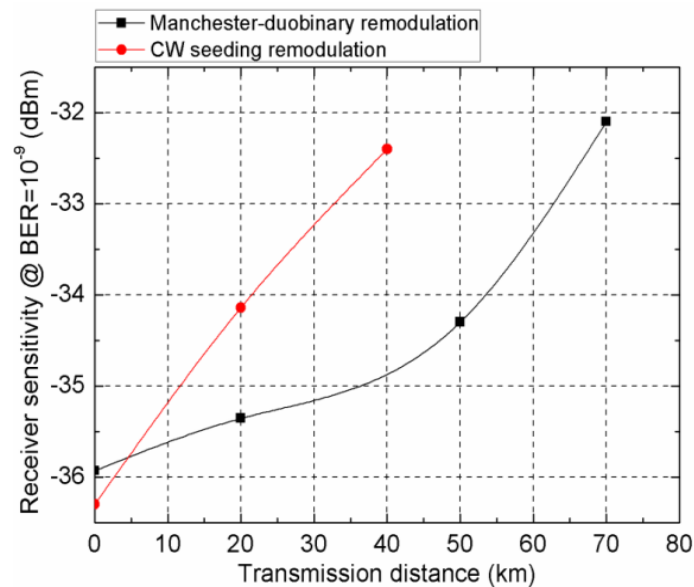


Fig. 4.15 Comparison of upstream sensitivity for re-modulating CW seeding and Manchester-duobinary downstream signal.

Figs. 4.14 (a) and (b) show the measured bit-error-rate (BER) curves for both the downstream and the upstream signals. Error free transmission was achieved after 70-km SSMF transmission without dispersion compensation. The BtB sensitivity (at

BER of  $10^{-9}$ ) for the 10-Gb/s downstream Manchester-duobinary signal and the 1.25-Gb/s upstream re-modulated NRZ-OOK signal were measured to be -27.05 dBm and -32.97 dBm, respectively. After 70-km transmission, their respective sensitivities were measured to be -28.37 dBm and -32.10 dBm, giving -1.05-dB and 0.87-dB penalty. Without HPF, error free downstream transmission could not be attained. Fig. 4.15 compares the upstream receiver sensitivity for different downstream light sources, including CW and Manchester-duobinary signal, at different transmission distances. Manchester-duobinary downstream signal outstood the CW case by achieving 70-km bi-directional transmission. When CW re-modulation was used, error-free upstream transmission over 50 km could not be achieved, due to the low frequency OBN.

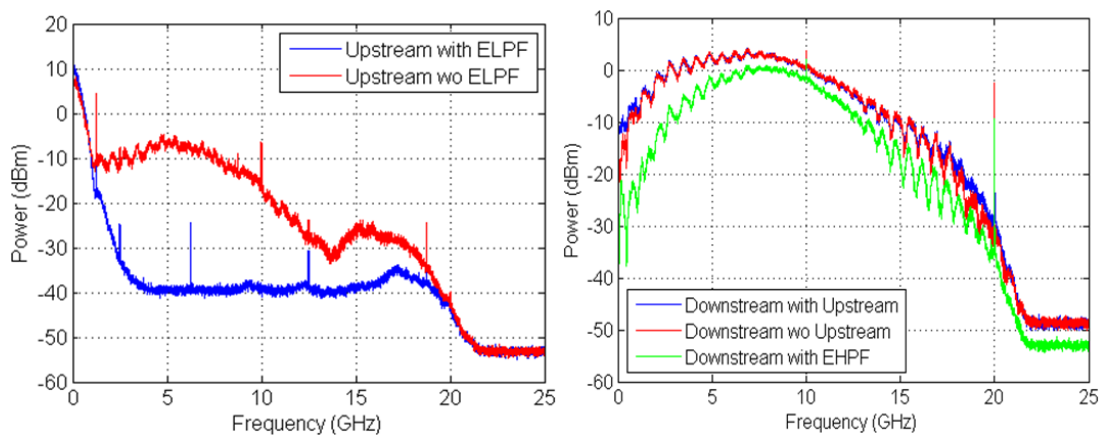


Fig. 4.16 Measured RF spectra for (a) upstream and (b) downstream paths with and without LPF and HPF. (Res: 10 MHz)

Fig. 4.16 (a) and (b) show the electrical spectrum for both upstream and downstream signals with and without the electrical filter. As shown in Fig. 4.16 (a), the spectrum of OBN for upstream signal lied within the high frequency region, attributed to the Manchester-duobinary format of the backscattered downstream signal. Therefore the upstream signal could be recovered by using the LPF to suppress the OBN. Similarly, the downstream signal could be restored by using the HPF, as the filtering of the low-frequency OBN would not affect the downstream signal.

## 4.4 Summary

In this chapter, we realized a modulation format by combining the Manchester coding and duobinary coding. The dispersion tolerance characteristics of the Manchester-duobinary signal is investigated and compared with that of Manchester signal. Two Manchester-duobinary transmitters, the MZM based transmitter and CML based transmitter, are reviewed and compared. Our proposed CML-based Manchester-duobinary transmitter has low complexity and is cost-effective in practical realization. Experiment results indicate that Manchester-duobinary coding exhibits much more compact optical spectrum compared with that using the Manchester signal and, thus, demonstrate much larger tolerance against chromatic dispersion. The dispersion tolerance of the Manchester-duobinary signal is increased by more than three times compared with that using the Manchester signal. In the CML-based Manchester-duobinary generation scheme, proper OSR control in the CML is needed to assure good signal quality and transmission performance.

Based on our proposed Manchester-duobinary transmitter, we have experimentally demonstrated and characterized a 70-km-reach CLS bi-directional WDM-PON. After carefully review the problem and progress of bi-directional WDM-PON. We demonstrate a By employing proper electrical filters and the dispersion tolerant Manchester-duobinary downstream signal generated by a CML, 10-Gb/s downstream and 1.25-Gb/s upstream transmissions over 70 km have been realized.

# Chapter 5. Electronic Equalizer for Manchester Coded Signal

## 5.1 Introduction

In chapter 4, we have discussed the application as well as the pros and cons of Manchester coded signal and have introduced a modified version of Manchester format named Manchester-duobinary, which shows apparent advantage in dispersion tolerance and spectrum efficiency. By combining Manchester with duobinary, the dispersion tolerance of Manchester-duobinary format can be increased by three times than that of conventional Manchester. However, the reported CD tolerance at 2-dB power penalty is 920 ps/nm, which corresponds to about 50 km for Manchester-duobinary signal at 10 Gb/s [120]. Still, it could not fulfill the requirement for modern metro and long-reach access networks, which requires uncompensated transmission distance of more than 80 km [136].

With the recent advent of low-cost high-speed electronics, electronic dispersion compensation (EDC) has become a cost-effective technique to dynamically compensate CD accumulated in optical transmission systems and networks. At the receiver side, EDC can be realized by employing an analogue feed forward equalizer (FFE) and/or decision feedback equalizer (DFE) [82], [137]. Compared with digital maximum-likelihood sequence estimation (MLSE), FFE-DFE is relatively simple and easy to implement, especially for high bit rate signals. Its CD compensation capability was demonstrated for various modulation formats [138]-[140]. However, there is yet no report for EDC with FFE-DFE for Manchester coded signal. Therefore, it is worth to study the capability of EDC for CD compensation of Manchester signal.

In Chapter 2, we have discussed the commonly used transmission impairment as well as technologies for impairment compensation. It is true that dispersion can be perfectly compensated in optical domain by using in-line compensation techniques



such as dispersion compensation fiber (DCF) or dispersion compensation module (DCM). However, compare with optical compensations, electronic compensation techniques has several crucial advantages that make it an irresistible trend. We have concluded its advantages as follows:

1. Reduce costs by eliminating the need for optical DCMs. The removal of DCMs will reduce the first-installed cost including the cost of DCMs and the associated cost for compensating the loss from the DCMs, simplify the deployment and configuration, and reduce the linear impairments caused by optical filtering.
2. Offer flexibility and adaptive compensation which will be required in future dynamic optical networks.
3. Easy to integrated in transmitter and receiver

In this chapter we will first review the basics of CD mitigation techniques using electronic equalizer, including analog equalizer (FFE, DFE) and digital equalizer (MLSE). The performance and limitation of FFE-DFE and MLSE for CD compensation of Manchester signal are studied in details.

## 5.2 Electronic equalizer for CD compensation

### 5.2.1 Channel model

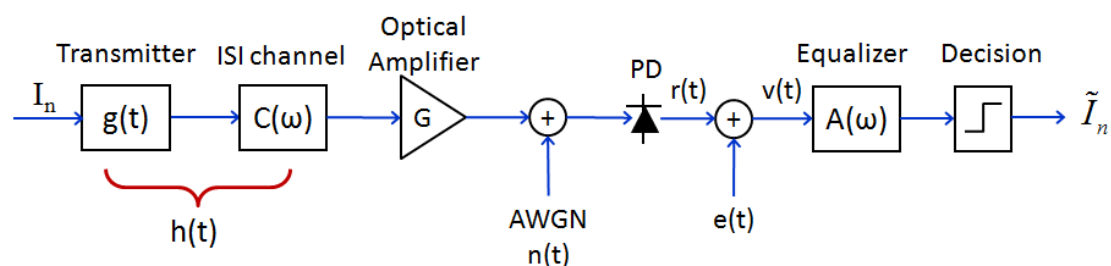


Fig. 5.1 Direct detected optical fiber communication OOK system with electronic equalizer

Fig. 5.1 depicts the model for IM-DD optical fiber communication system using equalizer at the receiver [141]. The EDFA is characterized by an optical field

amplifier with power gain  $G$  and an additive Gaussian white noise (AWGN) source  $n(t)$ , which corresponds to the spontaneous emission. Only linear distortion (CD, PDM) is assumed in the single-mode fiber. Therefore, the output can be obtained by convolving the data stream with the convolution of the pulse shape (generated by transmitter) with the impulse response of the fiber channel.

$$y(t) = \sum_{n=0}^N I_n \cdot h(t - nT) + n(t) \quad (5.1)$$

where  $h(t)$  is the convolution product between the transmitter response and the channel impulse response,  $T$  is the bit period,  $I_n$  is the bit sequence, and  $N$  is the number of interfering components for each bit. We assume the channel an ISI dominated channel as  $h(t)$  extends beyond  $T$  after a few tens of kilometers due to dispersion.

In IM-DD systems, the photodiode implements a square-law operation and the received electrical signal is represent as

$$r(t) = |y(t)|^2 + e(t) \quad (5.2)$$

where  $e(t)$  is the receiver additive white noise, which is assumed to be a zero mean, Gaussian distribution with variance  $\sigma_e^2$ .

Then, an equalizer follows the PD to mitigate the distorted signal. The equalizer only mitigates the ISI. The channel state is defined by using the noise free version of  $r(t)$ , i.e.,

$$c(t) = \left| \sum_{n=0}^N I_n \cdot h(t - nT) \right|^2 \quad (5.3)$$

In an optically amplified system the conditional probability density function (PDF) is noncentral chi square [149] and the SNR is given by

$$SNR = \frac{E(c(t)^2)}{2N\sigma^4 + 4\sigma^2 E(c(t))} \quad (5.4)$$

where the term in the denominator is the variance of noncentral chi-square distribution,  $N = 2BT + 1$  is the noncentral chisquare degrees of freedom,  $B$  is the ASE noise bandwidth, and  $T$  is the bit period.

### 5.2.2 FFE-DFE

FFE-DFE is a suboptimum channel equalization approach to compensate for the inter-symbol-interference (ISI). It employs a linear transversal filter that has a computational complexity that is a linear function of the channel dispersion.

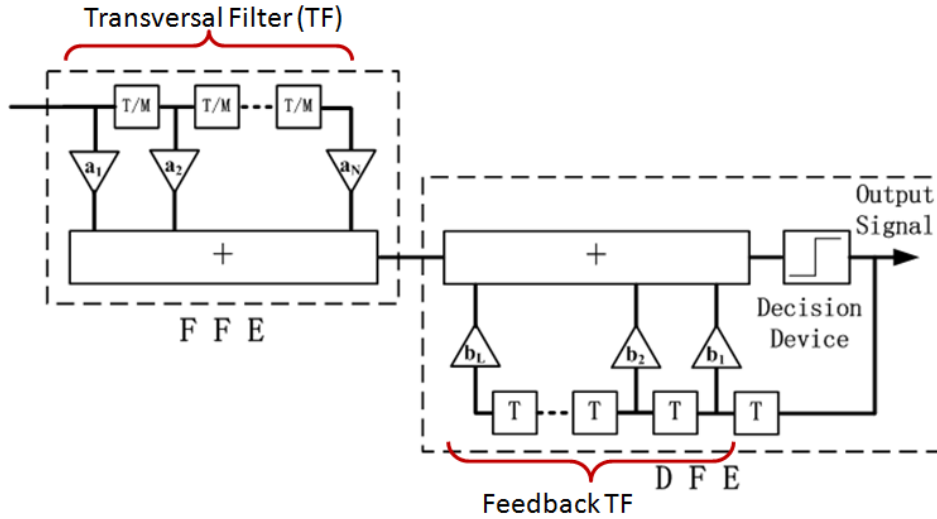


Fig. 5.2 Structure of FFE-DFE

Fig. 5.2 illustrates the structure of an FFE-DFE equalizer, which is a cascaded structure of FFE and DFE [143]. FFE consists of a linear transversal filter (TF) followed by a nearest neighbor quantizer (decision circuit). Its taps can be symbol-spaced (tap delay= $T$ ,  $T$  is the symbol duration) or fractionally spaced (tap delay= $T/M$ ). Its input sequence  $\mathbf{v}_k$  is obtained by sampling the electrical signal  $v(t)$  in Fig. 5.1 and its output is the estimated information sequence  $\tilde{I}_n$ . The estimate of the  $k$ th symbol can be expressed as

$$\tilde{I}_k = \sum_{j=-K}^K a_j v_{k-j} \quad (5.5)$$

where  $a_j$  are the the  $2K+1$  valued tap weight coefficients of the filter. The estimate  $\tilde{I}_k$  is quantized to the nearest information symbol to form the decision. If  $\tilde{I}_k$  is not identical to the transmitted information symbol  $I_k$ , an error has been made for feedback tap weight update. DFE is constructed by another feedback TF except the feedback control is done by using the detected bit.

The combination of FFE and DFE takes advantages of the two equalizers and has better performance [144]-[145]. FFE+DFE can also adaptively compensate the impairments. Adaptive electronic equalizer with control feedback by using both eye monitoring and pseudo-error count have been proposed.

Considerable research has been performed on the criterion for optimizing the filter coefficients. Since the most meaningful measure of performance for a digital communication system is the average probability of error, it is desirable to choose the coefficients to minimize it. Two criteria have found widespread use in optimizing the equalizer coefficients. One is the peak distortion criterion and the other is the least mean-square-error criterion (LMS) [143].

### 5.2.3 MLSE

The MLSE is a DSP equalizer proposed [146]. It achieves optimum detection by looking for the most likely bit sequence formed by the distorted bits. Mathematically, the criterion of MLSE can be expressed as

$$\mathbf{d} = \arg \max_{\mathbf{s} \in \mathbf{S}} \{p(\mathbf{r} | \mathbf{s})\} \quad (5.6)$$

where  $\mathbf{d}$  is the decided symbol sequence,  $\mathbf{s}$  is one of the possible transmitted symbol sequence,  $\mathbf{S}$  is the set of all the possible transmitted symbol sequences,  $\mathbf{r}$  is the

received signal after sampling and ADC, and  $p(\mathbf{r}|\mathbf{s})$  is the probability density function of the received signal conditioned on the transmitted symbol sequence  $\mathbf{s}$ .

The decision criterion implies that the MLSE is not tailored to a specific distortion but is optimum for any kind of optically distorted signal detected by the photodiode, provided the ISI does not exceed  $N+1$  symbol each with a period, where  $N$  is the maximum number of state considered in MLSE.

The implementation using the Viterbi algorithm is an efficient realization of the MLSE scheme [147]. The Viterbi algorithm models the transmitted symbol sequence as a state sequence in which

- the state at time  $n$  is  $(a_{n-L}, a_{n-L+1}, \dots, a_{n-1})$ ,  $L$  is the channel memory
- not all the transition between any two state pair is possible

Therefore, we cannot decide which state sequence corresponds to the maximum probability (or has the maximum metric) until all the symbols are received. However, when applying the algorithm, we can discard the state sequences beginning with certain state sequences which, based on already received (but not all the) symbols, surely does not contain the state sequence with the maximum metric.

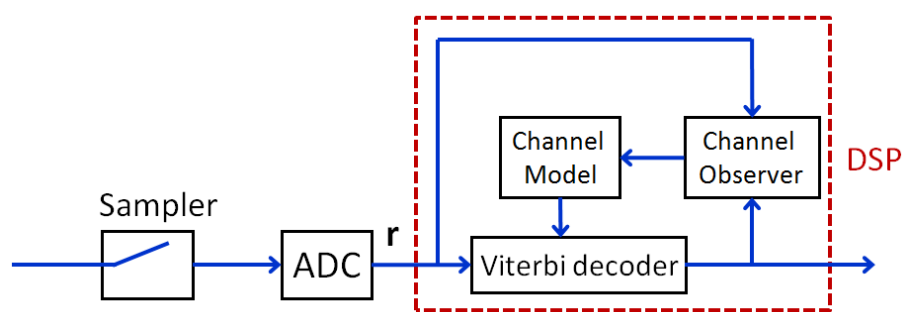


Fig. 5.3 Architecture of MLSE receiver

The principle architecture of an MLSE receiver is shown in Fig. 5.3. It consists of an analog to digital converter (ADC), a clock recovery (CR), and a digital signal

processing (DSP) that performs Viterbi algorithms. The software module in DSP contains a Viterbi detector, a channel model (CM) and a channel observer (CO).

The CO uses decision directed channel output observations to determine the metrics (CM) used in the Viterbi processor and comes in two flavors: a parametric CO estimates the parameters of closed-form approximations to the metrics-relevant data-dependent amplitude distributions, whereas a non-parametric CO uses empirical conditional amplitude histograms.

The choice of the architecture is influenced by the trade-off among performance improvement, complexity and cost. The most important choice regarding the allowable channel memory (ISI) is the number of trellis states in the Viterbi detector. Beyond that, clock recovery as well as ADC resolution and numerical resolution must be considered.

### **5.3 FFE-DFE for Manchester signal**

In this section, we experimentally investigate the performance of FFE-DFE for mitigating CD accumulated in Manchester signal, for both cases of single-end detection (SD) and balanced detection (BD). According to Nyquist criterion, a sampling rate of four samples per bit is needed to fully reconstruct the waveform of the Manchester signal, which means the best performance of FFE-DFE can be achieved when the FFE takes four samples from each bit. To compromise between complexity and performance, we also show and compare the results for FFE-DFE at a sampling rate reduced to 2 samples per bit.

### 5.3.1 Experimental setup for CD compensation of Manchester signal using FFE-DFE

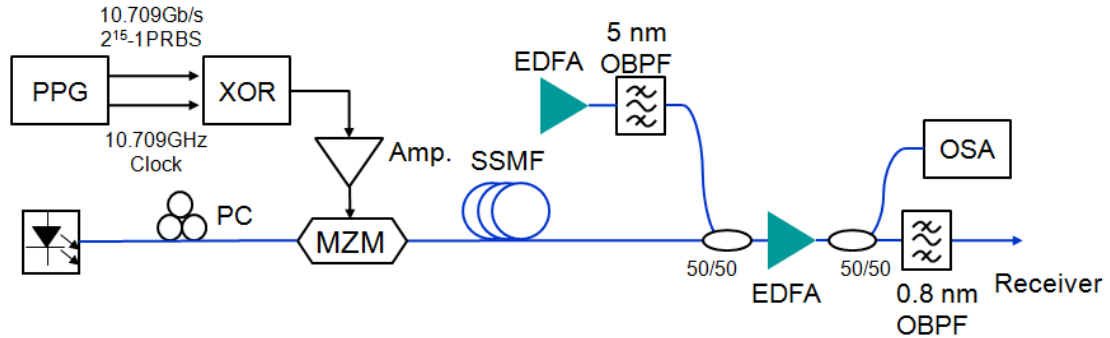


Fig. 5.4 Experimental setup for CD compensation of Manchester signal using FFE-DFE. PPG: pattern generator, XOR: exclusive-OR, OSA: optical spectrum analyzer, OBPF: optical bandpass filter.

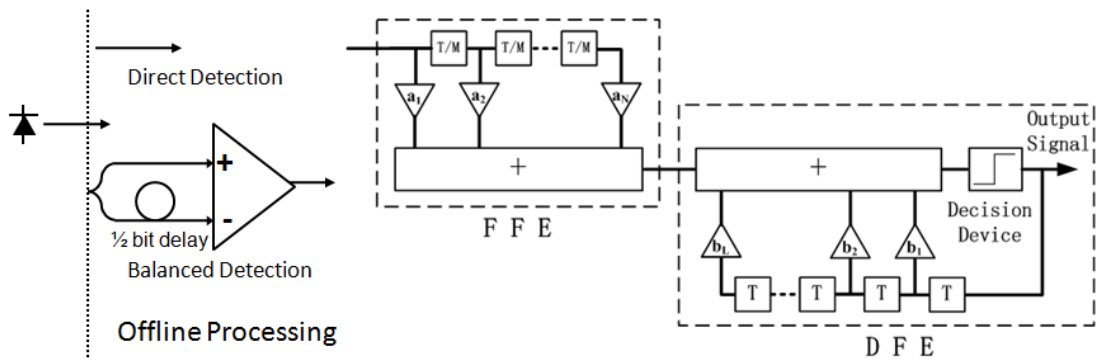


Fig. 5.5 Receivers for Manchester signal and the structure of FFE-DFE

Fig. 5.4 shows the experimental setup to evaluate the CD compensation capability of FFE-DFE for optical Manchester signal. In the transmitter, the electrical Manchester signal is generated by a typical Manchester encoder, which takes the exclusive OR (XOR) of two input signals, one of which is a 10.709-Gb/s NRZ signal carrying  $2^{15}-1$  PRBS, and the other is its clock signal. The signal bandwidth is doubled through Manchester encoding. Then the electrical Manchester signal is amplified by a 22-GHz electrical amplifier to drive a quadrature-biased Mach-Zehnder modulator, which takes a continuous wave input light at 1550.12 nm. The peak-to-peak amplitude ( $V_{pp}$ ) of the amplified electrical Manchester signal equals the  $V_{\pi}$  ( $\sim 6V$ ) of the MZM.

Different lengths of standard single-mode fiber (SSMF) with a dispersion coefficient of about 17 ps/nm·km at 1550 nm are utilized to study the CD tolerance of the FFE-DFE for the optical Manchester signal. In order to avoid any significant fiber nonlinearity, the power of the optical Manchester signal is kept below 0 dBm. After transmission over the SSMF, the optical signal-to-noise ratio (OSNR) of the optical signal is adjusted by injecting filtered ASE noise from an EDFA. The signal is then further boosted by another EDFA before being filtered by a 0.8-nm optical bandpass filter (OBPF) to remove the out-of-band ASE noise. The filtered signal is finally detected, via a PIN photodiode. The detected electrical signal is then sampled by a Tektronix DSA72004 digital serial analyzer (DSA), operating at 50 GS/s. For each combination of CD and OSNR values, the duration of the sampling time is 100  $\mu$ s, which corresponds to more than 1 million bits of the signal. Equalization with FFE-DFE is realized by off-line digital signal processing on a personal computer. For performance comparison, we also performed similar measurements using optical balanced detection. According to Nyquist criterion for signal sampling, at least four samples for each Manchester bit are needed to fully reconstruct the waveform. Therefore, it is expected that the CD compensation capability of FFE-DFE can be fully exploited when its FFE stage takes four samples from each Manchester bit (i.e. 4 spb). At this sampling rate, we assume the four samples are taken at 0, 1/4T, 1/2T, and 3/4T of each symbol, where T is the bit period, as shown in Fig. 5.6(a). We have also investigated the CD compensation performance of FFE-DFE when the sampling rate is reduced to two samples per bit (i.e. 2 spb). In this case, the samples are taken at 1/4T and 3/4T, as shown in Fig. 5.6(b). The equivalent FFE-DFEs employed are the same as the one shown in Fig. 5.5 with  $M=4$  (4 spb) and  $M=2$  (2 spb). The tap weights of the FFE-DFE are adapted with the least mean square (LMS) algorithm, using the first 5000 bits for training before entering the decision-directed mode.



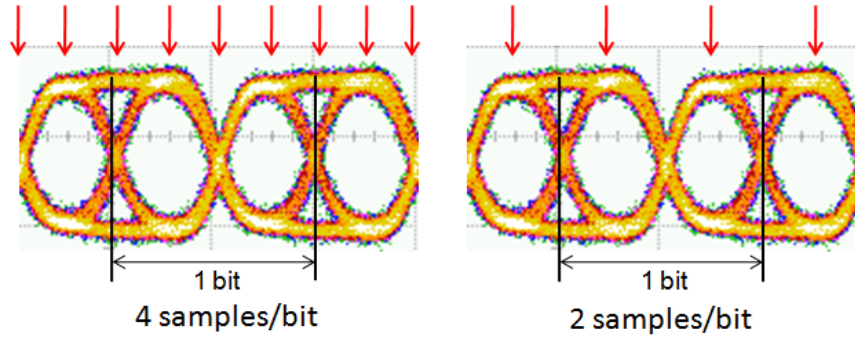


Fig. 5.6 Optical eye diagrams of Manchester signal and corresponding sampling schemes for equalization. (a) 4 spb sampling. (b) 2 spb sampling.

### 5.3.2 Results and discussion

#### A. FFE-DFE at 4spb

FFE-DFEs with different number of taps were used to evaluate their CD compensation capability for the optical Manchester signals. At the sampling rate of 4 spb, a minimum number of 9 FFE taps have been considered, which utilized the information from pre- and post-half symbol for equalization. Figs. 5.7 (a) & (b) show the required OSNR for the 10-Gb/s optical Manchester signal to achieve a bit-error-rate (BER) of  $10^{-3}$ , under various residual CD values when different kinds of FFE-DFEs and single-ended detection were employed. From both figures, it is shown that, without equalization, the required OSNR increased from 12.16 dB to 15.88 dB when the residual CD was raised from 0 to 338.06 ps/nm and the required OSNR increased drastically afterwards. When FFE-DFE was applied, about 2-dB improvement in the required OSNR was observed at zero CD value. Such improvement could be attributed to the emulation of balanced detection, via the FFE-DFE, by constraining the corresponding FFE-DFE coefficients for the first half bit and the second half bit to be of opposite numbers.

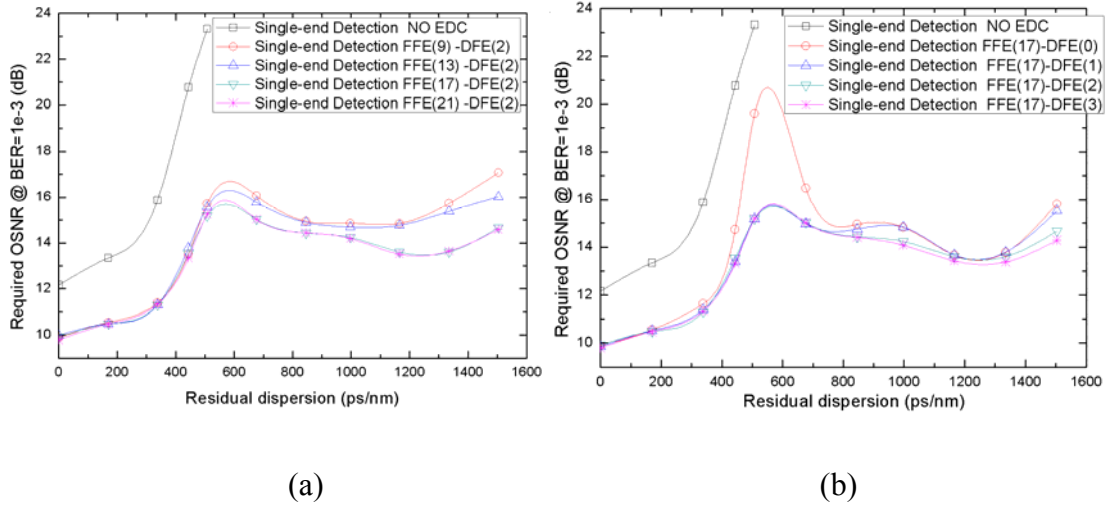


Fig. 5.7 Required OSNR vs. Residual CD for 10.709-Gb/s Manchester signal with different number of FFE/DFE taps using single-ended detection. (a) FFE with different number of taps followed by DFE(2). (b): FFE(17) followed by DFE with different number of taps.

Fig. 5.7 (a) shows the required OSNR curves when the number of DFE taps was fixed to 2. For all the FFE-DFEs with the number of FFE taps ranging from 9 to 21, the required OSNR curves first rose rapidly when the residual CD increased from 350 ps/nm to 500 ps/nm, then became leveled off at around 14 dB when the residual CD continued to increase from 500 ps/nm to 1533 ps/nm. At the residual CD value of 1673-ps/nm, in all cases, the measured BER was larger than  $1 \times 10^{-3}$ , even when the OSNR was increased to 24 dB. Thus, it was expected that the required OSNR curves would rise abruptly at the residual CD values beyond 1533-ps/nm. On the other hand, when the number of FFE taps was increased from 9 to 17, the performance of the FFE-DFE was enhanced, though any further increase in the number of taps did not give significant performance enhancement. Hence, it could be deduced that 17 taps were sufficiently optimal for the FFE stage. At a residual CD value of 1533 ps/nm, which corresponded to 90-km SSMF transmission, the required OSNR values for FFE tap number of 9, 13, 17 and 21 were 17.07 dB, 16.02 dB, 14.66 dB, and 14.57 dB, respectively. With the number of FFE taps being fixed to 17, the number of DFE taps was then varied between 0 and 3, and their required OSNR curves were shown in Fig.

5.7 (b). All the required OSNR curves coincided when the residual CD ranged from 0 to 440 ps/nm. However, they began to diverge when the transmission distance was further increased. The sudden rise in the required OSNR curve with FFE (17) - DFE (0) implied that DFE was indispensable for the CD compensation, and significant performance enhancement was observed when the number of DFE taps was increased from 0 to 3, though the performances of FFE(17)-DFE(2) and FFE(17)-DFE(3) were rather close to each other. Hence, it could be deduced that any further increase in the number of DFE taps would not give any further significant performance enhancement in CD compensation, thus FFE(17)-DFE(2) would be an optimal design for the electronic equalizer for the optical Manchester signals under single-ended detection.

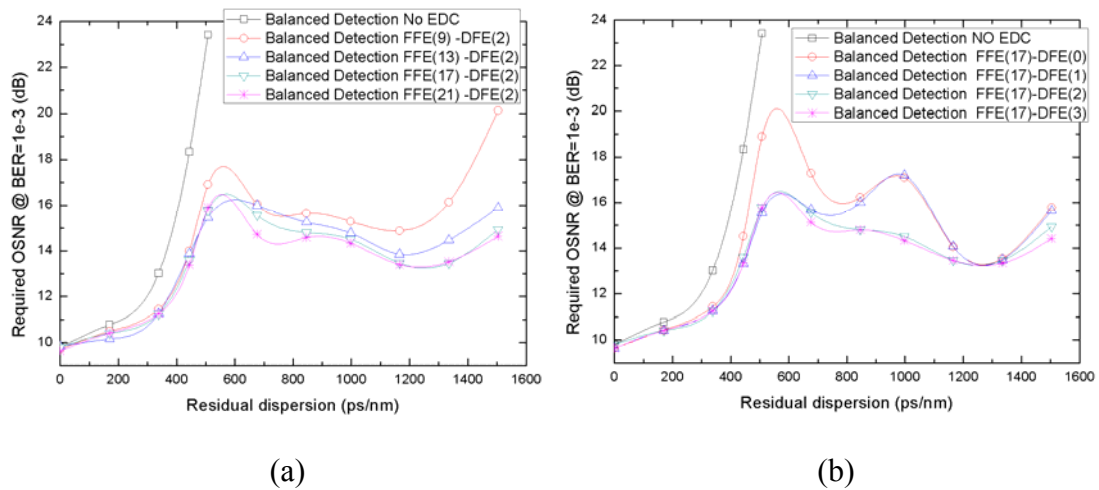


Fig. 5.8 Required OSNR vs. Residual dispersion for 10.709-Gb/s Manchester signal with different number of FFE/DFE taps using balanced detection. (a) FFE with different number of taps followed by DFE (2). (b): FFE (17) followed by DFE with different number of taps.

In view of the typical  $\sim 2$ -dB improvement in the required OSNR and larger tolerance to signal level fluctuation, balanced detection has also been widely considered for Manchester signal [141], [147-148]. Figs. 5.8 (a) and (b) show the required OSNR of the 10-Gb/s optical Manchester signal to achieve a bit-error-rate (BER) of  $10^{-3}$ , under various residual CD values when different kinds of FFE-DFEs

and balanced detection were employed. Fig. 5.8 (a) shows the performance with the FFE-DFE having different number of FFE taps and fixed 2 DFE taps. At zero CD value, the FFE-DFE could no longer enhance the performance as balanced detection has already been employed. Without equalization, the CD tolerance was still quite poor. When the FFE-DFE was applied, the required OSNR curves exhibited similar trend as those under single-ended detection, as in Fig. 5.7 (a). Hence, it could be deduced that 17 FFE taps were optimal to guarantee the performance of FFE-DFE, under balanced detection. From Fig. 5.8 (b), it was shown that the performances of FFE-DFE without DFE taps or with only one DFE tap were significantly inferior to that with two DFE taps. Hence, at least 2 DFE taps should be used for systems using balanced detection.

From the above results using single-ended or balanced detections schemes, it could be concluded that there was no benefit of using balanced detection for optical Manchester signal when FFE-DFE is used for CD compensation. In fact, adaptive filter like FFE-DFE can emulate balanced detection by properly constraining the coefficients of the FFE taps, for instance, by setting the weights of first two taps in the FFE with opposite polarity to that for the latter two taps for each bit. The performance was satisfactory when the FFE-DFE had 17 FFE taps and 2 DFE taps. From our results, any further increase in the number of FFE or DFE taps would not significantly further improve the CD tolerance.

## B. FFE-DFE at 2spb

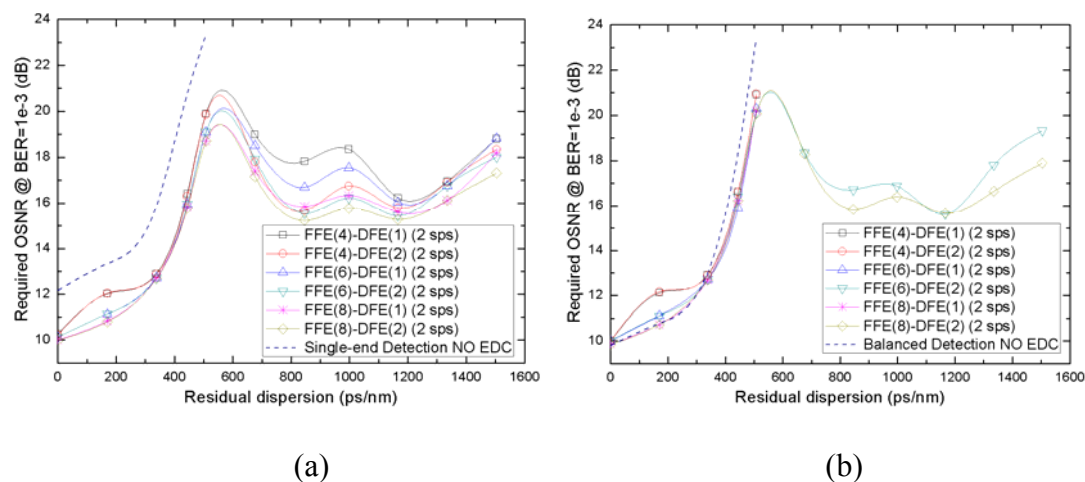


Fig. 5.9. Required OSNR vs. Residual dispersion for 10.709-Gb/s Manchester signal using different detector and 2 samples per symbol scheme with different number of FFE/DFE taps. (a): Single-end detector (b): Balanced detector

We have also investigated the CD compensation capability of FFE-DFE when its sampling rate was reduced by half to 2 spb. Similar to the case with FFE-DFE at 4 spb, both single-ended and balanced detection schemes were considered for FFE-DFE at 2 spb. As shown in Fig. 5.6(a), a minimum number of four FFE taps were required to utilize samples from the pre- and post- half symbols. Fig. 5.9(a) depicts the required OSNR curves for the 10-Gb/s optical Manchester signal with FFE-DFE having different number of DFE taps and FFE taps. As the signal was sampled at the maximum eye opening points in the first and the second half of each bit, the 2-dB improvement in the required OSNR at zero CD could still be achieved with FFE-DFE. When the number of DFE taps was 1, increasing the number of FFE taps showed remarkable improvement in the required OSNR. Nevertheless, when the number of DFE taps was 2, increasing the number of FFE taps from 4 to 8 would still reduce the required OSNR, but the benefit was less than 2 dB. The results implied that at least two DFE taps were needed in FFE-DFE at 2 spb, for optimal performance, and much fewer taps for FFE were required as compared to FFE-DFE at 4 spb. Besides, when the CD value ranged from 508 to 676 ps/nm, the required OSNR was quite large, thus

prohibited the use of FFE-DFE at 2 spb in such transmission distance. However, the required OSNR was well maintained at around 16 dB when the residual CD was between 845 and 997 ps/nm. Therefore, FFE-DFE at 2 spb offered a cost-effective solution to relax the requirement of OSNR in long-reach optical access network, which has typical transmission distances around 80 km (equivalent to a residual CD value of 1356 ps/nm). Fig. 5.9 (b) depicts the results when FFE-DFE at 2 spb was considered under balanced detection. It was shown that only FFE(6)-DFE(2) and FFE(8)-DFE(2) were capable of improving the CD tolerance while BER of  $10^{-3}$  cannot be achieved using other FFE-DFE for CD values beyond 508 ps/nm. Compared with single-ended detection, balanced detection was less robust when FFE-DFE at 2 spb was used to electronically compensate the CD for optical Manchester signals.

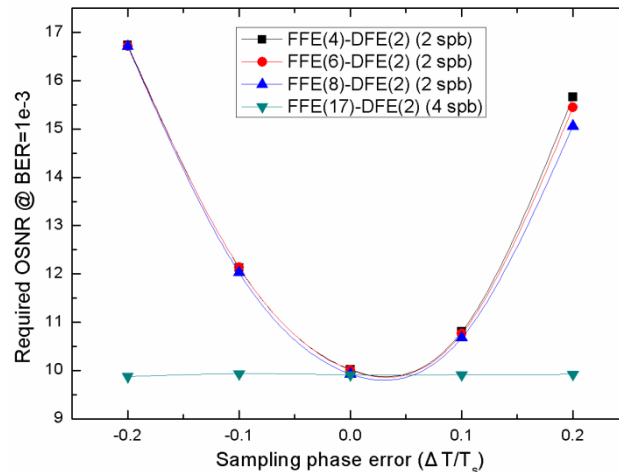


Fig. 5.10 Required OSNR vs. sampling phase error for 2-spb scheme at back-to-back.

As the 2 spb scheme required sampling at the  $1/4T$  and  $3/4T$  (maximum eye opening) points, the phase error tolerance has been studied. Fig. 5.10 shows the relationship between the sampling phase error and the required OSNR at BER of  $10^{-3}$ . The phase error was defined as the ratio of the sampling time misalignment ( $\Delta T$ ) and the symbol duration ( $T_s$ ). To maintain good performance ( $< 2$ -dB penalty in required OSNR), the phase error should be less than 0.1. The asymmetry of the phase error induced penalty was attributed to the asymmetric rising and falling edges of our

generated optical Manchester signal.

### C. Further Discussions

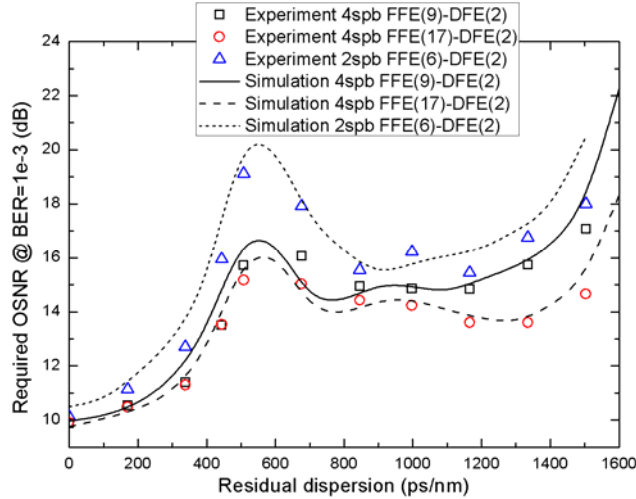


Fig. 5.11 Comparison of 2-spb scheme and 4-spb scheme for equalizer with different number of FFE taps.

The CD compensation ability of FFE-DFE has been verified by both numerical simulation and experiment. As shown in Fig. 5.11, using different FFE-DFEs and under either 2 spb or 4 spb schemes, the experimental results agreed with the numerical results very well. For most of the CD values, the increase in required OSNR of using FFE-DFE at 2 spb, compared with the 4-spb case, were less than 2 dB. At the CD values between 845 and 1172 ps/nm, such increase in required OSNR was less than 1 dB. However, such penalties were relatively large when the CD value was between 508 and 676 ps/nm, which prohibited the application of FFE-DFE at 2 spb in this range. In general, the results confirmed that FFE-DFE at 2 spb could reduce the number of FFE taps at the expense of the higher required OSNR (difference less than 2 dB). The simulated results have also showed that the required OSNR increased drastically in the presence of residual dispersion beyond 1533 ps/nm, regardless of the type of FFE-DFE and the sampling scheme utilized. This could be a fundamentally limitation caused by CD.

As shown in Fig. 5.11, there was a surge of the penalty in required OSNR for 10.709-Gb/s Manchester signal between CD values of 500 ps/nm and 600 ps/nm. In our numerical simulation, the maximum penalty point appeared at a CD value of 580 ps/nm. Such penalty surge in required OSNR could be explained by analyzing the eye diagrams and the FFE tap coefficients, as illustrated in Fig. 5.12. Fig. 5.12 (a), (b), (c), and (d) depicts the simulated eye diagrams at CD values of 380 ps/nm, 480 ps/nm, 580 ps/nm, and 680 ps/nm, respectively. Their corresponding FFE tap coefficients are shown in Fig. 5.12 (e), (f), (g), and (h), respectively, assuming FFE(9)-DFE(2) was adopted. The shaded areas in the eye diagrams were the eye opening areas of the transmitted symbol. FFE utilized both the first and the second half of the symbol for equalization. Therefore the corresponding coefficients for the samples of the first and the second half of each bit were opposite, which were indicated by the closed circles in the lower figures in Fig. 5.12. With the increase in the CD value, the eye opening was reduced and the eye became completely closed at the CD value of 580 ps/nm, and the FFE could hardly differentiate the two traces. This corresponded to the local maximum of the required OSNR, as in Fig. 5.11. However, any further increase in the CD value would lead to effective eye opening in the neighboring bits (see Fig. 5.12 (d)), and the FFE could then differentiate the two traces again. Therefore, the CD could be better compensated. Besides, similar to Figs. 5.7-5.9, the penalty curves in required OSNR exhibited surge at moderate residual CD and this could be attributed to the noise enhancement characteristics of the equalizer, as discussed in [82].



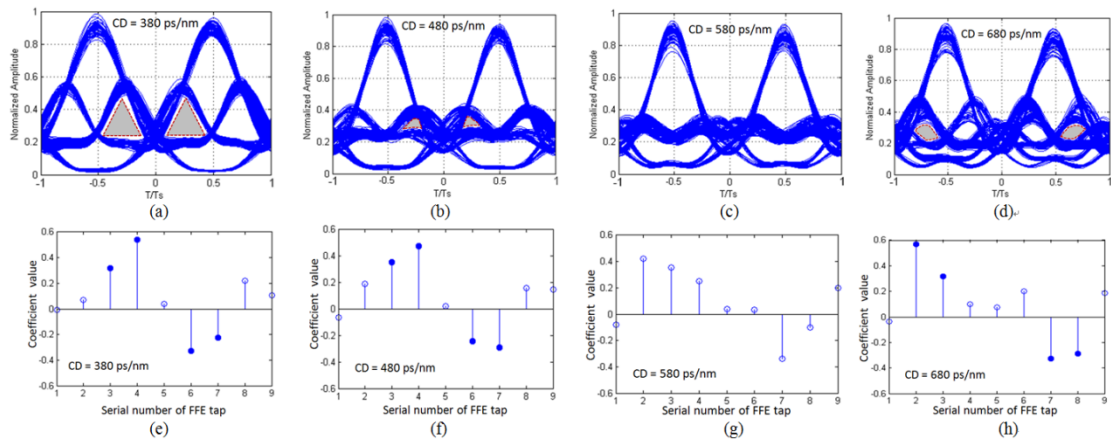


Fig. 5.12 Simulated eye diagrams for Manchester signal and corresponding FFE tap coefficients for FFE(9)-DFE(2) at different CD values. (a),(e): 380 ps/nm; (b),(f):480 ps/nm; (c),(g): 580 ps/nm; (d),(h): 680 ps/nm.

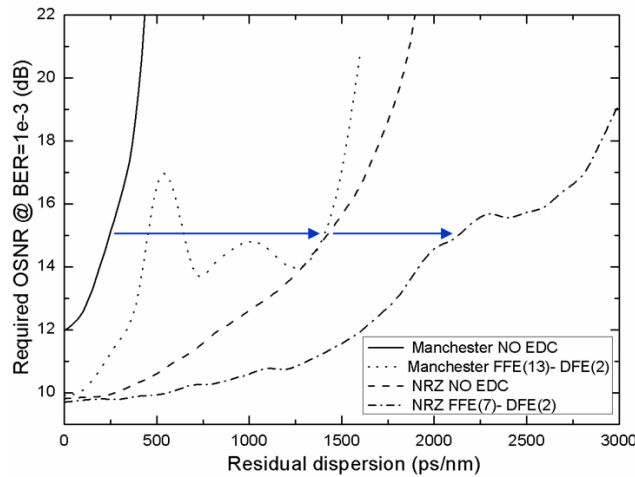


Fig. 5.13 Comparison of Manchester and NRZ for equalizer with different number of FFE taps.

Fig. 5.13 depicts the performance comparison between Manchester and NRZ-OOK formats with different number of FFE taps, via simulation. 4-spb FFE(13)-DFE(2) and 2-spb FFE(7)-DFE(2) were selected for Manchester signal and NRZ-OOK signal, respectively. The lower sampling rate of 2-spb was sufficient for the NRZ-OOK signal, due to its narrower bandwidth. The time spans within which the samples were utilized for both types of signals, were the same. As shown in Fig.5.13, although the performance of the Manchester signal with FFE-DFE was still worse than that of NRZ-OOK without equalization, except the residual CD ranges

between 1260 and 1417 ps/nm, the FFE-DFE did improve the dispersion tolerance of the Manchester signal significantly. For instance, at the required OSNR of 15 dB, the FFE-DFE increased the CD tolerance by about three times, while the improvement for NRZ-OOK was about 60%. Such drastic improvement for the Manchester signal would greatly enlighten its practical applications in optical access networks.

## 5.4 MLSE equalizer for Manchester signal

As discussed in chapter 2, EDC can be realized by an analogue FFE and/or DFE or by digital MLSE. In this section, we experimentally investigate the capability of EDC for Manchester signal. The performance of FFE/DFE and MLSE is demonstrated and compared with both single-end detection and balanced detection.

### 5.4.1 Experimental setup for CD compensation of Manchester format using MLSE

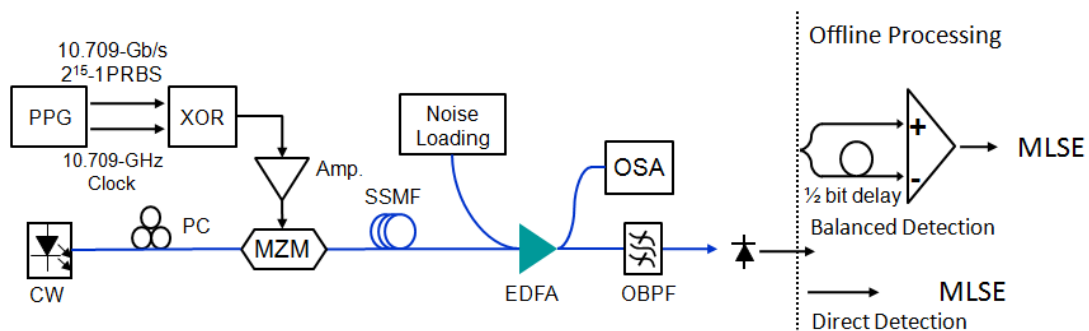


Fig. 5.14 Experimental setup for CD compensation of Manchester format using MLSE

Fig. 5.14 shows the experimental setup for evaluation the capability of EDC. The 10.709-Gb/s Manchester signal with an ER of 18 dB was generated by taking the exclusive OR (XOR) of NRZ signal with  $2^{15}-1$  PRBS and its clock. Continuous wave at 1550.12 nm was used as optical carrier for modulation. Different lengths of SSMFs with  $\sim 17$  ps/nm·km dispersion coefficient are utilized to introduce different amount of CD. In order to avoid significant fiber nonlinear effect the launch power of the optical Manchester signal is kept below 0 dBm. After transmission, noise loading for

adjusting the OSNR of the signal is realized by combining the optical signal with filtered ASE noise from an EDFA. With part of power tapped for OSNR measurement, the signal boosted by another EDFA is filtered by a 0.8-nm OBPF to remove out-band ASE noise. The filtered optical signal is converted to electrical signal by a PIN photodiode and sampled by a Tektronix DSA72004 digital serial analyzer (DSA) operating at 50GS/s. For each combination of CD and OSNR, the duration of the sampling time is 100  $\mu$ s, which corresponds to more than 1 million bits of the signal.

Balanced detection and equalization with FFE-DFE and MLSE are realized by off-line digital signal processing. According to the Nyquist criterion, at least 4 samples for each bit are needed to fully reconstruct the waveform. At this rate we take the four samples from each bit at 0, 1/4T, 1/2T, and 3/4T of the symbol, respectively.

### 5.4.1 Results and discussion

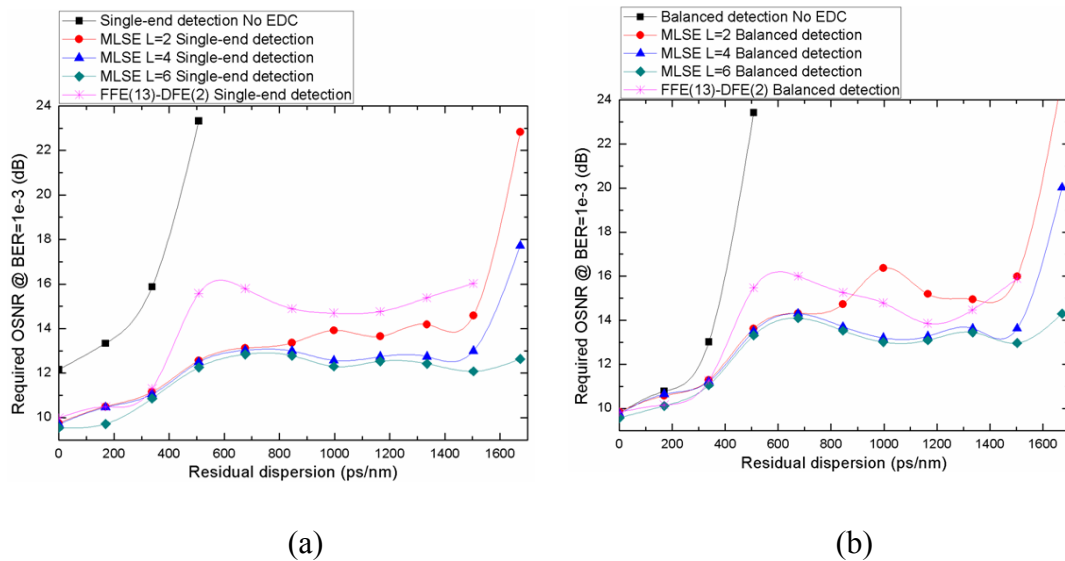


Fig. 5.15 Required OSNR vs. Residual dispersion for 10.709-Gb/s Manchester signal with/without equalization using (a) single-end detection and (b) balanced detection.

Fig. 5.15 (a) shows the required OSNR for a BER of 10<sup>-3</sup> as a function of CD for single-end detected Manchester signal. Memory length of 2, 4, and 6 (L=2, 4, 6) are chosen to exploit the CD compensation capability. For FFE-DFE the tap weight is adapted with least mean square (LMS) algorithm. We assume the Inter-channel

Interference (ISI) comes from adjacent bits. Thus FFE (13)-DFE (2) (13-delay tap FFE and 2-delay tap DFE) is used for comparison. Without equalization, the required OSNR increases from 12.16 dB to 15.88 dB after merely 20-km transmission and further increases dramatically afterwards. When equalization is applied, about 2-dB required OSNR improvement can be obtained at zero CD, regardless of the equalizer we use. As the accumulated CD increases, the required OSNR with MLSE equalization increases slowly and at 90 km the required OSNR is still smaller than 15 dB. When the transmission distance ranges from 0 km to 50 km, MLSE with different states shows similar performance. However, at the transmission distance between 50 km and 90 km, MLSE (4) and MLSE (6) achieve  $\sim 2$  dB lower required OSNR than MLSE (2). MLSE (6) can further increase the transmission distance to 100 km at merely 3.09-dB penalty, while MLSE (2) and MLSE (4) reach their limit at 90 km. Compared that with FFE/DFE, the required OSNR with MLSE does not have the sudden penalty rise at around 30-km SSMF distance and attains at least 2-dB lower required OSNR afterwards. With MLSE, the transmission distance of Manchester signal can be increased to 100 km, which fulfills the requirement of long-reach access network.

Characterized by  $\sim 2$ dB required OSNR improvement and large tolerance to signal level fluctuation, balanced detection is also widely used for Manchester signal [120]. The required OSNR curves for balanced detected Manchester signal with/without equalizer are shown in Fig. 5.15 (b). Without equalization, the CD tolerance is still not satisfactory, although there exists  $\sim 2$  dB required OSNR improvement at zero dispersion. When equalizer is applied, the required OSNR curves follow similar trend as those for single-end detection with equalization. However, their required OSNR at certain CD value are higher than that when single detector is used. It is because only first half bits carry information when balanced receiver is used all four samples are used in single-end receiver.

## 5.5 Summary

In this chapter, we first review the principle of electronic equalization. Particularly, we review the principle of FFE-DFE and MLSE in details. Then, we studied the capability of CD compensation using FFE-DFE for Manchester coded signal, under both single-ended and balanced detection schemes. Two fractional spaced FFE structure at both 4 spb and 2 spb have been further investigated and compared. With such electrical equalizer, the transmission distance of Manchester signal could be tripled. Our results have also showed that balanced detection did not effectively improve the receiver sensitivity in 4-spb based equalizer and was much less robust in 2-spb based equalizer. Two DFE taps were needed to ensure good CD tolerance. By taking two samples at the maximum eye opening points in the first and the second half symbol for equalization, the number of FFE taps could be remarkably reduced, at the expense of a certain penalty in required OSNR ( $< 2$  dB), which was induced by the possible frequency overlapping due to sub-sampling. For applications that such required OSNR penalty is tolerable, tradeoff could be made between the CD tolerance and the number of FFE taps.

In another study, the CD compensation capability of MLSE is experimentally investigated with 10.709 Gbit/s Manchester coded signal. MLSE equalizer with different number of states is used. The results show that MLSE improves the CD tolerance for Manchester signal by  $\sim 4$  times. By comparing the performance of equalizer with balanced detection with that with single-end detection, we can draw the conclusion that there is no benefit of using balanced detection for Manchester signal when equalizer is used.

# Chapter 6. Conclusion

## 6.1 Summary of this thesis

This thesis has investigated binary optical modulation formats and their applications in optical access networks. In this thesis, we have proposed and studied IRZ-duobinary, Manchester-duobinary, and Manchester formats, with focus on the format properties, transmitter and receiver design, and their system applications in optical access networks. We have proposed and studied these formats with a motivation of fulfilling various kinds of requirements for next-generation access networks. In each chapter that describing our original work, we have first explained the modulation format proposed, and then we have studied the properties of the proposed format, following by transmitter and receiver design, and have demonstrated system application in the end.

In chapter 1, we have introduced the basic concept and research thrust on optical access networks. In chapter 2, we have reviewed the basic concepts of optical modulation technologies, transmission impairments as well as common techniques for combating these impairments. These concepts are critical in understanding the whole thesis work. Particularly, we have reviewed the principle and some practical issues of the chirp managed laser (CML), which plays an important role in our innovations.

In chapter 3, we have explained the principle and applications of our proposed IRZ-duobinary format and compare them with conventional IRZ format. The relatively narrow IRZ-duobinary spectrum presents much better dispersion tolerance than conventional IRZ or RZ. Different configurations of generating IRZ-duobinary signal and the performance of the signal generated by the proposed transmitters are compared. After review IRZ-duobinary and its properties, we have proposed and experimentally demonstrated a WDM-PON with optical multicast overlay by using the bandwidth efficient IRZ-duobinary signal. In the proposal, multicast control can

be easily achieved by tuning bias of the downstream PtP modulator. Satisfactory transmission performances of the PtP and broadcast signals have been achieved, which provide sufficient power budget for the system. Another important application – wavelength reused WDM-PON, have also been characterized. In that work, an 80-km-reach CLS WDM-PON is experimentally demonstrated and characterized.

In chapter 4, we have proposed a novel and simple Manchester-duobinary transmitter. The dispersion tolerance characteristics of the Manchester-duobinary signal has been investigated and compared with that of Manchester signal. Two Manchester-duobinary transmitters, the MZM based transmitter and CML based transmitter, are proposed and compared. Experiment results indicate that Manchester-duobinary coding exhibits much more compact optical spectrum compared with that using the Manchester signal and, thus, demonstrate much larger tolerance against chromatic dispersion. The dispersion tolerance of the Manchester-duobinary signal is increased by more than three times compared with that using the Manchester signal. Based on our proposed Manchester-duobinary transmitter, a 70-km-reach CLS bi-directional WDM-PON is experimentally demonstrated and characterized.

In chapter 5, we have first reviewed the principle of different electronic equalizers, including FFE-DFE and MLSE. Then we have studied the capability of CD compensation for optical Manchester signal, with both FFE-DFE and MLSE. Two typical Manchester receivers, single-end receiver and balanced receiver, are used together with electronic equalizer to characterize the performance. In both studies, balanced detection with equalizer show worse performance than that of its single-end counterpart. Thus, we have drawn the conclusion that there is no benefit of using balanced detection for Manchester signal when equalizer is used.

## 6.2 Future work

In Chapter 4, we discussed a Rayleigh noise mitigated 70-km-reach bi-directional transmission WDM-PON, in which the downstream format is 10-Gb/s directly modulated Manchester-duobinary and the upstream format is realized by directly modulating a RSOA with 1.25-Gb/s NRZ-OOK single. Though the system performance is good, the upstream data rate is very limited. In practice, it is desired to increase the upstream transmission data rate to 2.5 Gb/s. However, this is not an easy task, because the broaden bandwidth of Rayleigh noise and the modulating chirp induced by directly modulating a RSOA may deteriorate signal quality and results in poor BER performance. To do so, the filters at both upstream receiver and downstream receiver need to be optimized, in both filter shape and bandwidth. A proper LPF is needed at the upstream receiver to filter out the Rayleigh noise induced by downstream signal. Similarly, A proper HPF or BPF is needed at the downstream receiver to recover the downstream data. The RSOA modulating chirp may lower down the transmission distance, the dispersion tolerance for 2.5-Gb/s upstream signal need to be evaluated.

In Chapter 5, we have shown the capability of dispersion compensation using EDC, including both FFE-DFE and MLSE, for Manchester signal. However, as we have discussed in Chapter 4, Manchester-duobinary format offer larger dispersion tolerance without using any compensation. It would be interesting to evaluate the performance of Manchester-duobinary under different electrical equalizers.



## References

- [1]. R. Ramaswami and K. Sivarajan, “Optical Networks: A Practical Perspective”, 2nd Edition, California: Morgan Kaufmann, 2002.
- [2]. G. Keiser, “FTTX Concepts and Applications”, New Jersey: John Wiley & Sons, 2006.
- [3]. US Census Bureau, “Manufacturing, Mining and Construction Statistics” Manufacturers’ Shipments Historic Timeseries, Aug. 29, 2005.
- [4]. C. Lam (Ed.), “Passive Optical Networks: Principles and Practice”, Academic Press-Elsevier, 2007, ISBN 0123738539
- [5]. Heavy Reading, “FTTH Technology Update & Market Forecast”, vol. 6, no.1, Feb., 2008
- [6]. Heavy Reading, “FTTH Technology & Market Forecast”, vol. 4, no.9, June, 2006.
- [7]. N.J. Frigo, “A Survey of Fiber Optics in Local Access Architectures,” in Optical Fiber Telecommunications, IIIA, edited by I.P. Kaminow and T.L. Koch, Academic Press, pp461–522, 1997.
- [8]. “Broadband optical access systems based on Passive Optical Network (PON),” ITU-T Recommendation G.983.1, 2005
- [9]. “Ethernet in the first mile,” IEEE Standard 802.3ah, 2004.
- [10]. “Gigabit-capable Passive Optical Networks (GPON),” ITU-T Recommendation G.984.1, 2003.
- [11]. H. Shinohara, “Broadband expansion in Japan,” Technical Digest of IEEE/OSA Optical Fiber Communication Conference, Plenary talk, Anaheim, 2005.

- [12]. V. O’Byrne, “Verizon’s fiber to the premises: lessons learned”, IEEE/OSA Optical Fiber Communication Conference / National Fiber Optic Engineers Conference (OFC/NFOEC), Paper OWP6, Anaheim, 2005.
- [13]. Y.C. Chuang, “Recent Advancement in WDM PON Technology,” European Conference on Optical Communications (ECOC), Paper Th.11.C.4, Geneva, Switzerland, 2011.
- [14]. D. K. Jung, S. K. Shin, C. H. Lee, and Y. C. Chung, “Wavelength-division-multiplexed passive optical network based on spectrum-slicing techniques,” IEEE Photon. Tech. Lett., vol. 10, no. 9, pp. 1334-1336, 1998.
- [15]. S. L. Woodward, P. P. Iannone, K. C. Reichmann, and N. J. Frigo, “A spectrally sliced PON employing Fabry-Perot Lasers,” IEEE Photon. Tech. Lett., vol. 10, no. 9, pp. 1337-1339, 1998.
- [16]. W.T. Holloway, A.J. Keating, and D.D. Sampson, “Multiwavelength source for spectrum sliced WDM access networks and LAN’s,” IEEE Photon. Tech. Lett., vol.9, no.7, pp1014–1016, July 1997.
- [17]. B. Zhang, Chinlon Lin, L. Huo, Z. X. Wang, C. K. Chan, “A simple high-speed WDM PON utilizing a centralized supercontinuum broadband light source for colorless ONUs,” IEEE/OSA Optical Fiber Communication Conference / National Fiber Optic Engineers Conference(OFC/NFOEC), Paper OTuC6, Anaheim, California, USA, 2006.
- [18]. C.F. Lam, M.D. Feuer, and N.J. Frigo, “Performance of pin and APD receivers in highspeed WDM data transmission systems employing spectrally sliced spontaneous emission sources,” Elect. Lett., vol.36, no.18, pp1572–1574, Aug. 31, 2000.

- [19]. K. M. Choi, C. H. Lee, "Colorless operation of WDM-PON based on wavelength locked Fabry-Perot laser diode," European Conference on Optical Communications (ECOC), Paper We3.3.4, Glasgow, UK, 2005.
- [20]. S. J. Park, G. Y. Kim, T. Park, E. H. Choi, et al., "WDM-PON system based on the laser light injected reflective semiconductor optical amplifier," European Conference on Optical Communications (ECOC), Paper We3.3.6, Glasgow, UK, 2005.
- [21]. C. Arellano, C. Bock, and J. Prat, "RSOA-based optical network units for WDM-PON," IEEE/OSA Optical Fiber Communication Conference / National Fiber Optic Engineers Conference (OFC/NFOEC), Paper OTuC1, Anaheim, California, USA, 2006.
- [22]. E. Wong, X. Zhao, C. J. Chang-Hasnain, W. Hoffman, M. C. Amann, "Uncooled, optical injection-locked 1.55 $\mu$ m VCSELs for upstream transmitters in WDM-PONs," IEEE/OSA Optical Fiber Communication Conference / National Fiber Optic Engineers Conference (OFC/NFOEC), Paper PDP50, Anaheim, California, USA, 2006.
- [23]. C. W. Chow, "Wavelength Remodulation Using DPSK Down-and-Upstream With High Extinction Ratio for 10-Gb/s DWDM-Passive Optical Networks," IEEE Photon. Tech. Lett., vol. 20, no. 1, pp. 12-14, Jan. 2008.
- [24]. W. Hung, C. K. Chan, L. K. Chen, F. Tong, "An optical network unit for WDM access networks with downstream DPSK and upstream re-modulated OOK data using injection-locked FP laser," IEEE Photon. Tech. Lett., vol. 15, no. 10, pp. 1476-1478, Oct. 2003.
- [25]. G. W. Lu, N. Deng, C. K. Chan, L. K. Chen, "Use of downstream inverse-RZ signal for upstream data re-modulation in a WDM passive optical network," IEEE/OSA Optical Fiber Communication Conference / National Fiber Optic

Engineers Conference (OFC/NFOEC), Paper OFI8, Anaheim, California, USA, Mar. 2005

- [26]. A. Chowdhury, H-C. Chien, M-F. Huang, Jianjun Yu, and G-K. Chang, “Rayleigh backscattering noise-eliminated 115-km long-reach bidirectional centralized WDM-PON with 10-Gb/s DPSK downstream and remodulated 2.5-Gb/s OCS-SCM upstream signal”, IEEE Photon. Tech. Lett., vol. 20, no. 24, pp. 2081-2083, 2008.
- [27]. Z. Liu, M. Li, and C.K. Chan, “Rayleigh Noise Mitigated 70-km-Reach Bi-directional WDM-PON with 10-Gb/s Directly Modulated Manchester-duobinary as Downstream Signal,” IEEE/OSA Optical Fiber Communication Conference / National Fiber Optic Engineers Conference (OFC/NFOEC), Paper OW1B.2, Los Angeles, California, USA, 2012.
- [28]. Y. J. Lee, K. Y. Cho, A. Murakami, A. Agata, Y. Takushima, and Y. C. Chung, “Reflection tolerance of RSOA-based WDM PON”, IEEE/OSA Optical Fiber Communication Conference / National Fiber Optic Engineers Conference (OFC/NFOEC), Paper OTuH5, San Diego, USA, Feb. 2008.
- [29]. M. J. Wale, “PICs for Next-Generation Optical Access Systems,” IEEE/OSA Optical Fiber Communication Conference / National Fiber Optic Engineers Conference (OFC/NFOEC), Paper OTh1F7, Los Angeles, California, USA, 2012.
- [30]. B. Schrenk, J. A. Lazaro, and J. Prat, “Employing feed-forward downstream cancellation in optical network units for 2.5G/1.25G RSOA-based and 10G/10G REAM-based passive optical networks for efficient wavelength reuse”, International Conference on Transparent Optical Networks (ICTON), Paper Th.B3.4, June 2009.

- [31]. F.-T. An, K. S. Kim, D. Gutierrez, S. Yam, E. Hu, K. Shrikhande, and L. G. Kazovsky, "SUCCESS: A next-generation hybrid WDM/TDM optical access network architecture," *J. Lightw. Technol.*, vol. 22, no. 11, pp. 2557–2569, Nov. 2004.
- [32]. Y.-L. Hsueh, M. S. Rogge, S. Yamamoto, and L. G. Kazovsky, "A highly flexible and efficient passive optical network employing dynamic wavelength allocation," *J. Lightw. Technol.*, vol. 23, no. 1, pp. 277–286, Jan. 2005.
- [33]. J. Bauwelinck, W. Chen, D. Verhulst, Y. Martens, P. Ossieur, X.-Z. Qiu, and J. Vandewege, "A high-resolution burst-mode laser transmitter with fast and accurate level monitoring for 1.25 Gb/s upstream GPONs," *IEEE J. Solid-State Circuits*, vol. 40, no. 6, pp. 1322–1330, Jun. 2005.
- [34]. S. Brigati, P. Colombara, L. D'Ascoli, U. Gatti, T. Kerekes, and P. Malcovati, "A SiGe BiCMOS burst-mode 155 Mb/s receiver for PON," *IEEE J. Solid-State Circuits*, vol. 37, no. 7, pp. 887–893, Jul. 2002.
- [35]. M. Nakamura, Y. Imai, Y. Umeda, J. Endo, and Y. Akatsu, "1.25-Gb/s burst-mode receiver ICs with quick response for PON systems," *IEEE J. Solid-State Circuits*, vol. 40, no. 12, pp. 2680–2688, Dec. 2005.
- [36]. M. Noda, S. Yoshima, K. Ishii, S. Shirai, M. Nogami, and J. Nakagawa, "Dual-rate Optical Transceiver incorporating Fully Optimized Burst-mode AGC/ATC Functions for 10G-EPON Systems," *European Conference on Optical Communications (ECOC)*, Paper Mo.2.B.2, Torino, Italy, 2010.
- [37]. P.-U. Han and W.-Y. Choi, "1.25/2.5-Gb/s burst-mode clock recovery circuit with a novel dual bit-rate structure in 0.18- $\mu$ m CMOS," in *Proc. Circuit Syst.*, pp. 3069–3072, 2006.

- [38]. S. Vatannia, P.-H. Yeung, and C. Ju, "A fast response 155-Mb/s burstmode optical receiver for PON," *IEEE Photon. Technol. Lett.*, vol. 17, no. 5, pp. 1067–1069, May 2005.
- [39]. N. Suzuki, K. Nakura, S. Kozaki, H. Tagami, M. Nogami, and J. Nakagawa, "Single Platform 10G-EPON 10.3-Gbps/1.25-Gbps Dual-Rate CDR with Fast Burst-Mode Lock Time Employing 82.5 GS/s Sampling IC and Bit-Rate Adaptive Decision Logic Circuit," *European Conference on Optical Communications (ECOC)*, Paper Mo.2.B.3, Torino, Italy, 2010.
- [40]. H. Nishizawa, Y. Yamada, K. Habara, and T. Ohyama, "Design of a 10-Gb/s Burst-Mode Optical Packet Receiver Module and Its Demonstration in a WDM Optical Switching Network," *J. Lightw. Technol.*, vol. 20, no. 7, pp. 1078–1083, July 2002.
- [41]. Y. Kai, S. Yoshida, K. Sone, G. Nakagawa, and S. Kinoshita, "MSA Compatible Package Size, Dual-Channel Fast Automatic Level Controlled SOA Subsystems for Optical Packet and PON Signals," *European Conference on Optical Communications (ECOC)*, Paper Mo.A.2, Geneva, Switzerland, 2005.
- [42]. G. P. Agrawal, "Fiber-Optic Communication Systems," 3rd Edition. New York: John Wiley & Sons, 2002.
- [43]. P. Gysel and R.K. Staubli, "Statistical Properties of Rayleigh Backscattering in Single-Mode Fibers," *J. Lightwave Technol.*, vol. 8, no. 4, pp. 561-567, Apr. 1990.
- [44]. S. K. Liaw, S. L. Tzeng and Y. J. Hung, "Rayleigh backscattering induced power penalty on bidirectional wavelength-reuse fiber systems," *Opt. Commun.*, vol. 188, no. 1-4, pp. 63-67, Feb. 2001.

- [45]. M. O. van Deventer, "Polarization properties of Rayleigh backscattering in single-mode fibers," *J. Lightw. Technol.*, vol. 11, pp. 1895–1899, Dec. 1993.
- [46]. Darren P. Shea and John E. Mitchell, "," *J. Lightw. Technol.*, vol. 25, no. 3, pp. 685-693, Mar. 2007.
- [47]. Rasmus Kjær, Idelfonso Tafur Monroy, Leif K. Oxenløwe and Palle Jeppesen, "Bi-directional 120 km long-reach PON link based on distributed Raman amplification," in *Proc. Photonics Switching*, 2007.
- [48]. R. P. Davey, D. B. Grossman, M. Rasztovits-Wiech, D. B. Payne, D. Nettet, A. E. Kelly, A. Rafel, S. Appathurai, and S. Yang, "Long-Reach Passive Optical Networks," *J. Lightw. Technol.*, vol. 27, no. 3, pp. 273-291, Feb. 2009.
- [49]. G. de Valicourt, D. Maké, J. Landreau, M. Lamponi, G. H. Duan, P. Chanclou, and R. Brenot, "High Gain (30 dB) and High Saturation Power (11 dBm) RSOA Devices as Colorless ONU Sources in Long-Reach Hybrid WDM/TDM-PON Architecture," *IEEE Photon. Tech. Lett.*, vol. 22, no. 3, pp. 191-193, Feb. 2010.
- [50]. T. Nakanishi, K-I. Suzuki, Y. Fukada, N. Yoshimoto, M. Nakamura, K. Kato, K. Nishimura, Y. Ohtomo and M. Tsubokawa, "High sensitivity APD burst-mode receiver for 10Gbit/s TDM-PON system," *IEICE Electronics Express*, vol. 4, no. 10, pp. 588-592, 2007.
- [51]. H. Song, B. Kim, and B. Mukherjee, "Long-Reach Optical Access Networks: A Survey of Research Challenges, Demonstrations, and Bandwidth Assignment Mechanisms," *IEEE Communications Surveys & Tutorials*, vol. 12, no. 1, First Quarter 2010.
- [52]. J. Cho, J. Kim, D. Gutierrez, and L. G. Kazovsky, "Broadcast Transmission in WDM-PON Using a Broadband Light Source," *IEEE/OSA Optical Fiber*

Communication Conference / National Fiber Optic Engineers Conference (OFC/NFOEC), Paper OWS7, Anaheim, California, USA, Mar. 2007.

- [53]. M. Khanal, C. J. Chae, R. S. Tucker, "Selective broadcasting of digital video signals over a WDM passive optical network," *IEEE Photon. Technol. Lett.*, vol. 17, no. 9, pp. 1992-1994, Sept. 2005.
- [54]. N. Deng, C. K. Chan, L. K. Chen, and C. Lin, "A WDM passive optical network with centralized light sources and multicast overlay," *IEEE Photon. Technol. Lett.*, vol. 20, no. 2, pp. 114–116, Jan. 2008.
- [55]. L. Cai, Z. Liu, S. Xiao, M. Zhu, R. Li and W. Hu, "Video-service-overlaid wavelength-division-multiplexed passive optical network," *IEEE Photon. Technol. Lett.*, vol. 21, no. 14, pp. 990-992, 2009.
- [56]. Y. Dong, Z. Li, C. Lu, Y. Wang, Y. J. Wen, T. H. Cheng, and W. Hu, "Improving dispersion tolerance of Manchester coding by incorporating duobinary coding," *IEEE Photon. Technol. Lett.*, vol. 18, no. 16, pp. 1723–1725, Aug., 2006.
- [57]. G. P. Agrawal, "Fiber - Optic Communications Systems" , third edition, 2002, Wiley Series in microwave and optical engineering.
- [58]. D. V. D. Borne, "Robust optical transmission systems", Technische Universiteit Eindhoven, 2008.
- [59]. P. J. Winzer, and R.J. Essiambre, "Advanced Optical Modulation Formats," *Proceedings of the IEEE*, Vol. 94, No. 5, May 2006
- [60]. Y. Matsui, D. Mahgerefteh, X. Zheng, C. Liao, Z. F. Fan, K. McCallion, and P. Tayebati, "Chirp-Managed Directly Modulated Laser (CML)," *IEEE Photonics Technology Letters*, vol. 18, no. 2, pp. 385-387, Jan. 2006.



- [61]. D. Mahgerefteh, Y. Matsui, X. Zheng, and K. McCallion, "Chirp Managed Laser and Applications," *IEEE J. Sel. Top. Quantum Electron.*, vol. 16, no.5, Sept./Oct. 2010.
- [62]. X. Zheng, D. Mahgerefteh, Y. Matsui, X. Ye, V. Bu, K. McCallion, H. Xu, M. Deutsch, H. Ereifej, R. Lewén, J. Wesström, R. Schatz, and P. Rigole, "Generation of RZ-AMI using a widely tunable modulated grating Y-branch chirp managed laser," presented at the Optical Fiber Communication/National Fiber Optic Engineers Conf. (OFC/NFOEC), Paper OThE5, San Diego, CA, 2010.
- [63]. W. Jia, J. Xu, Z. Liu, K. H. Tse, and C.K. Chan, "Generation and Transmission of 10-Gb/s RZ-DPSK Signals Using a Directly Modulated Chirp-Managed Laser," *IEEE Photonics Technology Letters*, vol. 18, no. 2, pp. 385-387, Jan. 2011.
- [64]. W. Jia, J. Xu, Z.X. Liu, C.K. Chan, L.K. Chen, "Generation of 20-Gb/s RZ-DQPSK Signal using a Directly Modulated Chirp Managed Laser," *IEEE/OSA Optical Fiber Communication Conference / National Fiber Optic Engineers Conference, OFC/NFOEC 2011*, Paper OThE4, Los Angeles, California, USA, 2011.
- [65]. C.K. Chan, W. Jia, Z.X. Liu, "Advanced Modulation Format Generation using High-Speed Directly Modulated Lasers for Optical Metro/Access Systems," *Asia Communications and Photonics Conference (ACP)*, Paper 8309-32 (Invited), Shanghai, PRC, Nov. 2011.
- [66]. Z. Liu and C.K. Chan, "Generation of Dispersion Tolerant Manchester-duobinary Signal Using Directly-modulated Chirp Managed Laser," *IEEE Photonics Technology Letters*, vol. 23, no. 15, pp. 1043-1045, Aug. 2011.

- [67]. T.L. Koch and R.A. Linke, "Effect of nonlinear gain reduction on semiconductor laser wavelength chirping," *Appl. Phys. Lett.*, vol. 48, pp. 613-615, Mar. 1986
- [68]. C. H. Henry, "Theory of the linewidth of semiconductor lasers," *IEEE J. Quantum Electron.*, vol. 18, pp. 259-264, Feb. 1982.
- [69]. B. W. Hakki, "Evaluation of Transmission Characteristics of Chirped DFB Lasers in Dispersive Optical Fiber," *J. Lightw. Technol.*, vol. 10, no. 7, pp. 964-970, July 1992.
- [70]. W. D. Cornwell, I. Andonovic, A. Zadok, and M. Tur, "The Role of Thermal Chirp in Reducing Interferometric Noise in Fiber-Optic Systems Driven by Directly Modulated DFB Lasers," *J. Lightw. Technol.*, vol. 18, no. 2, pp. 154 - 160, Feb. 2000.
- [71]. Lightwave on-line, <http://www.lightwaveonline.com/articles/2005/08/chirp-managed-laser-technology-delivers-gt-250-km-reach-53915052.html>  
[on-line]
- [72]. A. J. Price and N. L. Mercier, "Reduced Bandwidth Optical Digital Intensity Modulation with Improved Chromatic Dispersion Tolerance," *Electron. Lett.*, vol. 31, no. 1, pp. 58–59, Jan. 1995.
- [73]. A Lender , "Correlative Digital Communication Techniques," *IEEE Trans. on Communication Technology*, vol. 12, no. 4, pp. 128–135, Dec. 1964.
- [74]. K. Yonenaga, S. Kuwano, S. Norimatsu, and N. Shibata, "Optical Duobinary Transmission System with no Receiver Sensitivity Degradation," *Electron. Lett.*, vol. 31, no. 4, pp. 302–304, Feb. 1995.

- [75]. C. C. Chien, and I. Lyubomirsky, "Comparison of RZ Versus NRZ Pulse Shapes for Optical Duobinary Transmission," *J. Lightw. Technol.*, vol. 25, no. 10, pp. 2953-2958, Oct 2007.
- [76]. I. Lyubomirsky and C.-C. Chien, "Optical duobinary spectral efficiency versus transmission performance: Is there a tradeoff?" presented at the Conf. Lasers Electro-Optics/Quantum Electron. Laser Science Conf. (CLEO/QELS), Paper JThE72, Baltimore, MD, 2005.
- [77]. G. P. Agrawal, "Nonlinear fiber optics," 3rd edition, Academic Press, USA, 2001.
- [78]. R. J. Nuyts, Y. K. Park, and P. Gallion, "Dispersion equalization of a 10 Gb/s repeatered transmission system using dispersion compensation fibers", *IEEE Journal of Lightwave Technology*, vol. 15, pp. 31-42, 1997.
- [79]. O. Leclerc, B. Lavigne, E. Balmefrezol, P. Brindel, L. Pierre, D. Rouvillain, and F. Segumineau, "Optical regeneration at 40 Gb/s and beyond," *J. Lightw. Technol.*, vol. 21, no. 11, pp. 2779–2790, Nov. 2003.
- [80]. J. H. Winters, R. D. Gitlin, and S. Kasturia, "Reducing the effects of transmission impairments in digital fiber optic systems", *IEEE Communications Magazine*, vol. 31, pp. 68-76, 1993.
- [81]. H. Bulow, "PMD mitigation techniques and their effectiveness in installed fiber", *IEEE/OSA Optical Fiber Communication Conference (OFC)*, vol. 3, pp. 110-112, 2000.
- [82]. H. Bülow, F. Buchali, and A. Klekamp, "Electronic dispersion compensation," *J. Lightw. Technol.*, vol. 25, no. 7, pp. 1742–1753, Jul. 2008.

- [83]. T. Miyazaki and F. Kubota, "2-bit per symbol modulation/demodulation by DPSK over inverse-RZ optical pulses," in Proc. CLEO 2004, Paper CThBB2, San Francisco, CA, 2004.
- [84]. Siu-Sun Pun, Chun-Kit Chan, and Lian-Kuan Chen, "Demonstration of a Novel Optical Transmitter for High-Speed Differential Phase-Shift-Keying/Inverse-Return-to-Zero (DPSK/Inv-RZ) Orthogonally Modulated Signals," IEEE Photon. Technol. Lett., vol. 17, no. 12, pp. 2763 - 2765, Dec. 2005.
- [85]. T. Miyazaki and F. Kubota, "Superposition of DQPSK over inverse-RZ for 3-bit/symbol modulation-demodulation," IEEE Photon. Technol. Lett., vol. 16, no. 12, pp. 2643–2645, Dec. 2004.
- [86]. Murat Serbay1, "42.8 Gbit/s, 4 Bits per Symbol 16-ary Inverse-RZ-QASKDQPSK Transmission Experiment without Polmux", IEEE/OSA Optical Fiber Communication Conference / National Fiber Optic Engineers Conference (OFC/NFOEC), Paper OThL2, Anaheim, California, USA, Mar. 2007.
- [87]. T. Miyazaki, and F. Kubota, "PSK Self-Homodyne Detection Using a Pilot Carrier for Multibit/Symbol Transmission With Inverse-RZ Signal," IEEE Photon. Technol. Lett., vol. 17, no. 16, pp. 1334–1336, June. 2005.
- [88]. J. Yu, X. Zhou, L. Xu, P. N. Ji, Y. Yeo, T. Wang, and G. K. Chang, " Experimental Demonstration of a Label-Switched and 50GHz Channel Spacing DWDM Network with 50Gbit/s DQPSK Payload and 3.125Gb/s inversion-RZ OOK Label," IEEE/OSA Optical Fiber Communication Conference / National Fiber Optic Engineers Conference (OFC/NFOEC), paper OThF4, Anaheim, California, USA, Mar. 2007.

- [89]. J. Yu, L. Xu, Y.K. Yeo, P. N. Ji, T. Wang, and G.K. Chang, "A Novel Scheme for Generating Optical Dark Return-to-Zero Pulses and Its Application in a Label Switching Optical Network," *IEEE Photon. Technol. Lett.*, vol. 18, no. 14, pp. 1524–1526, July. 2006.
- [90]. C. W. Chow, C. H. Kwok, H. K. Tsang, and Chinlon Lin, "Optical label switching of DRZ/DPSK orthogonal signal generated by photonic-crystal fiber," *Opt. Lett.* Vol. 31, no.17, pp. 2535-2537, 2006.
- [91]. L. Cai, S. Xiao, Z. Liu, R. Li, M. Zhu, and W. Hu, "Cost-effective WDM-PON for simultaneously transmitting unicast and broadcast/multicast data by superimposing IRZ signal onto NRZ signal," *European Conference on Optical Communications (ECOC)*, Paper Th.1.F.4.m Brussels, Belgium, 2005.
- [92]. G. W. Lu, N. Deng, C. K. Chan, and L. K. Chen, "Use of downstream IRZ signal for upstream data re-modulation in a WDM passive network," *IEEE/OSA Optical Fiber Communication Conference / National Fiber Optic Engineers Conference (OFC/NFOEC)*, Paper OFI8, Anaheim, California , USA, Mar., 2005.
- [93]. H. S. Chung, B. K. Kim, and K. Kim, "Performance comparison between Manchester and inverse-RZ coding in a wavelength re-modulated WDM-PON," *IEEE/OSA Optical Fiber Communication Conference / National Fiber Optic Engineers Conference (OFC/NFOEC)*, Paper JThA94, San Diego, USA, Feb. 2008.
- [94]. C.K. Chan, Z. Liu, W. Jia, "Optical Inverse-RZ Duobinary Format for High-Speed Optical Transmission," *International Conference on Optical Communications and Networks (ICOON)*, Invited Paper, Nanjing, PRC, Oct, 2010.

- [95]. Z. Liu, Y. Qiu, J. Xu, C.K. Chan, “An Optical Multicast Overlay Scheme for a WDM PON using Inverse-RZ-Duobinary Signals” *IEEE Photonics Technology Letters*, vol. 23, no. 4, pp. 257-259, Feb. 2011.
- [96]. M. Khanal, C. J. Chae, and R. S. Tucker, “Selective broadcasting of digital video signals over a WDM passive optical network”, *IEEE Photon. Technol. Lett.*, vol. 17, no. 9, pp. 1992–1994, Sep. 2005.
- [97]. Y. Zhang, N. Deng, C. K. Chan, and L. K. Chen, “A multicast WDM-PON architecture using DPSK/NRZ orthogonal modulation”, *IEEE Photon. Technol. Lett.*, vol. 20, no. 17, pp. 1479–1481, Sep., 2008.
- [98]. Z. Liu, Y. Qiu, J. Xu, C. K. Chan and L.K. Chen, “A WDM-PON optical multicast overlay scheme using inverse-RZ-duobinary signal,” *IEEE/OSA Optical Fiber Communication Conference / National Fiber Optic Engineers Conference (OFC/NFOEC)*, Paper OThG5, San Diego, California, USA, 2010.
- [99]. R. Maher, L. P. Barry, and P. M. Anandarajah, “Cost Efficient Directly Modulated DPSK Downstream Transmitter and Colourless Upstream Remodulation for Full-Duplex WDM-PONs,” *IEEE/OSA Optical Fiber Communication Conference / National Fiber Optic Engineers Conference (OFC/NFOEC)*, Paper JThA29, San Diego, California, USA, 2010.
- [100]. W. Hung, C. Chan, L. Chen, and F. Tong, “An optical network unit for WDM access networks with downstream DPSK and upstream remodulated OOK data using injection-locked FP laser, ” *IEEE Photon. Technol. Lett.*, vol. 15, no. 10, pp. 1476–1478, Oct. 2003.
- [101]. Z. Liu, J. Xu, Y. Qiu, C.K. Chan, “An 80-km-Reach Centralized-light-source WDM PON utilizing Inverse-RZ-Duobinary Downstream Signals, ” *European Conference on Optical Communications, (ECOC)*, Paper P6.12, Torino, Italy, Sep. 2010.

- [102]. Y.Matsui, D.Mahgerefteh, X.Zheng, C. Liao, Z. F. Fan, K.McCallion, and P. Tayebati, "Chirp-managed directly modulated laser (CML)," *IEEE Photon. Technol. Lett.*, vol. 18, no. 2, pp. 385–388, 2006.
- [103]. T. V. Muoi, "Receiver design for digital fiber optic transmission systems using manchester (biphase) coding," *IEEE Trans. Commun.*, vol.31, no. 5, pp. 608–619, May 1983.
- [104]. T. Yoshida, S. Kimura, H. Kimura, K. Kumozaki, and T. Imai, "A new single-fiber 10-Gb/s optical loopback method using phase modulation for WDM optical access networks," *J. Lightw. Technol.*, vol. 24, no. 12, pp. 786-796, Dec. 2006.
- [105]. H. Nishizawa, Y. Yamada, K. Habara, and T. Ohyama, "Design of a 10-Gb/s Burst-Mode Optical Packet Receiver Module and Its Demonstration in a WDM Optical Switching Network," *J. Lightw Technol.*, vol. 20, no. 7, pp. 1078-1083, July 2002.
- [106]. J. Zhang, N. Chi, P. V. Holm-Nielsen, and P. Jeppesen, "Performance of manchester-coded payload in an optical FSK labeling scheme," *IEEE Photon. Techol. Lett.*, vol. 15, no. 8, pp. 1174–1176, Aug. 2003.
- [107]. J. Zhang, N. Chi, P. V. Holm-Nielsen, C. Peucheret, and P. Jeppesen, "10 Gbit/s manchester-encoded FSK-labelled optical signal transmission link," *Electron. Lett.*, vol. 39, no. 16, pp. 1193–1194, Aug 2003.
- [108]. B.K. Kim, H. Park, S. Park and K. Kim, "Optical access network scheme with downstream Manchester coding and upstream NRZ remodulation," *Electron. Lett.*, vol.42, no.8, pp. 484–485, April 2006.
- [109]. H.S. Chung, B.K. Kim, and K. Kim, "Performance comparison between Manchester and inverse-RZ coding in a wavelength re-modulated WDM-PON," in *Proc. OFC'08, San Diego, CA, 2008*, paper JThA94.

- [110]. S. P. Jung, Y. Takushima, K. Y. Cho, S. J. Park and Y. C. Chung, "Demonstration of RSOA-based WDM PON Employing Self-Homodyne Receiver with High Reflection Tolerance," in Proc. OFC'09, San Diego, CA, 2009, paper JWA69.
- [111]. A. Murakami, Y. J. Lee, K. Y. Cho, Y. Takushima, A. Agata, K. Tanaka, Y. Horiuchi, and Y. C. Chung, "Enhanced reflection tolerance of upstream signal in RSOA-based WDM-PON using Manchester coding," in Proc. SPIE, 2007, vol. 6783, p. 67832I.
- [112]. Z. Li, Y. Dong, Y. Wang, and C. Lu, "A novel PSK-Manchester modulation format in 10-Gb/s passive optical network system with high tolerance to beat interference noise," IEEE Photon. Technol. Lett., vol. 13, no. 5, pp. 1118–1120, May 2005.
- [113]. I. Lyubomirsky and C. Chien, "Optical duobinary spectral efficiency versus transmission performance: Is there a tradeoff?," CLEO/QELS, pp. 1774–1776, 2005.
- [114]. W. Kaiser, T. Wuth, M. Wichers, and W. Rosenkranz, "Reduced complexity optical duobinary 10-Gb/s transmitter setup resulting in an increased transmission distance," IEEE Photon. Technol. Lett., vol. 13, no. 8, pp. 884–886, Aug. 2001.
- [115]. T. Ono, Y. Yano, K. Fukuchi, T. Ito, H. Yamazaki, M. Yamaguchi, and K. Emura, "Characteristics of optical duobinary signals in terabit/s capacity, high-spectral efficiency WDM systems," J. Lightw. Technol., vol. 16, no. 5, pp. 788–797, May 1998.
- [116]. S. Walklin and J. Conradi, "On the relationship between chromatic dispersion and transmitter filter response in duobinary optical communication systems," IEEE Photon. Technol. Lett., vol. 9, no. 7, pp. 1005–1007, Jul. 1997.



- [117]. H. Kim and C. X. Yu, "Optical duobinary transmission system featuring improved receiver sensitivity and reduced optical bandwidth," *IEEE Photon. Technol. Lett.*, vol. 14, no. 8, pp. 1205–1207, Aug. 2002.
- [118]. X. Zheng, F. Liu, and P. Jeppesen, "Receiver optimization for 40-Gb/s optical duobinary signal," *IEEE Photon. Technol. Lett.*, vol. 13, no. 7, pp. 744–746, Jul. 2002.
- [119]. A. Royset and D. Roar, "Symmetry requirement for 10-Gb/s optical duobinary transmitters," *IEEE Photon. Technol. Lett.*, vol. 10, no. 2, pp. 273–275, Feb. 1998.
- [120]. Y. Dong, Z. Li, C. Lu, Y. Wang, Y. Wen, T. Cheng, and W. Hu, "Improving Dispersion Tolerance of Manchester Coding by Incorporating Duobinary Coding," *IEEE Photon. Technol. Lett.*, vol. 18, no. 16, pp. 1723–1725, 2006.
- [121]. Z. Liu, C.K. Chan, "Generation of Dispersion Tolerant Manchester-duobinary Signal Using Directly-modulated Chirp Managed Laser," *IEEE Photonics Technology Letters*, vol. 23, no. 15, pp. 1043-1045, Aug. 2011.
- [122]. Z. Liu, J. Xu, Q.K. Wang, C.K. Chan, "Rayleigh Noise Mitigated 70-km-Reach Bi-directional WDM-PON with 10-Gb/s Directly Modulated Manchester-duobinary as Downstream Signal," *IEEE/OSA Optical Fiber Communication Conference / National Fiber Optic Engineers Conference (OFC/NFOEC)*, Paper OW1B.2, Los Angeles, California, USA, 2012.
- [123]. Y. Matsui, D. Mahgerefteh, X. Zheng, C. Liao, Z. F. Fan, K. McCallion, and P. Tayebati, "Chirp-managed directly modulated laser (CML)," *IEEE Photon. Technol. Lett.*, vol. 18, no. 2, pp. 385–388, 2006.
- [124]. Arshad Chowdhury, Hung-Chang Chien, Ming-Fang Huang, Jianjun Yu, and Gee-Kung Chang, "Rayleigh Backscattering Noise-Eliminated 115-km Long-Reach Bidirectional Centralized WDM-PON With 10-Gb/s DPSK

- Downstream and Remodulated 2.5-Gb/s OCS-SCM Upstream Signal, ” IEEE Photon. Technol. Lett., vol. 20, no. 24, pp. 2081–2083, Dec. 2008.
- [125]. Y. C. Chung, “Recent Advancement in WDM PON Technology,” European Conference on Optical Communications (ECOC), Paper Th.11.C.4, Geneva, Switzerland, 2011.
- [126]. M. O. van Deventer, Fundamentals of Bidirectional Transmission Over a Single Optical Fiber. Boston, MA: Kluwer, 1996.
- [127]. H. Hu and H. Anis, “Degradation of Bi-Directional Single Fiber Transmission in WDM-PON Due to Beat Noise,” J. Lightw. Technol., vol. 26, no. 8, pp. 870–881, Apr. 2008.
- [128]. Z. Al-Qazwini and H. Kim, “10-Gbps Single-Feeder, Full-Duplex WDM-PON Using Directly Modulated Laser and RSOA,” IEEE/OSA Optical Fiber Communication Conference / National Fiber Optic Engineers Conference (OFC/NFOEC), Paper OTh1F.5, Los Angeles, California, USA, 2012.
- [129]. M. Omella, P. Chanclou, J. A. Lazaro, J. Prat, “RSOA as a Sawtooth Generator for Rayleigh Backscattering Effect Mitigation,” European Conference on Optical Communications, (ECOC), Paper Mo.1.B.5, Torino, Italy, Sep. 2010.
- [130]. T. Yoshida, S. Kimura, H. Kimura, K. Kumozaki, and T. Imai, “A new single-fiber 10-Gb/s optical loopback method using phase modulation for WDM optical access network,” J. Lightw. Technol., vol. 24, no. 2, pp. 786–796, 2006.
- [131]. C. W. Chow, G. Talli, and P. D. Townsend, “Rayleigh noise reduction in 10-Gb/s DWDM-PONs by wavelength detuning and phase-modulation-induced phase-modulation-induced spectral broadening,” IEEE Photon. Technol. Lett., vol. 19, no. 6, pp. 423–425, Mar. 2007.

- [132]. J. A. Lazaro, C. Arellano, V. Polo, and J. Prat, "Rayleigh scattering reduction by means of optical frequency dithering in passive optical networks with remotely seeded ONUs," *IEEE Photon. Technol. Lett.*, vol. 19, no. 2, pp. 64–66, Jan. 2007.
- [133]. H. H. Lin, C. Y. Lee, S. C. Lin, S. L. Lee, and G. Keuser, "WDM-PON systems using cross-remodulation to double network capacity with reduced Rayleigh scattering effects," *IEEE/OSA Optical Fiber Communication Conference / National Fiber Optic Engineers Conference, OFC/NFOEC 2008*, Paper OTuH6, San Diego, USA, Feb. 2008.
- [134]. A. Chowdhury, H-C. Chien, M-F. Huang, Jianjun Yu, and G-K. Chang, "Rayleigh backscattering noise-eliminated 115-km long-reach bidirectional centralized WDM-PON with 10-Gb/s DPSK downstream and remodulated 2.5-Gb/s OCS-SCM upstream signal", *IEEE Photon. Tech. Lett.*, vol. 20, no. 24, pp. 2081-2083, 2008.
- [135]. A. Murakami, Y. J. Lee, K. Y. Cho, Y. Takushima, A. Agata, K. Tanaka, Y. Horiuchi and Y. C. Chung, "Enhanced reflection tolerance of upstream signal in RSOA-based WDM-PON using Manchester coding", *Tech. Dig. of APOC*, paper 6783-87, Wuhan, China, 2007.
- [136]. R. P. Davey, D. B. Grossman, M. Rasztoivits-Wiech, D. B. Payne, D. Nettet, A. E. Kelly, A. Rafel, S. Appathurai, and S. Yang, "Long-Reach Passive Optical Networks," *J. Lightw. Technol.*, vol. 27, no. 3, pp 273-291, Feb. 2009.
- [137]. H. Louchet, A. Richter, "Electrical Equalization in Fiber-Optic Transmission Systems," *Military Communications Conference, MILCOM*, Oct. 2007.
- [138]. C. Xia and W. Rosenkranz, "Nonlinear Electrical Equalization for Different Modulation Formats With Optical Filtering," *J. Lightwave Technol.* vol. 25, no. no. 13, pp. 996-1001, July 2007.

- [139]. M. Cavalari, C. R. S. Fludger, and P. Anslow, "Electronic signal processing for differential phase modulation formats," IEEE/OSA Optical Fiber Communication Conference, (OFC), Paper TuG2, Los Angeles, USA, Feb. 2004.
- [140]. Ming Li, Fan Zhang, Zhangyuan Chen, and Anshi Xu, "Chromatic dispersion compensation and fiber nonlinearity mitigation of OOK signals with diverse-VSB-filtering FFE and DFE," Opt. Express vol. 16, no. 26, pp. 21991-21996, Dec. 2008.
- [141]. Gilad Katz and Dan Sadot, "Minimum BER Criterion for Electrical Equalizer in Optical Communication Systems," J. Lightw. Technol., vol. 24, no. 7, pp 2844-2850, July 2006.
- [142]. P. A. Humblet and M. Azizoglu, "On the bit error of lightwave system with optical amplifier," J. Lightw. Technol., vol. 9, no. 11, pp. 1576–1582, Nov. 1991.
- [143]. J. G. Proakis, Digital Communications, 4th ed. New York: McGraw-Hill, 2001.
- [144]. B. Franz, D. Roesener, F. Buchali, H. Bulow, G. Veith, "Adaptive electronic feed-forward equalizer and decision feedback equalizer for the mitigation of chromatic dispersion and PMD in 43 Gbit/s optical transmission systems", European Conference on Optical Communication (ECOC), Paper We1.5.1, 2006.
- [145]. B. Franz, F. Buchali, D. Rosener, H. Bulow, "Adaptation techniques for electronic equalizers for the mitigation of time-variant distortions in 43 Gbit/s optical transmission systems", IEEE/OSA Optical Fiber Communication Conference / National Fiber Optic Engineers Conference (OFC/NFOEC), Paper Paper OMG1, Anaheim, CA, 2007.

- [146]. G. D. Forney, Jr., "Maximum likelihood sequence estimation of digital sequences in the presence of intersymbol interference", IEEE Trans. Inform. Theory, IT-18, pp. 363-378, 1972.
- [147]. G. D. Forney, Jr., "The Viterbi Algorithm," Proc. IEEE, vol. 61, no. 3, pp. 268-278, Mar. 1973.
- [148]. H. Nishizawa, Y. Yamada, K. Habara, and T. Ohyama, "Design of a 10-Gb/s Burst-Mode Optical Packet Receiver Module and Its Demonstration in a WDM Optical Switching Network," IEEE/OSA J. Lightwave Technol., vol. 20, no. 7, pp. 1078-1083, July 2002.

# Appendix:

## A. List of abbreviations

ADC: analog to digital converter

ADD: delay-and-add ADD

AGC: automatic gain control

AMI: alternate mark inversion

ASE: amplified spontaneous emission

ATC: automatic threshold control

AWG: arrayed waveguide grating

AWGN: additive white Gaussian noise

BtB: back-to-back

BER: bit error rate

BPON: Broadband PON

CATV: community antenna television

CD: chromatic dispersion

CDR: clock and data recovery

CLS: centralized light source

CO: central office

CR: clock recovery

CM: channel model

CML: chirp managed laser

CW: continuous-wave

DCF: dispersion compensation fiber

DCM: dispersion compensation module

DD: direct detection

DFB: distributed feedback

DFE: decision feedback equalizer

DI: delay-interferometer

DL: delay line

DQPSK: Differential Quaternary Phase Shift Keying

DPSK: differential phase-shift keying

DSF: dispersion-shifted fiber

DSL: digital subscriber line

DSP: digital signal processing

EAM: electroabsorption modulator

EDC: electronic dispersion compensation

EDFA: erbium-doped fiber amplifier

EPON: ethernet PON

ER: extinction ratio

FFE: feed forward equalizer

FP-LD: Fabry-Perot laser diode

FSK: frequency-shift keying

FWM: Four-wave mixing

FTTC: fiber to the curb

FTTH: fiber to the home

FTTP: fiber to the premises

FTTx: fiber to the x

GPON: Gigabit PON

HDTV: high-definition television

HPF: high-pass filter

IM: intensity modulator

IPTV: Internet protocol TV

IRZ: inverse-return-to-zero

ISI: inter-symbol-interference

LPF: low pass filter

MLLD: mode-locked laser diode

MLSE: Maximum likelihood estimation

MZDI: Mach-Zehnder delay interferometer

MZM: Mach-Zehnder modulator

NG: next generation



NRZ: non-return-to-zero

OBPF: optical bandpass filter

OLT: optical line terminal

ONU: optical network unit

OOK: on-off keying

OSNR: optical signal to noise ratio

SSMF: standard single mode fiber

SPM: self-phase modulation

OTDM: optical time-division multiplexing

PC: polarization controller

PLC: planar lightwave circuit

PM: phase modulator

PON: passive optical network

PRBS: pseudorandom binary sequence

PtP: point-to-point

RBS: Rayleigh backscattering

RN: remote node

RSOA: reflective semiconductor optical amplifier

RZ: return-to-zero

SBS: stimulated brillouin scattering

SRS: stimulated Raman scattering

SMF: single mode fiber

SCM: Subcarrier multiplexing

SOA: semiconductor optical amplifier

TDM: time-division multiplexed

TDM-PON: time-division-multiplexed passive optical network

TF: transversal filter

VCSEL: vertical-cavity surface-emitting laser

VOA: variable optical attenuator

VoIP: voice over Internet Protocol

WDM-PON: wavelength-division-multiplexed passive optical network

XPM: cross-phase modulation

## **B. List of publications**

### **Journals**

- [1]. **Zhixin Liu**, Ming Li, Lu Lu, Chun-Kit Chan, Soung-Chang Liew, Lian-Kuan Chen, "Optical Physical-Layer Network Coding ," IEEE Photonics Technology Letters, vol. 24, no. 8, 2012.
- [2]. **Zhixin Liu**, Ming Li, and Chun-Kit Chan, "Chromatic Dispersion Compensation with Feed Forward Equalizer and Decision Feedback Equalizer for Manchester Coded Signals," IEEE Journal of Lightwave Technology, vol. 29, no. 18, 2011.
- [3]. **Zhixin Liu**, Chun-Kit Chan, "Generation of Dispersion Tolerant Manchester-duobinary Signal Using Directly-modulated Chirp Managed Laser," IEEE Photonics Technology Letters, vol. 23, no. 15, 2011.
- [4]. **Zhixin Liu**, Yang Qiu, Jing Xu, and Chun-Kit Chan, "An Optical Multicast Overlay Scheme for a WDM PON Using Inverse-RZ-Duobinary Signals," IEEE Photonics Technology Letters, vol.23, no. 4, 2011.
- [5]. Yang Qiu, **Zhixin Liu**, and Chun-Kit Chan, "A Centrally Controlled Survivable WDM-PON Based on Optical Carrier Suppression Technique," IEEE Photonics Technology Letters, vol.23, no. 6, 2011.
- [6]. Wei Jia, Jing Xu, **Zhixin Liu**, Kam-Hon Tse, Chun-Kit Chan, "Generation and Transmission of 10-Gb/s RZ-DPSK Signals using a Directly Modulated Chirp Managed Laser," IEEE Photonics Technology Letters, vol. 23, 2011.

### **Conferences**

- [1]. **Zhixin Liu**, Ming Li, and Chun-Kit Chan, "Fault Localization in Passive Optical Networks using OTDR Trace Correlation Analysis," OFC/NFOEC 2012, Paper OTu1H.2, Los Angeles, California, USA, 2012.
- [2]. **Zhixin Liu**, Jing Xu, Qike Wang, and Chun-Kit Chan, "Rayleigh Noise Mitigated 70-km-Reach Bi-directional WDM-PON with 10-Gb/s Directly

- Modulated Manchester-duobinary as Downstream Signal,” OFC/NFOEC 2012, Paper OW1B.2, Los Angeles, California, USA, 2012.
- [3]. **Zhixin Liu**, Jing Xu, Yang Qiu, and Chun-Kit Chan, "An 80-km-Reach Centralized-light-source WDM PON utilizing Inverse-RZ-Duobinary Downstream Signals," in European Conference on Optical Communications, ECOC 2010, paper P6.12, Torino, Italy, 2010.
- [4]. **Zhixin Liu**, Yang Qiu, Jing Xu, Chun-Kit Chan and Lian-Kuan Chen., “A WDM-PON Optical Multicast Overlay Scheme Using Inverse-RZ-Duobinary Signal,” OFC/NFOEC 2010, Paper OThG5, San Diego, California, USA, 2010.
- [5]. Jing Xu, **Zhixin Liu**, Lian-Kuan Chen, Chun-Kit Chan, "Time-Interleaved Phase Remodulation to Enable Broadcast Transmission in Bidirectional WDM-PONs without Additional Light Sources ,” OFC/NFOEC 2011, Paper OThK4, Los Angeles, California, USA, 2011.
- [6]. Chun-Kit Chan, **Zhixin Liu**, Wei Jia, “Optical Inverse-RZ Duobinary Format for High-Speed Optical Transmission,” in International Conference on Optical Communications and Networks (ICOON), **Invited Paper**, Nanjing, PRC, Oct, 2010.
- [7]. Wei. Jia, **Zhixin Liu**, Chun-Kit Chan, Generation and Transmission of 10.709-Gbaud RZ-DQPSK Using a Chirp Managed Laser, OptoElectronics and Communications Conference, OECC 2012, Paper SC2\_1067, Korea, Busan, 2012.
- [8]. Jing Xu, **Zhixin Liu**, Wei Jia, Lian-Kuan Chen, “A Novel Chirp-free Optical Manchester Signal Transmitter with Enhanced Dispersion Tolerance,” Asia Communications and Photonics Conference (ACP), Paper SA 2, Shanghai, China, 2010.
- [9]. Wei Jia, Jing Xu, **Zhixin Liu**, Chun-Kit Chan, Lian-Kuan Chen, "Generation of 20-Gb/s RZ-DQPSK Signal using a Directly Modulated Chirp Managed Laser," OFC/NFOEC 2011, Paper OThE4, Los Angeles, California, USA, 2011.

- [10]. Chun-Kit Chan, Wei Jia, **Zhixin Liu**, "Advanced Modulation Format Generation using High-Speed Directly Modulated Lasers for Optical Metro/Access Systems," Asia Communications and Photonics Conference (ACP), Paper 8309-32 (Invited), Shanghai, PRC, Nov. 2011.
- [11]. Yuan Luo, Lihua Li, **Zhixin Liu**, "A Hybrid Codebook Design Algorithm for MIMO Amplify-and-Forward Relaying System with Power Allocation and Precoding," IEEE GLOBECOM 2010, Miami, America, 2010.
- [12]. Yuan Luo, Lihua Li, Qiang Wang, and **Zhixin Liu**, "A Codebook-Based Precoding Method for MIMO Amplify-and-Forward Relaying System," Vehicular Technology Conference Fall (VTC 2010-Fall), Ottawa, ON, Canada, 2010.